

Single subject prediction of brain disorders in neuroimaging: Promises and pitfalls



Mohammad R. Arbabshirani^{a,b,*}, Sergey Plis^a, Jing Sui^{a,c}, Vince D. Calhoun^{a,d}

^a The Mind Research Network, Albuquerque, NM 87106, USA

^b Geisinger Health System, Danville, PA 17822, USA

^c Brainnetome Center and National Laboratory of Pattern Recognition, Institute of Automation, Chinese Academy of Sciences, Beijing 100190, China

^d Department of ECE, University of New Mexico, Albuquerque, NM, USA

ARTICLE INFO

Article history:

Accepted 25 February 2016

Available online 21 March 2016

Keywords:

Neuroimaging
Machine learning
Classification
Brain disorders
Prediction

ABSTRACT

Neuroimaging-based single subject prediction of brain disorders has gained increasing attention in recent years. Using a variety of neuroimaging modalities such as structural, functional and diffusion MRI, along with machine learning techniques, hundreds of studies have been carried out for accurate classification of patients with heterogeneous mental and neurodegenerative disorders such as schizophrenia and Alzheimer's disease. More than 500 studies have been published during the past quarter century on single subject prediction focused on a multiple brain disorders. In the first part of this study, we provide a survey of more than 200 reports in this field with a focus on schizophrenia, mild cognitive impairment (MCI), Alzheimer's disease (AD), depressive disorders, autism spectrum disease (ASD) and attention-deficit hyperactivity disorder (ADHD). Detailed information about those studies such as sample size, type and number of extracted features and reported accuracy are summarized and discussed. To our knowledge, this is by far the most comprehensive review of neuroimaging-based single subject prediction of brain disorders. In the second part, we present our opinion on major pitfalls of those studies from a machine learning point of view. Common biases are discussed and suggestions are provided. Moreover, emerging trends such as decentralized data sharing, multimodal brain imaging, differential diagnosis, disease subtype classification and deep learning are also discussed. Based on this survey, there is extensive evidence showing the great potential of neuroimaging data for single subject prediction of various disorders. However, the main bottleneck of this exciting field is still the limited sample size, which could be potentially addressed by modern data sharing models such as the ones discussed in this paper. Emerging big data technologies and advanced data-intensive machine learning methodologies such as deep learning have coincided with an increasing need for accurate, robust and generalizable single subject prediction of brain disorders during an exciting time. In this report, we survey the past and offer some opinions regarding the road ahead.

© 2016 Elsevier Inc. All rights reserved.

Introduction

Neuroimaging has opened up an exciting non-invasive window into the human brain over the past few decades. This interdisciplinary field has attracted scientists from areas such as medicine, engineering, mathematics, physics, statistics, computer science, and psychology (Epstein et al., 2001). Imaging modalities such as magnetic resonance imaging (MRI) and magnetoencephalography (MEG) along with more traditional methods such as electroencephalography (EEG) have made it possible to non-invasively study various aspects of the human brain with unprecedented accuracy. MRI-related techniques such as structural MRI (sMRI), functional MRI (fMRI) and diffusion MRI (dMRI)

have the benefit of providing localized spatial information about the brain structure and function as well as detailed functional and structural connectivity maps. These techniques have provided new insight into the human brain and have brought hope to researchers trying to unravel the secrets of one of the most complex systems in the universe, the human brain.

Structural MRI has made it possible to visualize the brain at high spatial resolution (one cubic millimeter or less) (Liang and Lauterbur, 2000). sMRI high resolution images of the brain are ideal for studying various brain structures and also for detecting physical abnormalities, lesions and damages. dMRI is an imaging technique for visualization of anatomical connections between different brain regions (Le Bihan et al., 2001; Merboldt et al., 1985). Functional MRI measures brain activity by detecting changes in the blood oxygenation (DeYoe et al., 1994; Ogawa et al., 1990). fMRI makes it possible to study

* Corresponding author at: The Mind Research Network, 1101 Yale Blvd., NE, Albuquerque, NM 87106, USA.

functional regions and networks of the brain as well as temporal associations among them.

Unfortunately, brain disorders are major health problems in the US and the rest of the world that not only impair the lives of millions of people but also impose huge financial burdens on societies (DiLuca and Olesen, 2014; Ernst and Hay, 1994; Rice, 1999). Moreover, there are no clinical tests to identify many brain disorders such as schizophrenia. One of the major hopes underlying the advanced neuroimaging tools mentioned above is to provide new understanding of brain disorders such as schizophrenia, bipolar disorder, autism spectrum disorder (ASD), Alzheimer's disease (AD), major depressive disorders, attention-deficit hyperactivity disorder (ADHD) and mild cognitive impairment (MCI). Brain disorder research aims at understanding the impact of each disease on the brain's function and structure from the cellular to system level, as well as the pathogenesis of these complex disorders. As a result, thousands of studies have been published on different aspects of brain disorders to show aberrations of some features (structural or functional) in a patient group usually in comparison with a healthy cohort (Jack et al., 1997; Jafri et al., 2008; Lorenzetti et al., 2009; McAlonan et al., 2005). While these studies are valuable in terms of finding relevant disease biomarkers, they are not sufficient for direct clinical diagnostic/prognostic adoption. The main reason is that many of these findings are statistically significant at the group level, but the individual discrimination ability of the proposed biomarkers is not typically evaluated. Since classification provides information for each individual subject, it is considered a much harder task than reporting group differences.

In recent years, there has been a growing trend in designing neuroimaging-based prognostic/diagnostic tools. As a result, there have been a lot of efforts using neuroimaging methods to automatically discriminate patients with brain disorders from healthy control or from each other (Klöppel et al., 2012). Many of these studies have reported promising prediction performances with the claim that complex diseases can be diagnosed robustly, accurately and rapidly in an automatic fashion. However, until now, these tools have not been integrated into the clinical realm. We believe that the main reason for this is that many of the studies of this nature, despite the promising results on a specific research dataset, are not designed to generalize to other datasets, specifically the clinical ones.

The purpose of this study was two-fold. First, we reviewed a large number of MRI-based brain disorder diagnostic/prognostic studies in schizophrenia, ASD, ADHD, depressive disorder, MCI and Alzheimer's disease. These studies are compared in a number of key aspects such as type of features, classifier and reported accuracies. Next, we formed our opinion on the issues associated with how machine learning is applied in neuroimaging and have suggested solutions that might address these pitfalls. Considering the immense potential of neuroimaging tools for clinical adoption, careful implementation and interpretation

of machine learning in neuroimaging is crucial. Machine learning is a relatively new domain for many neuroimaging researchers coming from other fields and therefore pitfalls are unfortunately not rare. We attempt to identify and emphasize some common mistakes that resulted in these shortcomings and biases. At the end, we discuss emerging trends in neuroimaging such as data sharing, multimodal brain imaging and differential diagnosis.

Group difference vs. classification

As pointed out in the Introduction section, many brain disorder studies have shown abnormality in the average sense in one or more brain features in a patient cohort in comparison with a healthy group using statistical tests. The success of such methodology is usually measured by the means of p-values. On the other hand, the goal of single subject prediction is to automatically classify each subject into one of the groups in the study (e.g., healthy vs. patient). The success of classification studies is usually measured by accuracy.

These two problems are very different in essence as they try to address distinct research questions. In general, showing group differences is much easier compared to single subject prediction. To better illustrate the difference between these types of analysis, we show an example in Fig. 1. Suppose there are two groups each with 100 samples (subjects) and we have measurements of one brain feature for each subject. Fig. 1A shows a case where the mean values of the two groups are different as measured by a two-sample t-test. The difference is statistically significant (p -value = 0.001). However, if one tries to classify subjects based on a threshold on this brain feature (the dotted red line placed between the mean of two groups), a weak classification rate of 60.0% will be achieved. The reason for this is the range of values for that specific feature is highly overlapping for the two groups. So, a highly significant group difference does not necessarily translate into a strong classification result. But the opposite is also true, as high classification based on a feature doesn't necessarily mean that group-level mean differences exist. Fig. 1B shows a case where the two-sample t-test on the two groups is not significant (p -value = 0.86) but the classification based on two thresholds (red dotted lines placed between each mode of group 2 and mean of group 1) is very strong (94.5%). In this case, the abnormality is bidirectional, which does not cause significant mean differences but makes it possible to separate the groups with two thresholds (dotted lines). Interestingly, bidirectional abnormalities are observed in neuroimaging studies (Arbabshirani and Calhoun, 2011; Calhoun et al., 2006b). Fig. 1C shows a case where strong group differences and successful classification go hand in hand. The abnormality is one-directional and the mean difference is very significant (p -value < $2e-16$). The mean of two groups is so far apart that the values of most of the samples of the two groups do not overlap. Therefore, a strong classification rate of 93.5% is achieved (based on one threshold).

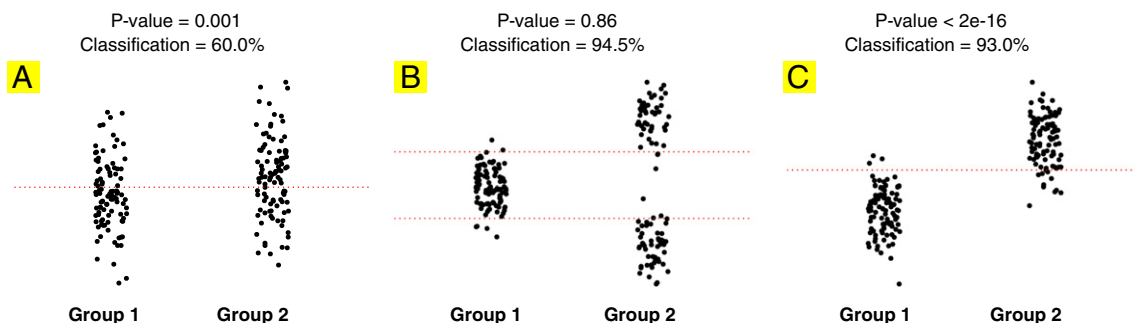


Fig. 1. Comparison of group difference analysis and classification in three different scenarios using toy data. Group difference is analyzed by two-sample t-tests and classification is performed by simple thresholding (red dotted lines). Each group/class has 100 samples. A: Significant group difference (p -value < 0.001) but poor classification (60.0%). B: Insignificant group difference (p -value = 0.865) but high classification accuracy (94.5%). C: Significant group difference (p -value < $2e-16$) and high classification accuracy (93.0%). Significant group difference doesn't necessarily cause high classification and vice versa.

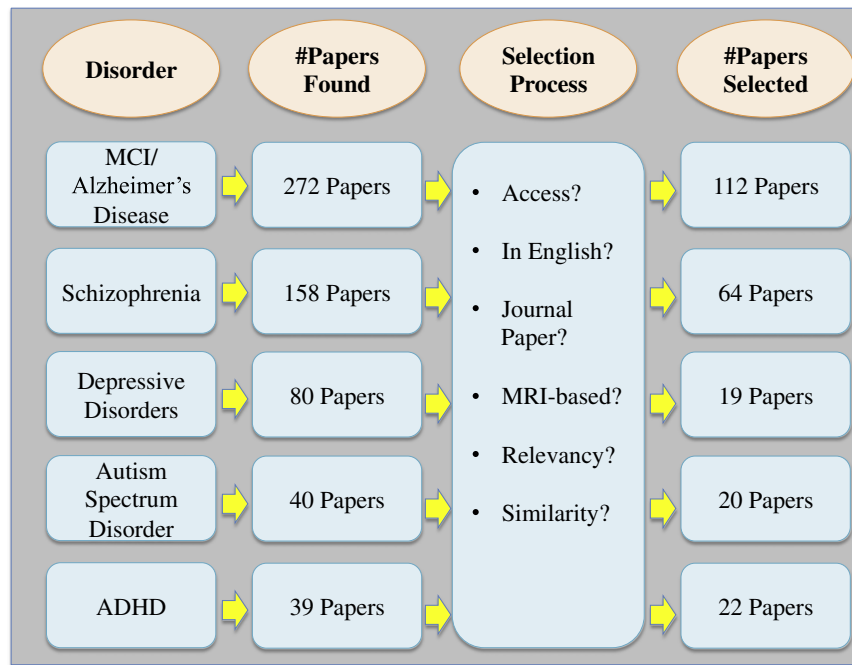


Fig. 2. The literature review procedure, the inclusion criteria and the number of surveyed studies for each modality.

The main purpose of example in Fig. 1 is to show that group level analysis and classification are two different methods for different problems. We will return to this example later for criticism of selecting features based on p-value.

Survey of MRI-based single-subject prediction of brain disorders

Based on a search on PubMed from 1990 to 2015,¹ more than 500 papers on MRI-based single subject prediction of brain disorders were found. Fig. 2 summarizes the paper selection procedure for this study. More than 200 papers were eventually selected for this survey (112 AD/MCI, 64 schizophrenia, 19 depressive disorders, 20 ASD and 22 ADHD papers).

We limited our search to journal papers in English published up to December 2015. In a few instances, the full paper was not found and therefore those studies were excluded from this survey. Also, in cases of very similar papers from the same authors, only one was selected. Key aspects of each study such as modality, machine learning method, sample size and extracted features were investigated. A list of all abbreviations used in the tables and the manuscript itself is provided in Table 1.

Mild cognitive impairment/Alzheimer's disease

MCI entails cognitive decline more than what is expected for an individual's age and education level, but not to the extent that it interferes notably with activities of daily life (Albert et al., 2011). Unfortunately, more than 50% of the MCI patients progress to dementia within 5 years (Gauthier et al., 2006). So, it is considered a prodromal phase to dementia especially the AD type (Gauthier et al., 2006). The

heterogeneous etiology of MCI includes degenerative diseases (AD, fronto-temporal lobe degeneration, dementia with Lewy bodies) as well as vascular and psychiatric disorders (Petersen and Negash, 2008). AD is the most common neurodegenerative disorder, which is increasingly prevalent among adults aged 65 years and older. AD is characterized by the progressive impairment of neurons and their connections, which result in decline and loss of cognitive functions. In 2007, it was estimated that more than 26 million people suffer from AD worldwide (Brookmeyer et al., 2007). In 2001 it was predicted that AD will triple in prevalence by 2050 (Hebert et al., 2001). The detection of AD is based on clinical examinations and an evaluation of the patient's perception and behavior. Considering the prevalence and severity of MCI/AD, the largest number of neuroimaging-based, automatic prediction/classification publications has been devoted to these conditions. Also, a number of these studies, investigated the possibility of automatic classification of stable MCI (sMCI) from progressive MCI (pMCI) using neuroimaging data (Eskildsen et al., 2013). Table 2 summarizes the 112 studies that we reviewed in this survey including 16 studies that also reported sMCI versus pMCI classification results.

Schizophrenia

Schizophrenia is among the most prevalent mental disorders and affects about 1% of the population worldwide (Bhugra, 2005). This devastating, chronic heterogeneous disease is usually characterized by disintegration in perception of reality, cognitive problems, and a chronic course with lasting impairment (Heinrichs and Zakzanis, 1998). Considering the absence of standard clinical test for schizophrenia, there is a growing interest in automatic diagnosis of schizophrenia based on neuroimaging features. We surveyed 64 papers, which are tabulated in Table 3.

Depressive disorders

Major depressive disorder (MDD) or unipolar depression characterized by a pervasive low mood, self-esteem and lack of interest in enjoyable activities is a common mental illness affecting adolescents. The lifetime prevalence of MDD is approximately 15–20% (Kessler et al.,

¹ Search term: ("Machine Learning" OR SVM OR "automatic Classification" OR "discriminant analysis" OR "neural Network" OR "Logistic Regressions" OR "decision tree") AND (MRI OR "Magnetic Resonance" OR fMRI OR "functional MRI" OR "structural MRI" OR "Diffusion MRI" OR DTI OR DSI) AND (schizophrenia OR bipolar OR Alzheimer's OR "Mild Cognitive Impairment" OR MCI OR autism OR "autism spectrum disorder" OR ASD OR depression OR "depressive disorder" OR ADHD OR "Attention Deficit Hyperactivity Disorder") concluded on 12/08/2015.

Table 1
Glossary of the abbreviations used in the manuscript and tables.

Abbreviation	Full term
AAL	automated anatomical labeling
ABIDE	autism brain imaging data exchange
ACC	anterior cingulate cortex
AD	alzheimer's disease
ADAS	alzheimer's disease assessment scale
ADHD	attention deficit hyperactivity disorder
ADHD-C	ADHD combined
ADHD-HI	hyperactive/impulsive ADHD
ADHD-IA	inattentive ADHD
ADNI	alzheimer's disease neuroimaging initiative
ADOS	autism diagnostic observation schedule
AG	angular gyrus
ALFF	amplitude of low frequency fluctuations
aMCI	amnestic MCI
ANN	artificial neural network
ANOVA	analysis of variance
AOD	auditory oddball
ASD	autism spectrum disease
AUC	area under curve
AX-CPT	AX version of continuous performance task
BOLD	blood-oxygen level dependent
BP	bipolar disorder
CFT	complex figure test
cMCI	MCI converter
CN	cognitively normal
CSF	cerebrospinal fluid
DA	axial diffusion
DAT	dementia of the Alzheimer's type
DLPFC	dorsolateral prefrontal cortex
DMN	default-mode network
dMRI	diffusion magnetic resonance imaging
DR	radial diffusion
DRS	dementia rating scale
EC	elderly controls
EEG	electroencephalography
ELM	extreme learning machines
eMCI	early MCI
ERC	entorhinal cortex
FA	fractional anisotropy
FALLF	fractional amplitude of low frequency fluctuations
FBIRN	functional biomedical informatics research network
FC	functional connectivity
FDG	fluorodeoxyglucose
FDG-PET	fluorodeoxyglucose positron emission tomography
FFT	fast Fourier transform
fMRI	functional magnetic resonance imaging
FNC	functional network connectivity
FTD	frontotemporal dementia
GLM	general linear modeling
GM	gray matter
GMD	gray matter density
HC	healthy controls
ICA	independent component analyses
ITG	inferior temporal gyrus
jICA	joint independent component analysis
LBD	Lewy body dementia
LDA	linear discriminant analysis
LDDMM	large deformation diffeomorphic metric mapping
LLD	late-life depression
LLE	locally linear embedding
LMCI	late MCI
MA	mean anisotropy
mCCA	multi-set canonical correlation analysis
MCI	mild cognitive impairment
MCIC	multi-site clinical imaging consortium
MD	mean diffusivity
md-aMCI	multiple domains MCI
MDD	major depressive disorder
MEG	magnetoencephalography
MLSP	machine learning for signal processing
mMLDA	modified maximum uncertainty linear discriminant analysis
MMSE	mini mental state examination
MPFC	medial prefrontal cortex
MRI	magnetic resonance imaging
MRMR	minimum redundancy maximum relevancy

Table 1 (continued)

Abbreviation	Full term
MRS	magnetic resonance spectroscopy
MTL	medial temporal lobe
MTR	magnetization transfer ratio
MVPA	multi voxel pattern analysis
N/A	no answer (we couldn't find it in the paper)
NC	normal controls
ncMCI	MCI non-converter
NDD	non-refractory depressive disorder
NMF	non-negative matrix factorization
OCD	obsessive compulsive disorder
ODVBA	optimally-discriminative voxel-based analysis
orPLS	ordinary partial least square
PANSS	positive and negative syndrome scale
PCA	principal component analysis
PCC	posterior cingulate cortex
pdf	probability distribution function
PET	positron emission tomography
pMCI	progressive MCI
PPI	psychophysiological interaction
QDA	quadratic discriminant analysis
RAVENS	regional analysis of brain volumes in normalized space
RBF	radial basis function
RDD	refractory depressive disorder
ReHo	regional homogeneity
RMD	remitted MDD
ROC	receiver operating characteristic
ROI	region of interest
rsfMRI	resting-state fMRI
RSN	resting-state networks
RVM	relevance vector machine
RVoxM	relevance voxel machine
RVR	relevance vector regression
sACC	subgenual anterior cingulate cortex
SBM	surface based morphometry
sd-aMCI	single domain amnestic MCI
sd-fMCI	single domain frontal MCI
SIFT	scale-invariant feature transform
sMCI	stable MCI
sMRI	structural magnetic resonance imaging
SN	saliency network
SNP	single nucleotide polymorphism
SSD	schizophrenia spectrum disorders
StD	late-life subthreshold depression
SUVr	standard uptake value ratio
SVM	support vector machine
SVM-FoBa	support vector machine with a forward-backward search strategy
SVM-RFE	support vector machine with recursive feature elimination
SZ	schizophrenia
SZA	schizoaffective
TD	typically developing
TDC	typically developing children
uMCI	unknown MCI
VaD	vascular dementia
VBM	voxel-based morphometry
VMHC	voxel-mirrored homotopic correlations
VOI	volume of interest
WFU	Wake Forest University
WM	white matter
WMD	white matter density
WMT	working memory task

2003; Lewinsohn et al., 1986). It is estimated that by the year 2020, depression will account for 15% of the disease burden in the world ranking second after heart disease (Kessler et al., 1994). We reviewed 19 studies that used neuroimaging for automatic diagnose MDD. Those studies are listed in Table 4.

Autism spectrum disorder

Autism spectrum disorder (ASD) is a serious neurodevelopmental condition characterized by impaired social communication, deficits in social-emotional reciprocity, deficits in nonverbal

Table 2

Summary of 112 MRI-based AD/MCI classification studies. Overall classification accuracy of stable (non-converting) MCI (sMCI or ncMCI) from progressive (converting) MCI (pMCI or cMCI) is indicated by MCI-Conv if applicable. N/A indicates information was not available or could not be found.

Modality	Disorder	Features	# of features	Classifier	Number of subjects	Overall accuracy	Reference
dMRI	AD	FA	1210	SVM	HC = 25, AD = 20, Total = 45	100%	Graña et al. (2011)
dMRI	AD/BP	FA maps	1500–14,000	SVM	HC = 25, BP = 12, AD = 20, Total = 57	100%	Bergouignan et al. (2011)
dMRI	AD/MCI	FA and MD Values	12–1080	SVM	EC = 50, AD = 37, MCI = 113, Total = 200	68.3–84.9%	Nir et al. (2015)
dMRI	MCI	Clustering coefficient of WM connectivity maps based on fiber count, FA, MD and principal diffusivities	3 (Most selected ROIs)	SVM	HC = 17, MCI = 10, Total = 27	88.90%	Wee et al. (2011)
dMRI	MCI	FA, DA, DR and MD	500	SVM	EC = 40, MCI = 33, Total = 73	93.00%	O'Dwyer et al. (2012)
dMRI	MCI	FA and the volume of fiber pathways from selected region	100–4500	SVM	NC = 45, MCI = 39, Total = 84	100%	Lee et al. (2013)
dMRI	MCI	FA maps	1000	SVM	sd-aMCI = 18, sd-fMCI = 13, ad-aMCI = 35, Total = 66	97%	Haller et al. (2013)
dMRI	MCI	FA, longitudinal, radial, and mean diffusivity features	N/A	SVM	HC = 35, MCI = 67, Total = 102	91.4–97.5%	Haller et al. (2010)
fMRI (confrontation naming task)	AD (low and high risk)	Fractional signal changes ROI	50	LDA + orPLS	Low AD Risk HC = 11, High AD Risk HC = 13, Total = 24	83.30%	Andersen et al. (2012)
rsfMRI	AD	Averaged voxel intensities of selected resting-state networks	4	Multivariate ROC	HC = 16, AD = 15, Total = 31	100%	Wu et al. (2013)
rsfMRI	AD	Graph measures based on FC analysis among ROIs	454	SVM	HC = 20, AD = 20, Total = 40	100%	Khazaei et al. (2015)
rsfMRI	AD/FTD	ROI-based difference between DMN and SN map	22	LDA	HC = 12, AD = 12, FTD = 12, Total = 36	92%	Zhou et al. (2010)
rsfMRI	AD/MCI	FC among selected AAL regions	3403	Bayesian Gaussian process logistic regression	HC = 39, aMCI = 50, AD = 27, Total = 116	75–90%	Challis et al. (2015)
rsfMRI	MCI	Local connectivity and global topological properties	450	Multiple kernel learning	HC = 25, MCI = 12, Total = 37	91.90%	Jie et al. (2014)
rsfMRI	MCI	N/A	465	N/A	HC = 21, MCI = 29, Total = 60	95.60%	Beltrachini et al. (2015)
sMRI	AD	Eigen brains of key slices	10	SVM	NC = 98, AD = 28, Total = 126	92.30%	Zhang et al. (2015)
sMRI	AD	ODVBA of RAVENS maps	N/A	SVM	HC = 50, AD = 50, Total = 100	90%	Zhang and Davatzikos (2011)
sMRI	AD	Hippocampus shape measures using LDDMM and PCA	20 principal components (3–4 selected by the classifier)	Logistic regression	HC = 26, DAT = 18, Total = 44	81.1–84.6%	Wang et al. (2007)
sMRI	AD	GM, WM, and CSF tissue densities along with age, gender and genotype	237–240	SVM	HC = 190, AD = 190, Total = 380	85.6–89.3%	Vemuri et al. (2008)
sMRI	AD	Cortical thickness measures along mesh vertices	82,000 mesh vertices	RVoxM	HC = 150, AD = 150, Total = 300	93.0% (AUC)	Sabuncu and Van Leemput (2012)
sMRI	AD	Whole brain and hippocampus VBM measures	N/A	SVM	EC = 31, AD = 31, Total = 62	74–79%	Polat et al. (2012)
sMRI	AD	Volumetric measures	45	SVM	HC = 20, AD = 14, Total = 34	88.20%	Oliveira et al. (2010)
sMRI	AD	Hippocampus morphometric measures	9	LDA	HC = 57, AD = 38, Semantic dementia = 6, Total = 101	77%	Miller et al. (2009)
sMRI	AD	GM maps	10–45	SVM, ELM, Self-adaptive Resource Allocation Network	HC = 30, AD = 30, Total = 60	97.1–99.7%	Mahanand et al. (2012)
sMRI	AD	GM distribution of ROIs	90	SVM	EC = 22, AD = 16, Total = 38	94.50%	Magnin et al. (2009)
sMRI	AD	Surface-based measures of	N/A	SVM	HC = 20, AD = 19, Total = 39	84.6–94.9%	Li et al. (2007)

(continued on next page)

Table 2 (continued)

Modality	Disorder	Features	# of features	Classifier	Number of subjects	Overall accuracy	Reference
sMRI	AD	hippocampus Cortical thickness	N/A	LDA, QDA and logistic regression	Total = 39 HC = 17, AD = 19, Total = 36	90–100%	Lerch et al. (2008)
sMRI	AD	Cortical thickness data and hippocampus shape	N/A	LDA	NC = 84, AD = 33, Total = 117	87.50%	Lee et al. (2014)
sMRI	AD	GM probability maps	Variable	Linear program boosting of voxel-wise weak classifiers with spatial constraints	Total = 183	82.0% (AUC)	Hinrichs et al. (2009)
sMRI	AD	WM and GM voxels selected by SVM-RFE	Variable	SVM	HC = 185, AD = 185, Total = 370	94.3–95.1%	Hidalgo-Muñoz et al. (2014)
sMRI	AD	Volumes of hippocampus–amygdala formation	1	Thresholding	HC = 28, AD = 27, Total = 55	89–96% (Sensitivity)	Hampel et al. (2002)
sMRI	AD	Linear measurements of several structures	12	LDA	HC = 31, AD = 46, Total = 77	81–87% (Sensitivity)	Frisoni et al. (1996)
sMRI	AD	Texture features	260	Linear discriminant function	HC = 40, AD = 24, Total = 66	91%	Freeborough and Fox (1998)
sMRI	AD	Percentage of brain volume changes	3	SVM	NC = 30, AD = 30, Total = 60	91.70%	Farzan et al. (2015)
sMRI	AD	GM, WM and CSF volumes and size of hippocampus	5	SVM, MLP, and J48 decision tree	NC = 48, AD = 37, Total = 85	93.70%	Farhan et al. (2014)
sMRI	AD	Brain volume, temporal lobe matter and CSF volume	4	Discriminant analysis	HC = 29, DAT = 31, Total = 60	100%	DeCarli et al. (1995)
sMRI	AD	Several voxel-based and cortical thickness-based schemes	Variable	Regularized SVM	CN = 162, AD = 137, Total = 299	83–91%	Cuingnet et al. (2013)
sMRI	AD	Atrophic patterns of hippocampus and entorhinal cortex	N/A	QDA	HC = 50, AD = 50, Total = 100	93%	Coupé et al. (2012)
sMRI	AD	SIFT features	133	Ensemble of SVMs	HC1 = 66, AD1 = 20, HC2 = 98, AD2 = 28, Total = 212	70–87%	Chen et al. (2014)
sMRI	AD	Pdf of VOI based on VBM	100	SVM	HC = 130, AD = 130, Total = 260	86%	Beheshti and Demirel (2015)
sMRI	AD	Generative–discriminative basis vectors based on RAVEN maps	30–50	Logistic model trees	HC = 63, AD = 54, Total = 117	87–89%	Batmanghelich et al. (2012)
sMRI	AD	Cortical thickness and volumetric measures	N/A	SVM	HC = 25, AD = 29, Total = 54	90.9% (AUC)	Arimura et al. (2008)
sMRI	AD	GM maps based on VBM	384,065	SVM	HC = 137, AD = 108, MCI = 203, Total = 448	63.7–80.3%	Adaszewski et al. (2013)
sMRI	AD	Gray matter probability maps	2.00E + 06	SVM	HC = 226, AD = 91, Total = 417	87%	Abdulkadir et al. (2011)
sMRI	AD/FTD	GM maps	N/A	SVM	HC = 91, AD = 85, FTD = 19, Total = 195	87–96%	Klöppel et al. (2008)
sMRI	AD/FTD	GM volume an thickness and complexity estimates	N/A	LDA	CN = 23 AD = 24, FTD = 19, Total = 66	81–96%	Young et al. (2009)
sMRI	AD/FTD	Morphometric measures of selected ROIs	2	Discriminant analysis	EC = 12, AD = 17, FTD = 16, Total = 45	91%	Kaufer et al. (1997)
sMRI	AD/MCI	3D hippocampal shape morphology	N/A	SVM	HC = 88, MCI = 103, AD = 71, Total = 262	MCI-Conv: 80%	Costafreda et al. (2011a)
sMRI	AD/MCI	GM, WM and CSF volumetric measures and ventricle shape	18	Particle swarm optimization SVM	HC = 17, AD = 17, MCI = 18, Total = 52	88.9–94.1%	Yang et al. (2013)
sMRI	AD/MCI	Coefficient of ICA on normalized brain images	N/A	SVM	HC1 = 316, AD1 = 98, Total1 = 416, HC2 = 200, AD2 = 200, MCI = 400, Total2 = 800,	67.5–99%	Yang et al. (2011)
sMRI	AD/MCI	Hippocampal volume, tensor-based morphometry, cortical thickness and manifold-based learning features	112–114	LDA and SVM	HC = 231, AD = 198, sMCI = 238, pMCI = 167, Total = 834	84.0–89.0% MCI-Conv: 68.0%	Wolz et al. (2011)
sMRI	AD/MCI	ROI-based and correlative features based on cortical and cerebral thickness and	N/A	Multi-kernel SVM	NC = 200, AD = 198, ncMCI = 111, cMCI = 89, Total	79.2–97.4% MCI-Conv: 75.1%	Wee et al. (2013)

Table 2 (continued)

Modality	Disorder	Features	# of features	Classifier	Number of subjects	Overall accuracy	Reference
sMRI	AD/MCI	WM volumes Intensity patches of selected ROIs around hippocampus	130–150 patches	SVM (in multiple instance-graph framework)	= 598 CN = 231, AD = 198, ncMCI = 238, cMCI = 167, Total = 834	82.9–89%-MCI-Conv: 70%	Tong et al. (2014)
sMRI	AD/MCI	Diffeomorphometry patterns of subcortical and ventricular structures	14	LDA	HC = 210, AD = 175, cMCI = 135, ncMCI = 87, Total = 607	MCI-Conv: 77.0%	Tang et al. (2015)
sMRI	AD/MCI	Hippocampus, amygdala, and ventricle shape measures	N/A	LDA	HC = 210, AD = 175, MCI = 369, Total = 754	86%	Tang et al. (2014)
sMRI	AD/MCI	Whole brain GM and WM maps	34–127	SVM	HC = 162, AD = 137, ncMCI = 134, cMCI = 76, Total = 509	72–76%, MCI-Conv: 66.0%	Salvatore et al. (2015b)
sMRI	AD/MCI	GM maps	6000	SVM	HC = 189, AD = 144, ncMCI = 166, cMCI = 136, Total = 635	80.0%-MCI-Conv: 70.7%	Retico et al. (2015)
sMRI	AD/MCI	Hippocampal surface deformation measures	19	LDA	HC = 26, DAT = 18, DAT-Converters = 9, Total = 53	77.0–87.0%	Qiu et al. (2008)
sMRI	AD/MCI	GM and WM maps	Variable	SVM, Bayes statistic and voting feature intervals	HC = 18, AD = 32, MCI = 24, Total = 74	92%-MCI-Conv: 75.0%	Plant et al. (2010)
sMRI	AD/MCI	Volumes of the hippocampus and ERC	2–4	Discriminant Function Analysis	HC = 59, AD = 48, MCI = 65, Total = 172	65.9–90.7%	Pennanen et al. (2004)
sMRI	AD/MCI	GM Density of ROIs	37	SVM	ncMCI = 38, cMCI = 39, Total = 77	MCI-Conv: 77.7%	Ota et al. (2014)
sMRI	AD/MCI	Hippocampal volumetric measures	5	LDA	HC = 53, AD = 18, MCI = 20, Total = 91	73.7–77.5%	Mueller et al. (2010)
sMRI	AD/MCI	GM density values and cognitive measures	309	Low density separation semi-supervised classifier	NC = 231, AD = 200, sMCI = 100, pMCI = 164, uMCI = 130, Total = 825	MCI-Conv: 76.6–90.0% (AUC)	Moradi et al. (2015)
sMRI	AD/MCI	Data-driven ROI GM from different templates	1500 from each template	SVM	NC = 128, AD = 97, sMCI = 117, pMCI = 117, Total = 459	91.6%, MCI-Conv: 72.4%	Min et al. (2014)
sMRI	AD/MCI	Longitudinal volumetric MR imaging measures	N/A	QDA	HC = 203 AD = 164, MCI = 317, Total = 684	85%	McEvoy et al. (2011)
sMRI	AD/MCI	Volumetric and cortical thickness measures	N/A	LDA	HC = 139, AD = 84, MCI = 175, Total = 398	89–92%	McEvoy et al. (2009)
sMRI	AD/MCI	GM maps	N/A	Ensemble of SVMs	NC = 229, AD = 198, MCI = 225, Total = 652	85.3–92.0%	Liu et al. (2014b)
sMRI	AD/MCI	GM maps registered to multiple templates	1500 for each template	Ensemble of SVMs	NC = 128, AD = 97, sMCI = 117, pMCI = 117, Total = 459	93.8% MCI-Conv: 80.9%	Liu et al. (2015)
sMRI	AD/MCI	Volume and cortical thickness values of ROIs	162 Original features reduced by LLE	Logistic regression, SVM and LDA	CN = 137, sMCI = 93, cMCI = 97, AD = 86, Total = 413	51–89% MCI-Conv: 68%	Liu et al. (2013)
sMRI	AD/MCI	Surface connectivity and center of mass markers	N/A	LDA	NC = 170, AD = 114, MCI = 240, Total = 524	76.6–87.7% (AUC)	Lillemark et al. (2014)
sMRI	AD/MCI	Proposed local binary pattern features	N/A	SVM	NC = 142, AD = 80, MCI = 141, Total = 363	61.5–82.8%	Li et al. (2014a)
sMRI	AD/MCI	Cortical thickness measures, cortex thinning dynamics and network features based	262	SVM	NC = 40, sMCI = 36, pMCI = 39, AD	81.7–96.1% MCI-Conv: 80.3%	Li et al. (2012)

(continued on next page)

Table 2 (continued)

Modality	Disorder	Features	# of features	Classifier	Number of subjects	Overall accuracy	Reference
sMRI	AD/MCI	on longitudinal thickness changes of different ROIs Hurst's exponents at different scales	N/A	SVM	= 37, Total = 152	97.1–97.5%	Lahmiri et al. (2014)
sMRI	AD/MCI	Volumetric measures	120 (115 brain features)	LDA	HC = 125, AD = 55, EMCI = 114, LMCI = 91, Total = 385	90.8–94.5%	Goryawala et al. (2015)
sMRI	AD/MCI	Spherical harmonics of hippocampi	2646	SVM	HC = 25, AD = 23, aMCI = 23, Total = 71	83–94%	Gerardin et al. (2009)
sMRI	AD/MCI	Three schemes: voxel-based features, cortical thickness features and hippocampus-based features	Variable	SVM	CN = 162, AD = 137, cMCI = 76, ncMCI = 134, Total = 509	81–95% (for AD vs CN)	Cuingnet et al. (2011)
sMRI	AD/MCI	Volume, thickness and surface area of selected ROIs	7 MRI, 2 CSF and 14 neuropsychological features	SVM	HC = 111, cMCI = 56, ncMCI = 111, AD = 96, Total = 350	MCI-Conv: 67.1%	Cui et al. (2011)
sMRI	AD/MCI	Hippocampus and parahippocampal gyrus GM maps	11,031	SVM	HC = 188, MCI = 260, AD = 131, Total = 579	70–85% MCI-Conv: 65%	Chu et al. (2012)
sMRI	AD/MCI	Intensity and texture of selected VOIs in MTL	>100,000	Ensemble of SVMs	HC = 189, ncMCI = 166, cMCI = 136, AD = 144, Total = 635	65–94% MCI-Conv: 74.0% (AUC)	Chincarini et al. (2011)
sMRI	AD/MCI	GM map	50,000–750,000	SVM, regularized logistic regression, linear regression classifier	HC = 205, MCI = 351, AD = 171, Total = 727	80–90%	Casanova et al. (2012)
sMRI	AD/MCI	Volumetric measures of amygdala, hippocampus, and parahippocampal gyrus	N/A	Discriminant function analysis	NEC = 20, MCI = 21, AD = 39, Total = 80	80.5–88.1%	Bottino et al. (2002)
sMRI	AD/MCI	Hippocampal volume and CSF A β , t-tau and p-tau levels, and ApoE4 stratification	N/A	SVM	NC = 111, AD = 95, MCI = 182, Total = 388	64–78%	Apostolova et al. (2014)
sMRI	AD/MCI	Cortical thickness and volumetric measures	57	SVM	HC = 110, AD = 116, MCI = 119, Total = 345	88.10%	Aguilar et al. (2013)
sMRI	AD/MCI/dementia	GM and WM maps	N/A	SVM	HC = 604, AD = 483, FTD = 51, LBD = 27, ncMCI = 290, cMCI = 128, Total = 1583	73–97% (AUC) MCI-Conv: 73.0% (AUC)	Klöppel et al. (2015)
sMRI	Dementia	Hippocampal head and body volumetric measures	4	LDA	HC = 17, Questionable dementia = 12, Mild dementia = 10, Total = 39	76.90%	Wolf et al. (2001)
sMRI	MCI	Graph properties based on inter-regional co-variation of cortical thickness	Variable	Multiple kernel learning	NC = 42, sd-aMCI = 38, md-aMCI = 32, Total = 112	56.0–62.0%	Raamana et al. (2014)
sMRI	MCI	Volume, mean T1, MTR and T2* for selected ROIs	7 ROIs	SVM	HC = 77, MCI = 42, Total = 119	75%	Granziera et al. (2015)
dMRI and sMRI	AD	FA and GM volumes	142	SVM	NC = 15, AD = 21, Total = 36	94.30%	Li et al. (2014b)
dMRI and sMRI	AD/MCI	Network topology, tractography connectivity and flow-based measures	N/A	SVM	NC = 50, AD = 38, EMCI = 74, LMCI = 38, Total = 200	59.2–78.2%	Prasad et al. (2015)
dMRI and sMRI	AD	FA and MD from dMRI and GMD and WMD from sMRI	26,000 FA, 128,000 MD, 41,000 WMD and 181,000 GMD	SVM	HC = 143, AD = 137, Total = 280	63.6–91.1%	Dyrba et al. (2013)
dMRI and sMRI	AD/VaD	Transcallosal prefrontal FA and Fazekas score	4	LDA	HC = 22, AD = 16, VaD = 13, Total = 51	87.50%	Zarei et al. (2009)
dMRI and sMRI	AD/MCI	Disease-specific spatial filters	N/A	LDA	NC = 22, AD = 19, aMCI-converter = 6, aMCI-stable = 16, Total = 63	MCI-Conv: 93.0% (AUC)	Oishi et al. (2011)

Table 2 (continued)

Modality	Disorder	Features	# of features	Classifier	Number of subjects	Overall accuracy	Reference
dMRI and sMRI	AD/MCI	Cortical thickness, subcortical volume and white matter integrity	2–5	SVM	SMI = 27, AD = 27, MCI = 138 Total = 192	70.5–96.3%	Jung et al. (2015)
dMRI and sMRI	MCI	Subcortical volumetric measures and FA values	68	SVM	HC = 204, aMCI = 79, Total = 283	71.10%	Cui et al. (2012)
sMRI and PET	AD/MCI	Volume of GM from sMRI and average intensity from PET of selected ROIs	186	Multi-task linear programming discriminant	sMCI = 226, pMCI = 167, Total = 393	MCI-Conv: 67.2%	Yu et al. (2014)
sMRI and PET	AD/MCI	GM density relative cerebral metabolic rate for glucose of ROIs	168–172	SVM	ncMCI = 40, cMCI = 40, Total = 80	MCI-Conv: 74.8–75.0% (AUC)	Ota et al. (2015)
sMRI and PET	MCI	ROI-based GM, WM and CSF volumes from sMRI and average intensity from PET	93 ROIs	Multiple Kernel Learning	ncMCI = 50, cMCI = 38, Total = 88	MCI-Conv: 78.4%	Zhang and Shen (2012b)
sMRI and PET	AD	Volumes of interest	12	SVM	HC1 = 28, AD1 = 28, HC2 = 13, AD2 = 21, Total = 90	86–100%	Dukart et al. (2013)
sMRI and PET	AD/MCI	Volumes of GM tissue of selected ROIs	93	Domain transfer SVM	NC = 52, AD = 51, cMCI = 43, ncMCI = 56, Total = 202	MCI-Conv: 79.4%	Cheng et al. (2015a)
sMRI and PET	AD/MCI	Functional and structural connectivity measures using sparse inverse covariance estimation	84	SVM	HC = 68, AD = 70, MCI = 111, Total = 249	84–92%	Ortiz et al. (2015)
sMRI and PET	AD/MCI	GM volume of ROIs from sMRI and average intensity of ROIs from PET	186 (original number of features)	Multi-kernel SVM	NC = 52, AD = 51, MCI = 99, Total = 202	78.8–94.8%	Liu et al. (2014a)
sMRI and rsfMRI	AD	GM volume from sMRI and ALFF, ReHo and FC from rsfMRI	Variable	Maximum uncertainty LDA and second level	HC = 22, AD = 16, Total = 38	89.50%	Dai et al. (2012b)
sMRI, FDG-PET	AD/MCI	ROI-based GM, volumes from sMRI and average intensity from PET	186	Multi-kernel SVM	NC = 52, AD = 51, ncMCI = 56, cMCI = 43, Total = 202	80.3–95.9%, MCI-Conv: 69.8%	Zu et al. (2015)
sMRI, FDG-PET	AD/MCI	Cortical and volumetric measures and surface based FDG uptakes	24	Partial least square LDA	NC = 85, AD = 71, MCI = 163, Total = 319	76.5–90.1%	Yun et al. (2015)
sMRI, FDG-PET	AD/MCI	GM and WM maps from sMRI and FDG-PET images	Variable	Multi-kernel learning	HC = 66, AD = 48, MCI = 119, Total = 233	87.60%	Hinrichs et al. (2011)
sMRI, FDG-PET and Florbetapir PET	AD/MCI	Mean volume of GM, SUVr value of FDG-PET and SUVr value of florbetapir PET for selected ROIs	90 per modality	Weighted multi-modality sparse representation-based classification	NC = 117, AD = 113, sMCI = 83, pMCI = 27, Total = 340	74.5–94.8%, MCI-Conv: 77.8%	Xu et al. (2015)
sMRI, FDG-PET, and CSF	AD/MCI	ROI-based GM, WM and CSF volumes from sMRI and average intensity from PET	189	SVM	HC = 52, AD = 51, ncMCI = 56, cMCI = 43, Total = 202	76.4–93.2%, MCI-Conv: 81.2%	Zhang et al. (2011)
sMRI, FDG-PET, and CSF data	AD/MCI	Volume of GM from sMRI and average intensity from PET of selected ROIs along with CSF measures	189	Graph-guided multi-task learning	NC = 52, AD = 50, MCI = 97, Total = 199	80.0–92.6%	Yu et al. (2015)
sMRI, FDG-PET, CSF and Genetics	MCI	ROI-based volumetric measures from sMRI, voxel-wise intensity measures from PET along with CSF and genetic features	>1E5	Random Forest	NC = 35, AD = 37, sMCI = 41, pMCI = 34, Total = 147	74.6–89.0%, MCI-Conv: 58.0%	Gray et al. (2013)
sMRI, FDG-PET, CSF, and APOE genotype	AD/MCI	ROI-based GMD maps, mean activity from PET	20 ROIs	Gaussian process classifier	HC = 73, AD = 63, ncMCI = 96, cMCI = 47, Total = 279	MCI-Conv: 74.1%	Young et al. (2013)
sMRI, PET, CSF and SNP	AD/MCI	GM volume and average intensity of ROIs along with CSF and SNP features	93 (sMRI, 93 (PET), 3 (CSF) and 5677 (SNP))	SVM	HC = 47, AD = 49, MCI = 93, Total = 189	71.0–94.8%	Zhang et al. (2014)
sMRI, rsfMRI and dMRI	AD	GM volume from sMRI, fiber tract integrity from dMRI and graph-theoretical measures from fMRI	N/A	SVM	HC = 25, AD = 28, Total = 53	74–85% (AUC)	Dyrba et al. (2015)

Table 3
Summary of 64 MRI-based schizophrenia classification studies. N/A indicates information was not available or could not be found.

Modality	Disorder	Features	# of features	Classifier	Number of subjects	Overall accuracy	Reference
dMRI	Schizophrenia	Discriminant PCA of FA maps	60	Fisher's linear discriminant	HC = 45, SZ = 45 Total = 90	80%	Caprihan et al. (2008)
dMRI	Schizophrenia	FA maps	13	LDA	HC = 24, SZ = 34 Total = 58	75%	Caan et al. (2006)
dMRI	Schizophrenia	Voxels of FA and MA maps reduced by PCA	11–13	LDA	HC = 50, SZ = 50 Total = 100	96%	Ardekani et al. (2011)
fMRI (sensorimotor, AOD, WMT tasks)	Schizophrenia	Mean activation of the largest activation cluster	1	Majority vote of 3 decision stumps	HC = 15, SZ = 13 Total = 28	96%	Honorio et al. (2012)
fMRI (AOD/Sternberg/sensorimotor tasks)	Schizophrenia	ICA spatial maps	10–14	Projection pursuit	HC = 91, SZ = 57 Total = 138	80–90%	Demirci et al. (2008a)
fMRI (AX-CPT task)	Schizophrenia (first-episode)	Voxels of left DLPFC in the contrast map	N/A	LDA	HC = 51, SZ = 51 Total = 102	62%	Yoon et al. (2012)
fMRI- (Monetary Incentive Delay task)	Schizophrenia	MVPA of task activation pattern (best result for right palladium)	N/A	Searchlight SVM	HC = 44, SZ = 44 Total = 88	93%	Koch et al. (2015)
fMRI (sensorimotor task) and SNP	Schizophrenia	Sparse representation based variable selection	200	Sparse representation based classifier	HC = 116, SZ = 92 Total = 208	77%	Cao et al. (2013)
fMRI (verbal fluency task)	Schizophrenia/bipolar	Thresholded voxels in activation map by ANOVA tests	N/A	SVM	HC = 40, SZ = 32, BP = 40 Total = 104	92%	Costafreda et al. (2011b)
fMRI (visual task)	Schizophrenia	Selected active voxels from the contrast map	346	MVPA	HC = 15, SZ = 19 Total = 34	59–72%	Yoon et al. (2008)
fMRI (WMT task)	Schizophrenia with and without OCD	MVPA on GLM contrast values	33	SVM	HC = 20, SZ (with OCD) = 16, SZ (without OCD) = 17, Total = 53	75–91%	Bleich-Cohen et al. (2014)
fMRI (AOD task)	Schizophrenia	ICA Spatial Maps of magnitude and phase data	135–243	Multiple kernel learning	HC = 21, SZ = 31 Total = 52	85%	Castro et al. (2014)
fMRI (AOD task)	Schizophrenia	ICA (temporal and DMN network) and GLM spatial maps parcellated into AAL atlas	116	Recursive composite kernels	HC = 54, SZ = 52 Total = 106	95%	Castro et al. (2011)
fMRI (AOD task)	Schizophrenia/bipolar	Distance to mean image for each group build using ICA spatial maps (DMN and temporal lobe)	3	Minimum distance	HC = 26, SZ = 21, BP = 14 Total = 61	83–95%	Calhoun et al. (2008)
fMRI (AOD task)	Schizophrenia/bipolar	ICA spatial maps (DMN and temporal lobe)	10	Bayesian generalized softmax perceptron	HC = 25, SZ = 21, BP = 14 Total = 60	82–90% (AUC)	Arribas et al. (2010)
rsfMRI	Schizophrenia	Functional connectivity among 116 regions in AAL atlas reduced by PCA	333	SVM	HC = 25, SZ = 24, Sibling HC = 22 Total = 71	62%	Yu et al. (2013b)
rsfMRI	Schizophrenia/MDD	FC among ROIs	6670	SVM	HC = 38, SZ = 32, MDD = 19, Total = 89	80.9%	Yu et al. (2013a)
rsfMRI	Schizophrenia	Functional connectivity among 347 nodes placed as a grid in the entire brain	3000	Fused Lasso, GraphNet	HC = 74, SZ = 71 Total = 145	91%	Watanabe et al. (2014)
rsfMRI	Schizophrenia	FALFF values of the left ITG	N/A	SVM	HC = 46, unaffected sibling of SZ patients = 46, Total = 92	75%	Guo et al. (2014b)
rsfMRI	Schizophrenia	FC among 90 ROIs	1096	Random forest	HC = 18, SZ = 18 Total = 36	75%	Venkataraman et al. (2012)
rsfMRI	Schizophrenia	FC among 90 regions in WFU atlas reduced by PCA	550	SVM	HC = 22, SZ = 22 Total = 44	93%	Tang et al. (2012)
rsfMRI	Schizophrenia	Functional connectivity (based on extended maximized mutual information) among 116 AAL regions	6670	SVM	HC = 32, SZ = 32 Total = 64	83%	Su et al. (2013)
rsfMRI	Schizophrenia	Dimension-reduced FC (local linear embedding) among AAL ROIs	12	C-means clustering	HC = 20, SZ = 32 Total = 52	86%	Shen et al. (2010)
rsfMRI	Schizophrenia	Functional connectivity among 116 regions in AAL atlas	6670	Deep neural network	HC = 50, SZ = 50 Total = 100	86%	Kim et al. (2015)
rsfMRI	Schizophrenia	Functional connectivity based on ICA decomposition	46	Regularized linear discriminant classifier	HC = 196, SZ = 71 Total = 267	75–84%	Kaufmann et al. (2015)
rsfMRI	Schizophrenia	Graph measures of functional connectivity	N/A	SVM	HC = 29, SZ = 19, Total = 48	80.0%	Cheng et al. (2015b)
rsfMRI	Schizophrenia	Local and global complex network measures	216	SVM	HC = 10, SZ = 8 Total = 18	100%	Fekete et al. (2013)
rsfMRI	Schizophrenia	Functional connectivity patterns	6–7 variable	Ensemble of SVM classifiers	HC = 31, SZ = 31 Total = 62	85–87%	Fan et al. (2011)
rsfMRI	Schizophrenia	Pearson correlation features derived from regional homogeneity, ALFF, FALFF	100	Ensemble of ELMs	HC = 74, SZ = 72 Total = 144	80–91%	Chyzyk et al. (2015)

Table 3 (continued)

Modality	Disorder	Features	# of features	Classifier	Number of subjects	Overall accuracy	Reference
rsfMRI	Schizophrenia	and voxel-mirrored homotopic connectivity Size of connected components in graphs build from correlation among time-courses for 90 AAL regions	N/A	SVM	HC = 29, SZ = 29 Total = 58	75%	Bassett et al. (2012)
rsfMRI	Schizophrenia	Functional network connectivity among 9 ICA time-courses	45	SVM (best result)	HC = 28, SZ = 28 Total = 56	96%	Arbabshirani et al. (2013)
rsfMRI	Schizophrenia	MVPA based on whole brain thalamic connectivity map	N/A	SVM	HC = 90, SZ = 90, Total = 180	73.9%	Anticevic et al. (2014)
rsfMRI	Schizophrenia	Graph metrics based on FNC computed from ICA	13	SVM	HC = 74, SZ = 72 Total = 146	65%	Anderson and Cohen (2013)
sMRI	Schizophrenia	Voxels from five regions based on optimally discriminative voxel-based morphometry	N/A	SVM	HC = 79, SZ = 69 Total = 148	71%	Zhang and Davatzikos (2013)
sMRI	Schizophrenia (first episode)	Whole brain volumetric measurements based on RAVENS	69	SVM	HC = 62, SZ = 62 Total = 124	73%	Zanetti et al. (2013)
sMRI	Schizophrenia (first-episode)	Volume and mean cortical thickness of selected ROIs	2.5	Discriminant function analysis	HC = 40, SZ = 52 Total = 92	80%	Takayanagi et al. (2011)
sMRI	Schizophrenia and psychosis	Cortical GMD	129	Sparse multinomial logistic regression classifier	HC = 36, SZ = 36 Total = 72	86%	Sun et al. (2009)
sMRI	Schizophrenia/bipolar	Voxel-wise GM maps	N/A	SVM	HC1 = 66, HC2 = 43, SZ1 = 66, SZ2 = 46, BP1 = 66, BP2 = 47 Total1 = 198, Total2 = 136	67–90%	Schnack et al. (2014)
sMRI	Schizophrenia	Texture and volumetric measures	N/A	LDA	HC = 24, SZ = 27, Total = 51	65.0–72.7%	Radulescu et al. (2014)
sMRI	Schizophrenia	Clinical, neuropsychological, biochemical and volumetric measures	1050	SVM	HC = 42, SSD = 36, Non-SSD = 45, Total = 123	81.0–99.0%	Pina-Camacho et al. (2015)
sMRI	Schizophrenia/bipolar	Volume of 23 ROIs along with 22 neuropsychological test scores	45	LDA	HC = 8, SZ = 10, BP = 10 Total = 28	96%	Pardo et al. (2006)
sMRI	Schizophrenia	GM and CSF volumetric measures of ROIs	4	LDA	HC = 105, HC2 = 23, SZ1 = 38, SZ2 = 23, Total = 189	70–76%	Ota et al. (2012)
sMRI	Schizophrenia	Gray matter densities based on voxel-based morphometry of top 10% voxels	15,700	SVM	HC1 = 111, HC2 = 122, SZ1 = 128, SZ2 = 155 Total1 = 239, Total2 = 277	71%	Nieuwenhuis et al. (2012)
sMRI	Schizophrenia	Volume of several ROIs in the brain	7	LDA	HC = 47, SZ = 57 Total = 104	78–86%	Nakamura et al. (2004)
sMRI	Schizophrenia/mood disorder	GM maps of regional analysis of brain volumes in normalized space (RAVENS)	170	SVM-RFE	Mood disorder = 104, SZ = 158 Total = 262	76%	Koutsouleris et al. (2015)
sMRI	Schizophrenia	The mean expression of eigen image derived from voxel-based morphometry	1	Simple Thresholding	HC = 46, SZ = 46 Total = 92	80–90%	Kawasaki et al. (2007)
sMRI	Schizophrenia (first-episode)	Whole brain voxel intensity values	N/A (probably thousands)	Maximum-uncertainty LDA	HC = 39, SZ = 39 Total = 78	72%	Kasperek et al. (2011)
sMRI	Recent onset Schizophrenia	Volumetric measurements of 95 ROIs	5	LDA	HC = 47, SZ = 28 Total = 75	72%	Karageorgiou et al. (2011)
sMRI	Schizophrenia	MR intensities, gray matter densities and deformation based morphometry	96 per feature category	Combination of mMLDA, centroid method, and the average linkage SVM	HC = 49, SZ = 49, Total = 98	81.6%	Janousova et al. (2015)
sMRI	Schizophrenia	GM and WM maps	N/A	SVM	HC = 20, SZ = 19, Total = 39	66.6–77%	Iwabuchi et al. (2013)
sMRI	Schizophrenia (identifying subtypes)	Multi-edge graphs build from Structural connectivity networks with 78 ROIs	N/A	Spectral clustering	HC = 29, SZ = 23 Total = 52	78%	Ingalhalikar et al. (2012)
sMRI	Schizophrenia (childhood onset)	Cortical thickness	74	Random Forrest	HC = 99, SZ = 98 Total = 197	74%	Greenstein et al. (2012)
sMRI	Schizophrenia (cognitive deficit and cognitive spared)	Whole brain voxel-based morphometry	N/A	SVM	HC = 163, SZ = 208, SZA = 41, Total = 412	56–72%	Gould et al. (2014)

(continued on next page)

Table 3 (continued)

Modality	Disorder	Features	# of features	Classifier	Number of subjects	Overall accuracy	Reference
sMRI	Schizophrenia	Volumetric measurements based on deformation-based morphometry	39/44	SVM	HC1 = 38, HC2 = 41, SZ1 = 23, SZ2 = 46 Total1 = 61, Total2 = 87	91%	Fan et al. (2007)
sMRI	Schizophrenia	Volumetric measures of all WM, GM and CSF	69	SVM-RFE	HC = 38, SZ = 23 Total = 61	92%	Fan et al. (2005)
sMRI	Schizophrenia	Whole brain volumetric measurements	N/A	Nonlinear classifier (not specified)	HC = 79, SZ = 69 Total = 148	81%	Davatzikos et al. (2005)
sMRI	Schizophrenia	Hippocampal and thalamic shape eigenvectors	25	Discriminant function analysis	HC = 65, SZ = 52 Total = 117	79%	Csernansky et al. (2004)
sMRI	Schizophrenia	Visual words extracted from DLPFC by SIFT and clustered by k-means	30	SVM with local kernel	HC = 54, SZ = 54 Total = 108	66–75%	Castellani et al. (2012)
sMRI	Schizophrenia	Surface morphological measures	N/A	Semi-supervised (hierarchical clustering)	HC = 40, SZ = 65, Total = 105	94.0%	Bansal et al. (2012)
sMRI and dMRI	Schizophrenia/MDD	Volume and FA of insula, thalamus, ACC, ventricles and corpus callosum	31	LDA	MDD = 25, SZ = 25 Total = 50	72–88%	Ota et al. (2013)
fMRI (AOD task) and rsfMRI	Schizophrenia	Kernel PCA on ICA spatial maps	53	Fisher's linear discriminant	HC = 28, SZ = 28 Total = 56	93–98%	Du et al. (2012)
fMRI (AOD task) and rsfMRI	Schizophrenia	FNC scores derived from ICA-based multi-network fusion template for functional normalization	3 and 100	LDA and shapelet based classifier	HC = 28, SZ = 27 Total = 55	72%	Çetin et al. (2015)
fMRI (AOD task) and SNP	Schizophrenia	Three types of features: selected voxels in fMRI activation map, selected SNPs and ICA components	261 voxels + 150 SNPs	Majority voting among 3 SVMs	HC = 20, SZ = 20 Total = 40	87%	Yang et al. (2010)
sMRI, rsfMRI and dMRI	Schizophrenia	Gray matter densities from structural, FA from DTI and ALFF from fMRI	1863	SVM	HC = 28, SZ = 35 Total = 63	79%	Sui et al. (2013b)

communicative behaviors used for social interaction and stereotypic behavior (Association et al., 2003). Although the causation of autism is still largely unknown, it has been suggested that genetic, developmental, and environmental factors could be involved alone or in combination as possible causal or predisposing effects toward developing autism (Minshew and Payton, 1988; Wing, 1997). ASD has an estimated prevalence of 1:68 in the US (Baio, 2012). We surveyed 20 papers in automatic diagnosis of ASD using MRI-based features. Those studies are listed in Table 5.

Attention deficit hyperactivity disorder

Attention deficit hyperactivity disorder (ADHD) is one of the most commonly found functional disorders affecting children. Approximately 3–10% of school aged children are diagnosed with ADHD (Biederman, 2005; Dey et al., 2012). Currently, no biological-based measure exists to detect ADHD and instead, behavioral symptoms are investigated to identify it. Despite all the research efforts, the root cause of ADHD is still unknown. In 2011, a global competition (called ADHD-200) was held in order to use neuroimaging as well as phenotypic measures to automatically detect ADHD (Consortium et al., 2012). Most of the studies reviewed in this survey were responses to that challenge. The main characteristics of those studies are tabulated in Table 6.

Analysis of the survey

In Fig. 3 we illustrate a couple of key aspects of this survey. Fig. 3A shows the number of papers published in each year for each disease type. The number of studies has been growing significantly since 2007. There is a peak for ADHD studies in 2012–2013 mainly due to ADHD-200 competition (Consortium et al., 2012) which attracted

many scientists. The total number of studies for each modality and each disorder is illustrated in Fig. 3B. It is clear that structural MRI is the most popular modality especially for MCI/AD studies thanks to Alzheimer's disease neuroimaging initiative (ADNI) dataset. Combined rest and task fMRI studies are most popular for ADHD and schizophrenia studies. Surprisingly, multimodal studies are more common compared to either task fMRI or diffusion MRI studies. Fig. 3C shows the overall accuracy against the total sample size used in the studies. Interestingly, almost all studies that reported very high accuracies, had sample sizes smaller than 100. The reported overall accuracy decreases with sample size in most of disorders such as schizophrenia and ADHD. This pattern raises a serious concern regarding generalizability of many of those studies with small sample sizes. Fig. 3D shows the sample size distribution. The dashed lines represent mean (red) and median (blue) sizes, which are 186 and 88 respectively. Finally, Fig. 3E illustrate the distribution and summary statistics of reported overall accuracy for each disorder along with the distribution of accuracies reported for classification of pMCI from sMCI (16 studies). On average (red diamonds) MCI/AD studies (usually against a healthy group) reported the highest accuracies and sMCI versus pMCI studies reported the lowest accuracies.

Based on Tables 2–6, the most common extracted features in the surveyed studies are volume and cortical thickness from structural MRI, the activation maps and functional connectivity among ROIs or ICA components from fMRI data and fractional anisotropy from dMRI data. Most common feature reduction methods (not reported in the tables) were based on PCA or univariate statistical tests.

In terms of classification methods, support vector machine (SVM) was by far the most popular method. Different flavors of SVM such as linear, non-linear with different kernel, SVM with recursive feature elimination, SVM with L1 regularization and SVM with L1 and L2 regularization (elastic net) have been used for classification of various

Table 4

Summary of 19 MRI-based depressive disorder classification studies. N/A indicates information was not available or could not be found.

Modality	Disorder	Features	# of features	Classifier	Number of subjects	Overall accuracy	Reference
dMRI	MDD	Whole-brain anatomical connectivity patterns	50	SVM	HC = 26, MDD = 22, Total = 48	91.7%	Fang et al. (2012)
fMRI (facial affect recognition task)	MDD	Brain activation maps and ROI-averaged activation features	N/A	One-class SVM	HC = 19, Depressed = 19, Total = 38	63–65.5% (estimated)	Mourão-Miranda et al. (2011)
fMRI (gender discrimination and emotional tasks)	MDD	Sparse network-based features of FC	9316	SVM	HC = 19, MDD = 19, Total = 38	78.9–85.0%	Rosa et al. (2015)
fMRI (social concept task)	MDD	GM maps of PPI analysis	N/A	Maximum entropy LDA	HC = 21, MDD = 25, Total = 46	78.1% (AUC)	Sato et al. (2015)
fMRI (verbal fluency task)	MDD	Voxel-wise contrast map	14,055	Regularized logistic regression, SVM (best performance)	HC = 31, MDD = 31, Total = 62	90.0–95.0%	Shimizu et al. (2015)
rsfMRI	MDD	FC maps of sACC	N/A	Label generation maximum margin clustering	HC = 29, MDD = 24, Total = 53	92.5%	Zeng et al. (2014)
rsfMRI	MDD	Hurst components of resting-state networks	12	SVM	HC = 20, MDD = 20, Total = 40	90%	Wei et al. (2013)
rsfMRI	MDD	Network-based measures based on FC among ROIs	2–25	SVM	HC = 22, MDD = 21, Total = 43	99%	Lord et al. (2012)
rsfMRI	MDD	FC among AAL regions	31	SVM	HC = 37, MDD = 39, Total = 76	76.6%	Cao et al. (2014)
rsfMRI	First-onset depressive disorder	Graph-theory measures	30	ANN	HC = 27, first-onset depression = 36, Total = 63	90.5%	Guo et al. (2014a)
rsfMRI	Subthreshold depression	ReHo features of ROIs	8 ROIs	Fisher stepwise discriminant analysis	NC = 19, StD = 19, Total = 37	91.9%	Ma et al. (2013)
sMRI	MDD/BP	GM, WM and ventricles volumetric maps (RAVENS)	53–99	SVM	HC1 = 33, HC2 = 38, MDD = 19, BP = 23, Total = 113	54.6–66.1%	Serpa et al. (2014)
sMRI	MDD/BP	Gray matter volumes of caudate and ventral diencephalon	4	SVM	HC = 61, BP = 40, MDD = 57, RMD = 35, Total = 193	59.5–62.7%	Sacchet et al. (2015)
sMRI	MDD/BP	Volumetric measurements	5	Discriminant function analysis	HC = 22, MDD = 32, BP = 14, Total = 68	81.0%	MacMaster et al. (2014)
sMRI	MDD/BP	Cortical thickness and surface area	18	SVM	HC = 29, MDD = 19, BP = 16	74.3%	Fung et al. (2015)
sMRI	MDD	Feature-based morphometric measures of GM maps	N/A	SVM and RVM	HC = 32, MDD = 30, Total = 62	90.3%	Mwangi et al. (2012)
sMRI	MDD	GM and WM densities	N/A	SVM	HC = 42, RDD = 23, NDD = 23, Total = 88	58.7–84.6%	Gong et al. (2011)
sMRI	MDD	Cortical thickness of several ROIs	68	SVM	HC = 15, MDD = 18, Total = 33	70%	Foland-Ross et al. (2015)
sMRI, rsfMRI and dMRI	LLD	Variety of features from each modality	13 feature sets	Alternating decision trees	EC = 35, LLD = 33, Total = 68	87.3%	Patel et al. (2015)

disorders. Linear discriminant analysis (under different names) and logistic regression were also popular classification methods among the surveyed studies.

Predicting continuous measures

Most of the studies surveyed above, conducted the diagnosis of a disorder (i.e., assigning a categorical label to each subject) using classification techniques. Pattern regression considers the problem of estimating continuous rather than categorical variables, which can be more challenging as compared to classification. Clinically, pattern regression can be used to estimate the disease stage and progression. Therefore, there is a growing interest in estimating continuous variables such as cognitive scores for brain disorders using neuroimaging measurements. We didn't survey those papers, but we will point out to some of those studies in this section.

Wang et al. proposed a general methodology for estimating continuous clinical variables from high-dimensional imaging data (Wang et al., 2010). Sato et al. used interregional cortical thickness measurements to estimate Autism Diagnostic Observation Schedule (ADOS) score in ASD patients (Sato et al., 2013). Stonnington et al. used relevance vector regression (RVR) to predict number of cognitive scores such as Dementia Rating Scale (DRS) and Alzheimer's Disease

Assessment Scale (ADAS) based on structural MRI measures (Stonnington et al., 2010). Tognin et al. used RVR to predict Positive and Negative Syndrome Scale (PANSS) scores of subjects at high risk of psychosis based on gray matter volume and cortical thickness measurements (Tognin et al., 2013). Yue et al. showed relationship between functional connectivity and neuropsychological assessment scores such as Rey–Osterrieth Complex Figure Test (CFT) in amnesic MCI patients (Yue et al., 2015). Zhang et al. used MRI, PET and CSF data to predict Mini Mental State Examination (MMSE) and ADAS scores in MCI and AD patients (Zhang and Shen, 2012a).

Detecting/characterizing at risk healthy subjects

The majority of studies surveyed above tried to automatically diagnose one or more disorders in patients. However, detecting or characterizing healthy individuals who are at high risk of brain disorders could potentially delay or prevent future symptoms. There has been a lot of such studies using genetics information but detecting or characterizing at risk subjects based on neuroimaging data is rare. Mourão-Miranda et al. used functional MRI to detect subjects at high risk of mood disorders (Mourão-Miranda et al., 2012). Guo et al. characterized activity of default-mode network in unaffected siblings of schizophrenia patients using resting-state functional data (Guo et al., 2014b). In another

Table 5

Summary of 20 MRI-based ASD classification studies. N/A indicates information was not available or could not be found.

Modality	Disorder	Features	# of features	Classifier	Number of subjects	Overall accuracy	Reference
dMRI	ASD	FA and MD of selected ROIs	18	SVM	TDC = 30, ASD = 45, Total = 75	80%	Ingalhalikar et al. (2011)
fMRI (social interaction task)	ASD	Activation of selected voxels processed by factor analysis	4 factors	Gaussian naïve Bayes	HC = 17, TDC = 17, Total = 34	97%	Just et al. (2014)
fMRI (two language tasks and a Theory-of-Mind task)	ASD	AG, MPFC and PCC based FC maps	N/A	Logistic regression	TD = 14, ASD = 13, Total = 27	96.0%	Murdaugh et al. (2012)
rsfMRI	ASD	ICA components of rsfMRI	10 components	Logistic regression	TDC = 20, ASD = 20, Total = 40	78.0%	Uddin et al. (2013)
rsfMRI	ASD	FC among ROIs	Variable	Logistic regression and SVM (best results)	TD1 = 59, TD2 = 89, ASD1 = 59, ASD2 = 89, Total = 296	76.7%	Plitt et al. (2015)
rsfMRI	ASD	FC among 90 ROIs	4005	Probabilistic neural network	TDC = 328, ASD = 312, Total = 640	90%	Iidaka (2015)
rsfMRI	ASD	Functional connectivity among 220 ROIs	24,090	Random forest	TDC = 126, ASD = 126, Total = 252	91%	Chen et al. (2015)
rsfMRI	ASD	FC among ROIs	26,393,745	Thresholding	TD = 40, ASD = 40, Total = 80	79.0%	Anderson et al. (2011)
sMRI	ASD	Thickness and volumetric of ROIs along with interregional features	N/A	Multi-kernel SVM	HC = 59, ASD = 58, Total = 117	96.3%	Wee et al. (2014)
sMRI	ASD	Voxel-wise GM and WM maps	N/A	SVM	TD = 24, ASD = 24, Total = 48	92.0%	Uddin et al. (2011)
sMRI	ASD	GM volume map	N/A	SVM	HC = 40, ASD = 52, ASD-Sib = 40	80.0–85.0%	Segovia et al. (2014)
sMRI	ASD	Regional thickness measurements extracted from SBM	7	Logistic model trees	HC = 16, ASD = 22, Total = 38	87%	Jiao et al. (2010)
sMRI	ASD	Morphometric features of selected ROIs	314	SVM	HC = 20, ASD = 21, Total = 41	74% (AUC)	Gori et al. (2015)
sMRI	ASD	GM and WM maps	>10,000	SVM	HC = 22, ASD = 22, Total = 44	77%	Ecker et al. (2010b)
sMRI	ASD	Volumetric and geometric features of selected cortical locations	5 features from each ROI	SVM	HC = 20, ASD = 20, Total=40	85%	Ecker et al. (2010a)
sMRI	ASD	Gray maps from VBM-DARTEL	200	SVM	TDC = 38, ASD = 30, Total = 76	80.0% (AUC)	Calderoni et al. (2012)
sMRI	ASD	Volumetric measures and cerebellar vermis area	9	Discriminant function analysis	TDC = 15, ASD = 52, Total = 67	92.3–95.8%	Akshoomoff et al. (2004)
fMRI-Task and dMRI	ASD	Causal connectivity weights, FC values and FA values	19	SVM	TDC = 15, ASD = 15, Total = 30	95.9%	Deshpande et al. (2013)
sMRI, dMRI and MRS	ASD	Cortical thickness, FA and neurochemical concentration	3	Decision tree	TD = 18, ASD = 19, Total = 37	91.9%	Libero et al. (2015)
sMRI and rsfMRI	ASD	Volume of selected subcortical regions, fALFF, number of voxels and Z-values of selected regions and global VMHC voxel number	22	Random tree classifier	TDC = 153, ASD = 127, Total = 280	70.0%	Zhou et al. (2014)

study, Fan et al. studied structural endophenotypes in unaffected family members of schizophrenia patients using machine learning methods (Fan et al., 2008a).

Semi-supervised studies

The main focus of this work is on supervised studies. However, in the cases that collecting data is difficult and costly, semi-supervised learning might help. This method uses both labeled and unlabeled data for building the predictive model. For example, predicting MCI patients that convert to AD (sMCI vs. pMCI) requires following up with the subjects for a long time which makes the data collection cumbersome. One remedy is to use labeled AD and healthy data to build a model for predicting labels for MCI subjects. A few studies have utilized this strategy and achieved accuracies comparable or even better than those obtained from fully supervised learning (Batmanghelich et al., 2012; Filipovych et al., 2011; Moradi et al., 2015; Zhang and Shen, 2012b).

Common machine-learning pitfalls in neuroimaging

In this section, common pitfalls among the surveyed papers are discussed.

Feature selection bias

Most of the papers we surveyed consisted of two consecutive parts: group difference analysis and classification. Usually, statistical tests such as t-tests are used to show group differences on a set of extracted features in the first part of the study, which is followed by a classification approach to assess the discrimination ability of those features on a single subject basis. Unfortunately, it is not rare to see that the results of first part (group differences) are used to select features for the classification part. In general, any use of test samples in any part of the training (such as feature extraction, feature selection and classifier training) poses a bias. Selecting features for classification based on the results of group tests that were conducted on the whole dataset is a form of double dipping and therefore leads to a biased (inflated) result (Bishop, 2006; Demirci et al., 2008b).

This form of feature selection also has another major problem. The significance of group statistical tests, which are the basis of feature selection in some of the studies, is mostly based on p-values. However, the relationship between p-value and discrimination power is not straightforward. Fig. 1 shows the p-value of a two-sample t-test as well as overall accuracy based on one or two thresholds in three different scenarios. It is seen that low p-value doesn't necessary mean a strong feature (Fig. 1A) and high p-value doesn't mean a weak feature

Table 6

Summary of 22 MRI-based ADHD classification studies. N/A indicates information was not available or could not be found.

Modality	Disorder	Features	# of features	Classifier	Number of subjects	Overall accuracy	Reference
fMRI (Stop Task)	ADHD	Whole brain GLM coefficient map	21,658	Gaussian process classifier	HC = 30, ADHD = 30, Total = 60	77%	Hart et al. (2014a)
fMRI (Six Tasks)	ADHD	Network measures based on FC values	N/A	SVM	ADHD-IA = 13, ADHD-C = 21, Total = 34	91.2%	Park et al. (2015)
fMRI (temporal discrimination task)	ADHD	Brain activation map	N/A	Gaussian process	HC = 20, ADHD = 20, Total = 40	75.0%	Hart et al. (2014b)
rsfMRI	ADHD	ReHo maps	N/A	PCA-based Fisher discriminative analysis	HC = 12, ADHD = 12, Total = 24	85.0%	Zhu et al. (2008)
rsfMRI	ADHD	ReHo maps	6500	SVM	HC = 23, ADHD = 23, Total = 46	80.0%	Wang et al. (2013)
rsfMRI	ADHD	FFT and different variation of PCA on the BOLD signals along with phenotypic measures	About 7000	SVM	HC = 429, ADHD-I = 98, ADHD-C = 141, Total = 668	68.86–76%	Sidhu et al. (2012)
rsfMRI	ADHD	ReHo, ALLF and RSN	400 for each feature type	Logistic regression (best performance)	HC = 546, ADHD-IA = 122, ADHD-HI = 12, ADHD-C = 249, Total = 929	54% ADHD Subtype: 67%	Sato et al. (2012)
rsfMRI	ADHD	Graph based features based on FC	150	SVM-based MVPA	TDC = 455, ADHD-I = 80, ADHD-C = 112, Total = 647	63.4–82.7%	Fair et al. (2012)
rsfMRI	ADHD	Graph-based measures compressed by multi-dimensional scaling	2	SVM	HC = 307, ADHD = 180, Total = 487	73.5%	Dey et al. (2014)
rsfMRI	ADHD	Directional connectivity measures	200	Artificial neural network	TDC = 744, ADHD = 433, Total = 1177	90%	Deshpande et al. (2015)
sMRI	ADHD/ Dyslexia	Morphometric measures of ROIs	6	Discriminant function analysis	HC = 10, ADHD = 10, Dyslexia = 10, Total = 30	60.0–87%	Semrud-Clikeman et al. (1996)
sMRI	ADHD	Cortical thickness measures	340	ELM	HC = 55, ADHD = 55, Total = 110	90.2%	Peng et al. (2013)
sMRI	ADHD	Voxel-wise GM volumetric measures	N/A	Gaussian process classifier	HC = 19, ASD = 19, ADHD = 20, Total = 58	68.2–85.2%	Lim et al. (2013)
sMRI	ADHD	WM maps	N/A	SVM	HC = 34, ADHD = 34, Total = 68	93%	Johnston et al. (2014)
sMRI	ADHD	Caudate nucleus volumetric measures	N/A	Adaboost and SVM	HC = 39, ADHD = 39, Total = 78	72.5%	Igual et al. (2012)
sMRI	ADHD	Texture features based on isotropic local binary patterns on three orthogonal planes	117–33,630	SVM	HC = 226, ADHD = 210, Total = 436	69.9%	Chang et al. (2012)
sMRI	ADHD	Surface morphometric measures	N/A	Semi-supervised (hierarchical clustering)	HC = 42, ADHD = 41, Total = 83	91.0%	Bansal et al. (2012)
sMRI, rsfMRI and phenotypic data	ADHD	Curvature index, folding index, Gaussian curvature, gray matter volume, mean curvature, surface area, thickness average, and thickness standard deviation along with functional connectivity measures and phenotypic data	20	NMF + decision tree	TD = 472, ADHD = 276, Total = 748	66.8%	Anderson et al. (2014)
sMRI and rsfMRI	ADHD	Various anatomical, network and non-imaging measures	5–6000	SVM	TDC = 491, ADHD = 285, Total = 776	80.0% (AUC)	Bohland et al. (2012)
sMRI and fMRI-task (Flanker/NoGo)	ADHD	Whole brain GLM coefficients and GM maps from VBM	N/A	SVM	HC = 18, ADHD = 18, Total = 36	61.1–77.8%	Iannaccone et al. (2015)
sMRI and rsfMRI	ADHD	Cortical thickness and GM maps from sMRI and ReHo and FC from rsfMRI	N/A	SVM and multi-kernel learning	TCD = 402, ADHD = 222, Total = 624	61.5%	Dai et al. (2012a)
sMRI and rsfMRI	ADHD	Morphological measures, FC, power spectra and graph measures	Variable (>100)	Multiple SVM	TD = 491, ADHD = 285, Total = 776	55%	Colby et al. (2012)

(Fig. 1B). However, if the abnormality is one-directional, then a very low p-value might translate to high classification accuracy (Fig. 1C). So, by discarding features just based on the result of statistical tests sensitive to group mean, valuable discriminatory information could be lost.

Instead of feature selection based on univariate group-level statistical tests, more common filtering and wrapper methods should be used (Blum and Langley, 1997; Hall and Smith, 1998; Kohavi and John, 1997). Filtering methods assign scores to each feature from which a number of top ones can be selected. A good filtering method should be sensitive to the discriminative power of the features. Most of these methods are univariate and therefore each feature is treated independently from other features. Filtering methods have the advantage of low

computational cost, but their main drawback is ignoring the relationship among features.

Wrapper methods, on the other hand, consider selection of a set of feature as a search problem. Different combinations are evaluated and finally the best set of features is selected. A popular wrapper method is the recursive feature elimination (RFE) algorithm (Guyon et al., 2002). Wrapper methods are computationally much more expensive than filtering methods, but can result in superior performance by considering interaction among features.

There are methods that aim at combining both filtering and wrapper methods. Minimum-redundancy maximum relevancy (mRMR) is one the methods popular for genetic feature selection. MRMR tries to select features with maximum mutual information with class labels while

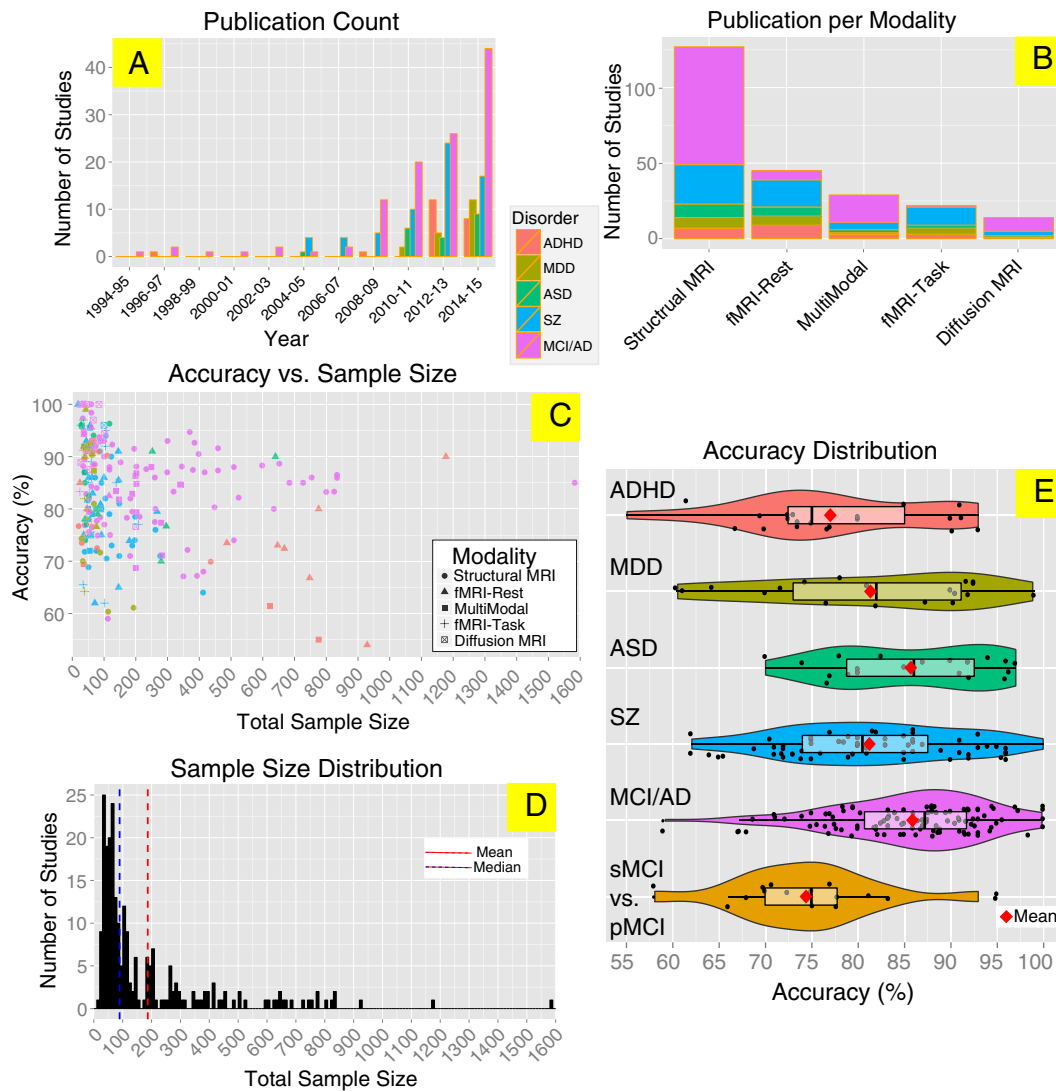


Fig. 3. Visual summary of Table 2–6. A: Total number of papers for two-year intervals for each modality. The legend shows the color code for each disorder. This legend also applies to parts B and C. B: Number of publications per modality for each disorder. C: Scatter plot of overall reported accuracy versus the total sample size. D: Histogram of the sample sizes of the surveyed studies. Vertical dashed lines indicate mean (red) and median (blue) sample size among all studies, which are 186 and 88 respectively. E: Disorder specific violin plots of reported overall accuracies of the surveyed papers with embedded boxplots and data points (each black dot corresponds to a study). This part also includes the accuracies of sMCI vs. pMCI studies. Red diamonds indicate the mean accuracy.

minimizing the mutual information among those features (Brown et al., 2012a).

Finally, there are embedded feature selection methods (Guyon and Elisseeff, 2003). These methods combine classification and feature selection into one unified step. Embedded methods learn the features that contribute the most to the accuracy of the model during the training phase. One of the common categories of the embedded methods is using regularization to enforce the learning algorithm to find more parsimonious models with lower complexity and therefore with fewer parameters. A post training analysis of the model coefficients, determines the selected features. Examples of regularization algorithms used in embedded feature selection methods are LASSO, elastic net and ridge regression (Hastie et al., 2004; Ng, 2004; Park and Hastie, 2007; Zou and Hastie, 2005).

Overfitting

Overfitting happens when a model describes noise in the data rather than the underlying pattern of interest. Overfitting results in very good

performance on the observed data and very poor performance on unseen data. Using models that are very complex or have many parameters on datasets with small number of samples and large number of features are more susceptible to overfitting. Neuroimaging datasets have limited number of samples and millions of voxels per sample. Based on Fig. 3D, the majority of surveyed studies built predictive models based on a very small number of subjects. It is evident from Fig. 3C that overall reported accuracy decreases with sample size in our survey. Therefore, it is plausible that many surveyed studies suffer from overfitting problem. It should be noted that by definition, overfitted models work well on the training data and poor on the test data. However, if the process of training and testing is repeated (by varying the model parameters) until a desirable performance on the test data is achieved, the model will likely overfit both the train and test datasets and will not generalize to an unseen dataset. Cross validation and regularization are common methods to control for overfitting. As mentioned earlier, more complex models have a greater chance of overfitting the data. For example, non-linear SVM is more powerful compared to linear SVM but has more hyperparameters and therefore

Confusion Matrix

		True Label	
		Condition Positive	Condition Negative
Predicted Label	Predicted Positive	True Positive (TP)	False Positive (FP)
	Predicted Negative	False Negative (FN)	True Negative (TN)

Performance Measures

Sensitivity (Recall) = $TP / (TP + FN)$

Specificity = $TN / (TN + FP)$

Precision = $TP / (TP + FP)$

Accuracy = $(TP + TN) / (TP + TN + FN + FP)$

F1 = $2TP / (2TP + FP + FN)$

Fig. 4. Confusion matrix and common performance measures for binary classification. Measures such as sensitivity, specificity, precision, accuracy and F1 score are easily computable based on the four elements of the confusion matrix.

is also potentially more capable of explaining noise in the data. As discussed in the previous section, proper feature selection can also help avoiding overfitting.

Reporting classification results

The result of classification is basically a confusion table/matrix also known as a contingency table. The confusion matrix summarizes the results in a table layout where each column represents the predicted class and each row represents the actual class. Confusion matrix is $m \times m$ where m represents the number of classes. In the case of binary classification, several statistical measures can be computed from the 2×2 confusion matrix, such as sensitivity (or recall), specificity, positive predictive value (or precision), negative predictive value, F1 score, odds ratio, kappa and false negative rate. Confusion matrix and some of the performance measures are shown in Fig. 4. In order to understand the performance of a classifier, it is important to report at least sensitivity/specificity or precision/recall along with the overall accuracy. We highly encourage reporting the confusion matrix itself as well. Some of the studies in this review just reported the overall accuracy, which can be very uninformative especially when classes have unequal sample sizes (Alberg et al., 2004). Suppose there are 20 patients and 80 controls in a test dataset. Reporting 80% accuracy is completely uninformative since the classification of all subjects as healthy could also result in 80% (one of the scenarios). This problem is easily detectable by looking at the confusion matrix or sensitivity and specificity measures. In unbalanced sample size cases, balanced specificity and sensitivity is more desirable than higher overall accuracy; therefore, measures such as F1 score (harmonic mean of precision and recall) are preferred for evaluating the classifier. The other very common way of reporting results for a binary classifier is by plotting “receiver operating characteristic” (ROC) curve. The ROC curve is the plot of sensitivity against “1-specificity” by changing the discrimination threshold and therefore provides a complete picture of classifier’s performance. The ROC curve is usually

summarized by the area under the curve (AUC), which is a number between 0 and 1.

The other common reporting issue is unjustified comparison of the achieved overall accuracy with the random chance. This issue is critical in this field due to small sample sizes. For example, an 80% achieved overall accuracy might not be significantly different from a 50% random chance in a statistical sense in a two-class problem if the sample size is too small. Any achieved accuracy in a test sample is just one estimate of the population accuracy. Like any other statistics, a confidence interval can be computed for that measure. In the case of a two-class problem, a binomial confidence interval can be computed for overall accuracy that serves as the basis for comparison with random chance, or any other accuracy. In our example (80% accuracy), if the test sample size is 10, then the 95% exact binomial confidence interval would be [0.444 0.975], which includes the random chance probability (0.50) and therefore is not statistically above chance (significance level of 0.05). Calculating this interval is straightforward using most of statistical and technical computing software such as R and Matlab. This approach should be employed when repeating the classification experiment for number of times is not feasible. However, in most cases, the null distribution of chance is empirically computable by randomly assigning labels to test samples and repeating classification for a number of times. This method, known as a permutation or randomization test, makes it possible to calculate the desired confidence interval of the chance, which consequently could be compared against the achieved classification accuracy using the correct labels (Collingridge, 2013; Fisher et al., 1960; Good, 2006; Mehta et al., 1988). Recently, for special cases such as SVM, fast analytical estimation of permutation testing has been proposed (Gaonkar and Davatzikos, 2013). Also, it has been shown that p-value for permutation testing can be written in the form of an infinite series whose terms are efficiently computable (Gill, 2007).

Comparison of accuracies across studies

It was frequently observed that authors claim that their proposed classification framework outperformed some other studies (and sometimes all other studies) just on the basis of overall accuracy. Considering the number of variables in each study—such as sample size, scanner parameters, sample age distribution, patients’ status (e.g., severity, medication), modality, length, type and design of study (for fMRI studies), preprocessing parameters, number and type of extracted features and type of classifier—such a comparison is essentially meaningless. Even in the case of standard neuroimaging datasets, the statistical comparison discussed in the previous section, should be employed to compare the results.

Hyperparameter optimization

Hyperparameter optimization or model selection is choosing a set of parameters for the learning algorithm in order to maximize the performance of the algorithm. Hyperparameters should be chosen during training, usually via an inner loop cross validation inside the training data. SVM, which is one of the most popular classifiers in this review and in neuroimaging in general (Orrù et al., 2012), has at least one hyperparameter (linear SVM) called soft margin. In addition to soft margin, non-linear SVM has one or more hyperparameters depending on the kernel (e.g. sigma/gamma for RBF kernel and degree for polynomial kernel). Some of the studies that we reviewed just used the default values for these parameters. A lack of parameter optimization can degrade the classification performance significantly. To show this, a toy example is illustrated in Fig. 5. SVM with three different kernels is used to classify this simulated two-class problem. In the top row, 1.0 is chosen for soft margin hyperparameter (which is the default of most machine learning software packages) for all kernels, degree of 3 was chosen for the polynomial kernel and gamma of 0.01 was selected

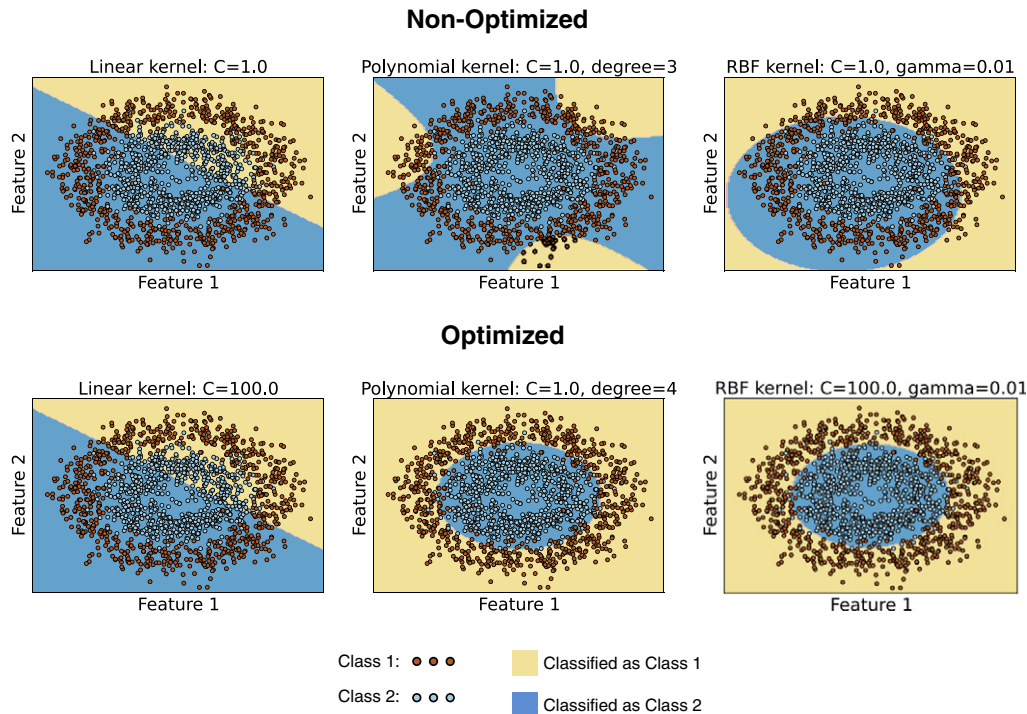


Fig. 5. An example to show the effect of SVM hyperparameter optimization on classification accuracy for linear, polynomial and RBF kernels. Top row: un-optimized, bottom row: optimized. Since the underlying pattern is non-linear, SVM with linear kernel fails to perform well in both scenarios. Performance of SVM with both polynomial and RBF kernels significantly improve when the parameters are optimized.

for RBF kernel. In the second row, the hyperparameters are optimized. First, it is evident that the linear kernel failed to learn the non-linear pattern under both settings. Increasing the polynomial kernel degree by one, dramatically improved the classifier. Also, increased soft margin value, significantly improved SVM with RBF kernel. So, both the choice of kernel and hyperparameters are crucial for building a successful SVM-based classifier. SVM hyperparameters are usually selected based on a grid search over plausible values.

Machine learning in neuroimaging: shortcomings and emerging trends

Machine learning has more than two decades of history in neuroimaging and despite all of the promising results of numerous studies, it is still immature and not ready for integration into clinical healthcare. In this section, we review some of the challenges and emerging solutions.

Sample size in neuroimaging studies

The most limiting factor in this field is by far the limited sample size issue. As summarized in Fig. 3B, the majority of studies in this review and in general have sample size of less than 150. This sample size is miniscule in comparison with other fields in which machine learning is used. As an example, ImageNet,² which is commonly used as standard computer vision dataset, has over one million samples and 1000 classes. As a result of such big datasets, dramatic improvement has been achieved in the field of computer vision in the past few years. However, sample size limitations in neuroimaging pose several problems. First, the classifier performance is directly affected by the sample size. It is shown that large training data sets increase classification accuracy (Franke et al., 2010; Klöppel et al., 2009). Small sample size does not represent the patient population and therefore promising results

may not generalize to other patient groups. In a study conducted by Nieuwenhuis et al., it was shown that for small training sample sizes ($N < 130$) the predictive model for classification of schizophrenia patients based on sMRI was not stable (Nieuwenhuis et al., 2012). More than 63% of the studies we reviewed didn't meet this criterion. Large datasets may reduce problems with disease heterogeneity as they can represent the whole spectrum of the disorder. Although there are some machine learning methods that are less sensitive to data, a limited number of data samples can cause model overfitting, resulting in poor generalization of the method to independent data sets (Pereira et al., 2009).

To understand the etiology of complex conditions such as mental health, we must develop a better understanding of the structure of the signals and measurements we make of the brain. Thanks to advances in imaging and assaying technology, we can gather increasingly detailed information about individuals, but the cost and complexity of these techniques means that individual researchers may not have sufficient data to build a compact and informative representation of the data. For example, a single sMRI may have tens of thousands of voxels, but a single site may have only a hundred subjects in their study. With increasingly complex data, the classical “curse of dimensionality” would seem to indicate that there is no way to determine signal from noise in this setting. To address the “small N ” problem in other settings, many researchers have proposed open sharing of data to leverage data from multiple sites as well as commercial cloud computing infrastructures to handle the additional computational burden. In the past few years, several multi-site data sharing initiatives such as FBIRN, MCIC and COBRE for schizophrenia, ADNI for Alzheimer's disease, ABIDE for ASD, ADHD-200 for children with ADHD and Functional Connectomes project for healthy have been started.

In neuroscience, measurements often come from human subjects; in some cases legal, ethical, and sociological concerns may preclude or prohibit such open sharing. In particular, local administrative rules, concerns about re-identification of study participants, and a desire to maintain control over data in ongoing research projects may prevent

² <http://image-net.org/>.

individual research sites from sharing the data (Sarwate et al., 2014). The status quo is a patchwork of institution-to-institution data use agreements whose complexity stymies automated analyses across more than a handful of data sets.

Operating on decentralized data

We believe that a more convenient and scalable solution will come from design and implementation of algorithms which learn from data distributed across research groups. These algorithms shall include feature learning as well as classification, prediction and inference. Dropping the requirement of moving the data, these algorithms will better match the current decentralized and efficient organization of research society and substantially lower barriers to entry for collaborative work. The resulting network effect will enable new innovative opportunities for research that we cannot envision today. The need for such approaches to general data computation is realized by some researchers (Bai et al., 2005) but not yet fully appreciated by the neuroimaging field. The field is currently in the state of establishing central repositories of anonymized raw data (Bockholt et al., 2009; Buccigrossi et al., 2007; Di Martino et al., 2014; Jack et al., 2008; Keator et al., 2008; Landis et al., 2016; Marcus et al., 2007; Poldrack et al., 2013; Scott et al., 2011; Turner, 2014; Van Essen et al., 2013). In the past 10 years, release of multi-site neuroimaging datasets such as: FBIRN, MCIC for schizophrenia (Ford et al., 2009; Gollub et al., 2013), ADNI for Alzheimer's disease (Jack et al., 2008), ABIDE for ASD (Di Martino et al., 2014), ADHD-200 for children with ADHD (Consortium et al., 2012) and Functional Connectomes project for healthy subjects (Biswal et al., 2010) have been started.

Certainly, access to raw data is the best way to drill down to the finest details and resolve any inconsistencies due to data handling. However, even in the centralized repositories, it is often more convenient to start analysis from a point in the processing pipeline where less detailed but possibly more informative features are generated. Furthermore, there are three categories of data that pose challenges for public availability for easy access: (1) data that are non-shareable due to obvious re-identification concerns, such as extreme age of the subject or a zip code/disease combination that makes re-identification simple; (2) data that are non-shareable due to more complicated or less obvious concerns, such as genetic data or other data which may be re-identifiable in conjunction with other data not under the investigator's control; and (3) data that are non-shareable due to the local institutional review boards (IRBs) rules or other administrative decisions (e.g., stakeholders in the data collection not allowing sharing). For example, even with broad consent to share the data acquired at the time of data collection, some of the eMERGE sites were required to re-contact the subjects and re-consent prior to sharing within the eMERGE consortium, which can be a permanent show-stopper for some datasets (Ludman et al., 2010). An extensive account of the problems that go along with these concerns is given by Sarwate et al. (2014). An example of how a decentralized data feature learning algorithm could use decentralized data joint ICA in given by Baker et al. (2015). In short, the algorithm performs a joint ICA on datasets distributed across research sites which enables one to perform temporal ICA on fMRI data as an increasingly large data sample becomes available when many research groups join the collaboration. Importantly, Baker et al. have demonstrated (on synthetic data) that with their approach the estimated components are virtually identical for the pooled data (i.e. a central repository), two sites with data split in half, multiple sites with data evenly split across, and even a very large number of sites with very few subjects at each of them. Once globally consistent features are available they may be used in building classification algorithms.

Nevertheless, decentralized data computation under serious privacy concerns will need additional protection besides simple protection from only sharing summaries and not the raw data samples. A solution for

this setting has been offered in the ϵ -differential privacy model and explained extensively in the neuroimaging context with published examples (Dwork, 2006; Sarwate et al., 2014). This approach defines privacy by quantifying the change in the risk of re-identification as a result of publishing a function of the data. Notably, privacy is a property of an algorithm operating on the data, rather than a property of the sanitized data, which reflects the difference between semantic and syntactic privacy. Importantly for our applications, it can be applied to systems which do not share data itself but instead share data derivatives (functions of the data). Algorithms that guarantee differential privacy are randomized in how they manipulate the data values (e.g., by adding noise) to bound the risk. Enabling individual subject prediction in the classification framework is one of the applications where the above-described approaches can provide the most benefit—especially for rare conditions that are easy to identify by cross referencing when raw data is openly shared and hard to collect enough data at a single site to provide high generalization. The former is perfectly addressed by applying ϵ -differential privacy approach to classification (Chaudhuri et al., 2011), while the latter can be addressed by running decentralized algorithms over multiple sites. As mentioned already, differentially private algorithms provide guarantees by necessarily lowering the quality of the solution due to the required noise addition. The same happens to differentially private classifiers (Chaudhuri et al., 2011) and the effect is an undesirable increase in prediction error (Sarwate et al., 2014). Fortunately, combining the approaches (differential privacy and decentralized algorithms) can improve the situation considerably by dropping classification error from 25% to 5% while preserving all privacy guarantees (Sarwate et al., 2014).

In these “big data” times, the need for computation on large-scale datasets creates the best climate for software for distributed computation. Many useful and powerful projects came to the scene such as Apache Spark (Zaharia et al., 2010) and H2O (H2O [WWW Document], 2015). On closer inspection, these implementations are essentially striving for the efficiency of computation given a big data overload (typically easy to get data stored centrally). They suggest optimization toward an environment that is quite orthogonal to what we have to deal with—hard to get to and expensive to collect data spread across research labs around the nation and the world. The goal of decentralized approaches that we are describing here stands principally as preserving correctness of the computation while minimizing the data passed around and reducing the number of iterations. The tools and methods are not conflicting and decentralized data algorithms can and shall take advantage of what is being developed for large-scale computation in the distributed computing community.

Differential diagnosis and disease subtype classification

Using machine learning methods, promising results have been reported for automatic diagnosis of various cognitive and neurodegenerative disorders, usually from healthy controls based on neuroimaging features. However, one of the main challenges in psychiatric and neurology diagnoses is to differentially diagnose a disorder that shares symptoms with multiple other disorders. Examples of such overlapping disorders are schizophrenia, bipolar, schizoaffective, unipolar and mood disorders. Except for differentiating MCI for AD, only a few considered much needed automatic differential diagnosis in the studies we surveyed. Costafreda et al. used fMRI with a verbal fluency task to classify schizophrenia, bipolar and healthy controls (Costafreda et al., 2011b). Calhoun et al., and Arribas et al. both used fMRI with an auditory oddball task and an ICA approach to extract features from the default model network and the temporal lobe of the brain (Arribas et al., 2010; Calhoun et al., 2008). Both of these studies reported high differential accuracy between schizophrenia and bipolar disorder. Pardo et al. used a combination of volumes of 23 ROIs derived from structural MRI along with 22 neurophysiological test scores to automatically classify schizophrenia, bipolar and healthy controls (Pardo et al., 2006).

Recently, Schnack et al. proposed using gray matter densities for classification of schizophrenia, bipolar and healthy controls (Schnack et al., 2014). Koutsouleris et al., used gray matter maps from structural MRI to classify schizophrenia from mood disorder (Koutsouleris et al., 2015). Ota et al. combined volumetric measures derived from structural MRI with fractional anisotropy from dMRI in selected ROIs to classify schizophrenia from MDD (Ota et al., 2013). Sacchet et al. proposed using gray matter volumes of caudate and ventral diencephalon to differentiate MDD, bipolar and remitted MDD patients (Sacchet et al., 2015).

Pathologies like autism and schizophrenia are spectrum disorders with multiple etiologies under the umbrella of the same diagnostic category. While classification of these disorders using the generic category is commonly used to find diagnostic biomarkers, one of the key issues in mental healthcare is the differential diagnosis of patients across several disease subtypes. Common binary patient–control classification ignores the underlying heterogeneity of the disorder. Usually, the treatment path used for these subtypes differs from each other and therefore the correct subtype diagnosis is very important. For example, several cognitive deficits are observed in schizophrenia patients, but the magnitudes of such symptoms are highly variable among the patients. To reduce this phenotypic heterogeneity two major subtypes named “cognitive deficit” and “cognitively spared” have been defined (Green et al., 2013; Jablensky, 2006). These two subtypes exhibit different genetic and cognitive profiles (Green et al., 2013; Morar et al., 2011). An automatic classification of schizophrenia subtypes has been rarely studied. Ingahlhalikar et al. proposed that unsupervised spectral clustering of multi-edge graphs built from a structural connectivity network among 78 ROIs be used to identify subtypes of autism and schizophrenia (Ingahlhalikar et al., 2012). Gould et al. proposed using whole brain, voxel-based morphometry to classify schizophrenia patients with cognitive deficit from those that are cognitively spared (Gould et al., 2014).

There are several studies on automatic differentiation of stable MCI from progressive MCI (those that convert to AD within a certain amount of time). Most of these studies reported modest accuracies around 65–80% (Plant et al., 2010; Salvatore et al., 2015; Tangaro et al., 2015; Tong et al., 2014; Wolz et al., 2011; Zu et al., 2015). ADHD subtype studies are scarce and limited to few studies such as the one by Sato et al. with the intent to automatically differentiate ADHD-IA, ADHD-HI and ADHD-C using resting-state fMRI (Sato et al., 2012).

Again, one major limitation in differential diagnosis and disease subtype classification is the limited sample size. In most of the current datasets, the number of subjects in each disease subtype is small and therefore provides limited ability to develop robust single-subject predictor to accurately differentiate them.

Multimodal neuroimaging studies

Each imaging modality provides a different view of brain function or structure, and data fusion capitalizes on the strengths of each imaging modality/task and their inter-relationships in a joint analysis. This is an important tool to help unravel the pathophysiology of brain disease (Calhoun et al., 2006a; Sui et al., 2012). Recent advances in data fusion include integrating multiple (task) fMRI data sets (Kim et al., 2010; Sui et al., 2009, 2015) from the same participant to specify common versus specific sources of activity to a greater degree than traditional general linear model-based approaches. This can increase confidence in conclusions about the functional significance of brain regions and of activation changes in brain disease. In addition, the combination of function and structure may provide more informative insights into both altered brain patterns and connectivity in brain disorders (McCarley et al., 2008; Michael et al., 2009; Sui et al., 2011). These findings suggest that most studies favor only one data type or do not combine modalities in an integrated manner, and thus miss important changes which are only partially detected by each modality (Calhoun and Adali, 2009). On the other hand, multimodal fusion provides

a more comprehensive description of altered brain patterns and connectivity than a single modality, which has shown increasing utility in answering both scientifically interesting and clinically relevant questions.

Single-subject prediction using multimodal neuroimaging data

There is increasing evidence from multimodal studies that patients with brain disorders exhibit unique morphological characteristics, connectivity patterns, and functional alterations, which could not have been revealed through separate unimodal analyses as typically performed in the majority of neuroimaging experiments. Hence, applying classification techniques to these characteristics could identify biomarkers for psychiatric diseases. This could expedite differential diagnosis, thus leading to more appropriate treatment and improved outcomes for patients with brain disorders. There has been number of studies showing the benefits of combining both rest and task fMRI data for group differences in functional connectivity between schizophrenia patients and controls (Arbabshirani and Calhoun, 2011; Cetin et al., 2014). The change of functional connectivity from rest to task contains novel information present in neither of the states, which could be beneficial for single subject prediction (Arbabshirani and Calhoun, 2011). Based on these evidences, future studies might benefit from combining resting-state and task-based data for classification of brain disorders.

As another example, MCI is difficult to diagnose due to its rather mild and nearly insignificant symptoms of cognitive impairment. Wee et al. integrated information from DTI and resting fMRI by employing multiple-kernel SVM, yielding statistically significant improvement (>7.4%) in classification accuracy of predicting MCI from HC by using multimodal data (96.3%) compared to using each modality independently (Wee et al., 2012). There are additional studies that demonstrate the potential of the fusion of structural and functional data combined with multi-modal classification techniques to provide more accurate and early detection of brain abnormalities (Fan et al., 2008b). By taking advantage of these two complementary approaches, Sui et al. proposed a framework based on mCCA + jICA, that allows both high and weak connections to be detected and shows excellent source separation performance (Sui et al., 2011). It enables robust identification of correspondence among N diverse data types and enables one to investigate the important question of whether certain disease risk factors are shared or are distinct across multiple modalities, which can also serve as multimodal feature selection method for schizophrenia (Sui et al., 2013a, 2013b). Similarly, Jie et al. adopted SVM-FoBa to classify between bipolar versus unipolar disorders by combining GM and ALFF features, achieving an accuracy of 92%. This suggests that using complimentary multimodal biomarkers may be more informative and effective to discriminate brain disorders (Jie et al., 2015).

There are number of recent studies looking at combined biomarkers of sMRI, FDG-PET, and CSF (mostly for ADNI dataset) to discriminate between AD, MCI and HC (Gray et al., 2013; Xu et al., 2015; Yu et al., 2015; Zhang et al., 2011, 2014). Similarly, a few studies combined functional and structural data to build such predictive models (Dai et al., 2012b; Dyrba et al., 2015). Most of those studies reported superior performance of models built based on multimodal features compared to those based on a single modality (Calhoun and Sui, in press).

Deep learning in neuroimaging

In recent years, deep learning methodology has made significant improvement in representation learning and classification in various areas such as speech recognition, natural image classification and text mining. Two main features have made deep learning very attractive to machine learning researchers. First deep learning in contrast with traditional machine learning methods is capable of data-driven automatic feature learning. This important capability removes the subjectivity in selecting the relevant features especially in cases where too many features exist

or prior knowledge in selecting features is not conclusive. The second important feature of deep learning is the depth of models. By applying a hierarchy of non-linear layers, deep learning is capable of modeling very complicated data patterns in contrast with traditional shallow models.

Typical approaches in single subject prediction in neuroimaging consist of selecting features sometimes from thousands of voxels. As reviewed in this report, the basis for such a feature selection is usually inefficient univariate statistical tests. Recently, deep belief networks, a class of deep learning, has been applied to both structural and functional MRI data (Plis et al., 2014). Plis et al. showed that deep learning methods could produce physiologically meaningful features and reveal relations from high dimensional neuroimaging data (Plis et al., 2014). Hjelm et al. applied restricted Boltzmann machines (RBM) to identify intrinsic networks in fMRI data (Hjelm et al., 2014). They showed that RBMs could extract spatial networks and their activation with the accuracy of traditional matrix factorization methods such as ICA. Provably, deep models need exponentially smaller number of parameters in order to model the same thing shallow models can model (Bengio, 2012, 2013). Moreover, deep learning structures such as RBM are generative models and therefore it can be sampled from. This way it is easy to access uncertainty in the estimates compared to the point estimates of matrix factorization models. Furthermore, for deep learning RBM could be stacked to obtain deeper models as needed. This cannot be readily done with ICA, NMF, or sparse PCA.

Recently, deep learning is employed in classification of patients using neuroimaging data. Suk et al. used stacked autoencoder (another class of deep learning) to discriminate patients with AD from those with MCI (Suk et al., 2013). Kim et al. used deep learning for classification of schizophrenia patients from healthy controls based on functional connectivity patterns. They showed that their approach outperforms SVM by a significant margin (Kim et al., 2015).

Deep learning is a very promising tool for understanding the neural basis of brain disorders by extracting hidden patterns from high-dimensional neuroimaging data (Kriegeskorte, 2015). In our opinion, this method has the potential to improve brain disorder diagnosis—especially if larger neuroimaging datasets become available and/or improved methods of training based on existing data are developed (Castro et al., 2015).

Standard machine learning competitions in neuroimaging

The machine learning field has benefited hugely from standard competitions in many applications. In such competitions, usually the participants are provided with a labeled training dataset and an unlabeled testing dataset. The participants try to develop the best predictive model based on the training dataset, predict the labels of the provided testing dataset and submit the results. Such a setting ensures that the results are not biased. These competitions usually attract many groups, even those with less domain knowledge and expertise. By providing a standard dataset and some initial preprocessing, the participants can primarily concentrate on the machine learning aspect of the analysis.

Due to all of the data sharing problems previously discussed, such competitions are rare in neuroimaging. The ADHD-200 competition was held in 2011 with the goal of predicting ADHD from healthy controls in children and adults, using resting-state fMRI along with anatomical and phonotypical data of 776 subjects (491 TDC and 285 ADHD) for training along with additional 197 subjects for testing (Consortium et al., 2012). The competition was a successful example of large-scale ADHD data sharing among several sites. However, the ‘winning’ team of ADHD-200 competition didn’t use the imaging data in their predictive model (just the phenotypical data), which caused discussion in the community about usefulness of brain data in diagnosing a brain disorder (Brown et al., 2012b; Consortium et al., 2012).

More recently, The IEEE MLSP workshop held a schizophrenia classification challenge with the goal of automatic classification of

schizophrenia patients from healthy controls using just brain imaging features (Silva et al., 2014). Functional network connectivity values of resting-state fMRI along with ICA loadings of source-based morphometry of sMRI were calculated from 144 subjects (75 healthy controls, 69 schizophrenia patients) and shared with participants. Interestingly, 245 teams participated in the competition and the winning team achieved an AUC of around 0.90. Moreover, by combining the top three models, an AUC of around 0.94 was achieved (Silva et al., 2014). In our opinion, sharing ready to use, well-defined features as opposed to imaging data itself, was one of the success factors of the MLSP competition in both attracting numerous groups and also achieving high accuracy results. That experience shows that imaging data has a lot of predictive potential at least in the case of separating schizophrenia patients from healthy controls.

We believe that the field of neuroimaging can benefit a lot from standard machine learning competitions such as the ones discussed above. Such competitions can assess the realistic, unbiased, discriminative power of brain data for detecting brain disorders. Also, by attracting a large number of participants, a variety of machine learning methods will be examined for the specific problem. By providing brain features, machine learning experts with less neuroimaging domain knowledge can participate and develop predictive models.

Summary and conclusions

Previous single-subject prediction surveys

In this study, we comprehensively reviewed past efforts in neuroimaging-based single subject prediction in several brain disorders such as MCI, AD, ASD, ADHD, schizophrenia and depressive disorders. Previous reviews include disease-specific surveys such as schizophrenia (Calhoun and Arbabshirani, 2012; Dazzan, 2014; Demirci et al., 2008b; Kambeitz et al., 2015; Veronese et al., 2013; Zarogianni et al., 2013), autism spectrum disorder (Retico et al., 2013, 2014), Alzheimer’s disease (Falahati et al., 2014; Klöppel et al., 2008) and in general (Klöppel et al., 2012; Lemm et al., 2011; Orrù et al., 2012) as well as modality-specific reviews such as machine learning based on fMRI (Sundermann et al., 2014). Also, there are few children specific reviews such as a recent one by Levman et al. on multivariate analyses studies in neonatal and pediatric patients (Levman and Takahashi, 2015). Probably the most comprehensive review so far is the recent one by Wolfers et al., where they reviewed about 120 single subject prediction studies in schizophrenia, mood disorders, anxiety disorders, ADHD and ASD (Wolfers et al., 2015). While there is some overlap among the mentioned studies and this survey, to our knowledge, this is by far the largest survey in the field based on the number of papers reviewed (about 240 papers). Moreover, as discussed previously, the majority of single subject prediction studies have been published in recent years; consequently, an updated survey is much needed. In this work, several pitfalls such as feature selection bias, incomplete reporting of results, unfair comparison across studies and improper hyperparameter selection were discussed and suggestions to address those issues were provided. Moreover, emerging trends in this exciting field such as decentralized data sharing, differential diagnosis and disease subtype classification, multimodal neuroimaging, applications of deep learning in neuroimaging and merits of standard machine learning competitions were discussed in detail.

Limitations

There are several limitations in this work. We limited our search to MRI-based English journal papers in specific disorders. There are other single subject prediction studies that are based on other modalities such as EEG and MEG. Also, other brain disorders such Parkinson disease and anxiety disorders were not reviewed in this work. From the studies we reviewed, we tried to extract the key features as it relates to the

machine learning. Many of those studies contained multiple experiments under different scenarios but we just reported one of them (usually the most successful one) here. Also, there are many important details in each study and for that reason interested readers should always refer to each reference for full information on experiment setup and other details. The other reason for this, is the chance of error in reported information in Table 2–6, considering the large number of surveyed studies despite our efforts to be as accurate as possible.

In terms of common pitfalls, we mostly focused on the potential problems from the machine learning point of view. There are many other important potential issues in topics such as experimental design, effect of head motion and other factors such as the impact of draining veins on fMRI studies (Boubela et al., 2015; Power et al., 2012, 2014, 2015), wakefulness of subjects during rsfMRI (Tagliazucchi and Laufs, 2014) and the selecting of preprocessing steps (Vergara et al., 2015). Effect of those potential issues on single subject prediction deserves a full paper by itself.

In conclusion, we are optimistic about the use of brain imaging for single subject prediction, and many of the issues we recommend are within reach. Larger studies are available and repositories with pooled data across studies are growing rapidly (Eickhoff et al., 2016).

Acknowledgement

This work was supported by National Institutes of Health grants P20GM103472, R01EB005846, R01EB020407, 1R01DA040487 and NSF EPSCoR grant #1539067 (to V.D. Calhoun); “100 Talents Plan” of Chinese Academy of Sciences (to J. Sui); Chinese National Science Foundation No. 81471367 and the State High-Tech Development Plan (863) No. 2015AA020513. Also, we would like to thank Monica Jaramillo for the initial survey of neuroimaging studies. The authors report no financial relationships with commercial interests.

References

- Abdulkadir, A., Mortamet, B., Vemuri, P., Jack, C.R., Krueger, G., Klöppel, S., 2011. Effects of hardware heterogeneity on the performance of SVM Alzheimer's disease classifier. *NeuroImage* 58, 785–792. <http://dx.doi.org/10.1016/j.neuroimage.2011.06.029>.
- Adaszewski, S.S., Dukart, J., Kherif, F., Frackowiak, R., Draganski, B., 2013. How early can we predict Alzheimer's disease using computational anatomy? *Neurobiol. Aging* 34, 2815–2826. <http://dx.doi.org/10.1016/j.neurobiolaging.2013.06.015>.
- Aguilar, C., Westman, E., Muehlboeck, J.-S.S., Mecocci, P., Vellas, B., Tsolaki, M., Kloszewska, I., Soininen, H., Lovestone, S., Spenger, C., Simmons, A., Wahlund, L.-O.O., 2013. Different multivariate techniques for automated classification of MRI data in Alzheimer's disease and mild cognitive impairment. *Psychiatry Res.* 212, 89–98. <http://dx.doi.org/10.1016/j.psychres.2012.11.005>.
- Akshoomoff, N., Lord, C., Lincoln, A.J., Courchesne, R.Y., Carper, R.A., Townsend, J., Courchesne, E., 2004. Outcome classification of preschool children with autism spectrum disorders using MRI brain measures. *J. Am. Acad. Child Adolesc. Psychiatry* 43, 349–357. <http://dx.doi.org/10.1097/00004583-200403000-00018>.
- Alberg, A.J., Park, J.W., Hager, B.W., Brock, M.V., Diener-West, M., 2004. The use of “overall accuracy” to evaluate the validity of screening or diagnostic tests. *J. Gen. Intern. Med.* 19, 460–465.
- Albert, M.S., DeKosky, S.T., Dickson, D., Dubois, B., Feldman, H.H., Fox, N.C., Gamst, A., Holtzman, D.M., Jagust, W.J., Petersen, R.C., et al., 2011. The diagnosis of mild cognitive impairment due to Alzheimer's disease: Recommendations from the National Institute on Aging-Alzheimer's Association workgroups on diagnostic guidelines for Alzheimer's disease. *Alzheimers Dement.* 7, 270–279.
- Andersen, A.H., Rayens, W.S., Liu, Y., Smith, C.D., 2012. Partial least squares for discrimination in fMRI data. *Magn. Reson. Imaging* 30, 446–452. <http://dx.doi.org/10.1016/j.mri.2011.11.001>.
- Anderson, A., Cohen, M.S., 2013. Decreased small-world functional network connectivity and clustering across resting state networks in schizophrenia: an fMRI classification tutorial. *Front. Hum. Neurosci.* 7, 520. <http://dx.doi.org/10.3389/fnhum.2013.00520>.
- Anderson, A., Douglas, P.K., Kerr, W.T., Haynes, V.S., Yuille, A.L., Xie, J., Wu, Y.N., Brown, J.A., Cohen, M.S., 2014. Non-negative matrix factorization of multimodal MRI, fMRI and phenotypic data reveals differential changes in default mode subnetworks in ADHD. *NeuroImage* 102 (Pt 1), 207–219. <http://dx.doi.org/10.1016/j.neuroimage.2013.12.015>.
- Anderson, J.S., Nielsen, J.A., Froehlich, A.L., DuBray, M.B., Druzgal, T.J., Cariello, A.N., Cooperrider, J.R., Zielinski, B.A., Ravichandran, C., Fletcher, P.T., et al., 2011. Functional connectivity magnetic resonance imaging classification of autism. *Brain* 134, 3742–3754.
- Anticevic, A., Cole, M.W., Repovs, G., Murray, J.D., Brumbaugh, M.S., Winkler, A.M., Savic, A., Krystal, J.H., Pearlson, G.D., Glahn, D.C., 2014. Characterizing thalamo-cortical disturbances in schizophrenia and bipolar illness. *Cereb. Cortex* 24, 3116–3130. <http://dx.doi.org/10.1093/cercor/bht165>.
- Apostolova, L.G., Hwang, K.S., Kohannim, O., Avila, D., Elashoff, D., Jack, C.R., Shaw, L., Trojanowski, J.Q., Weiner, M.W., Thompson, P.M., 2014. ApoE4 effects on automated diagnostic classifiers for mild cognitive impairment and Alzheimer's disease. *Neuroimage Clin.* 4, 461–472. <http://dx.doi.org/10.1016/j.nicl.2013.12.012>.
- Arbabshirani, M.R., Calhoun, V.D., 2011. Functional network connectivity during rest and task: comparison of healthy controls and schizophrenic patients. *Engineering in Medicine and Biology Society, EMBC, 2011 Annual International Conference of the IEEE*, pp. 4418–4421.
- Arbabshirani, M.R., Kiehl, K.A., Pearlson, G.D., Calhoun, V.D., 2013. Classification of schizophrenia patients based on resting-state functional network connectivity. *Front. Neurosci.* 7, 10–3389.
- Ardekani, B.A., Tabesh, A., Sevy, S., Robinson, D.G., Bilder, R.M., Szeszko, P.R., 2011. Diffusion tensor imaging reliably differentiates patients with schizophrenia from healthy volunteers. *Hum. Brain Mapp.* 32, 1–9. <http://dx.doi.org/10.1002/hbm.20995>.
- Arimura, H., Yoshiura, T., Kumazawa, S., Tanaka, K., Koga, H., Mihara, F., Honda, H., Sakai, S., Toyofuku, F., Higashida, Y., 2008. Automated method for identification of patients with Alzheimer's disease based on three-dimensional MR images. *Acad. Radiol.* 15, 274–284. <http://dx.doi.org/10.1016/j.acra.2007.10.020>.
- Arribas, J.I., Calhoun, V.D., Adali, T., 2010. Automatic Bayesian classification of healthy controls, bipolar disorder, and schizophrenia using intrinsic connectivity maps from fMRI data. *IEEE Trans. Biomed. Eng.* 57, 2850–2860. <http://dx.doi.org/10.1109/TBME.2010.2080679>.
- Association, A.P., et al., 2003. *Diagnostic and Statistical Manual of Mental Disorders: DSM-5. ManMag*.
- Bai, Z.-J., Chan, R.H., Luk, F.T., 2005. Principal component analysis for distributed data sets with updating. *Proceedings of the 6th International Conference on Advanced Parallel Processing Technologies, APPT'05. Springer-Verlag, Berlin, Heidelberg*, pp. 471–483.
- Baio, J., 2012. Prevalence of autism spectrum disorders: autism and developmental disabilities monitoring network, 14 sites, United States, 2008. *Morb. Mortal. Wkly. Rep. Surveill. Summ.* 61 (3) (Centers Dis. Control Prev).
- Baker, B., Silva, R., Calhoun, V.D., Sarwate, A.D., Plis, S., 2015. Large scale collaboration with autonomy: decentralized data ICA. *IEEE Machine Learning for Signal Processing Workshop. Boston, MA*.
- Bansal, R., Staib, L.H., Laine, A.F., Hao, X., Xu, D., Liu, J., Weissman, M., Peterson, B.S., 2012. Anatomical Brain Images Alone Can Accurately Diagnose Chronic Neuropsychiatric Illnesses.
- Bassett, D.S., Nelson, B.G., Mueller, B.A., Camchong, J., Lim, K.O., 2012. Altered resting state complexity in schizophrenia. *NeuroImage* 59, 2196–2207. <http://dx.doi.org/10.1016/j.neuroimage.2011.10.002>.
- Batmanghelich, N.K., Taskar, B., Davatzikos, C., 2012. Generative-discriminative basis learning for medical imaging. *IEEE Trans. Med. Imaging* 31, 51–69. <http://dx.doi.org/10.1109/TMI.2011.2162961>.
- Beheshti, I., Demirel, H., 2015. Probability distribution function-based classification of structural MRI for the detection of Alzheimer's disease. *Comput. Biol. Med.* 64, 208–216. <http://dx.doi.org/10.1016/j.combiomed.2015.07.006>.
- Beltrachini, L., De Marco, M., Taylor, Z.A., Lotjonen, J., Frangi, A.F., Venneri, A., 2015. Integration of cognitive tests and resting state fMRI for the individual identification of mild cognitive impairment. *Curr. Alzheimer Res.* 12, 592–603.
- Bengio, Y., 2012. Deep learning of representations for unsupervised and transfer learning. *Unsupervised Transf. Learn. Challenges Mach. Learn.* 7, 19.
- Bengio, Y., 2013. Deep learning of representations: looking forward. *Statistical Language and Speech Processing. Springer*, pp. 1–37.
- Bergouignan, L., Lefranc, J.P., Chupin, M., Morel, N., Spano, J.P., Fossati, P., 2011. Breast cancer affects both the hippocampus volume and the episodic autobiographical memory retrieval. *PLoS One* 6, e25349. <http://dx.doi.org/10.1371/journal.pone.0025349>.
- Bhugra, D., 2005. The global prevalence of schizophrenia. *PLoS Med.* 2, 372.
- Biederman, J., 2005. Attention-deficit/hyperactivity disorder: a selective overview. *Biol. Psychiatry* 57, 1215–1220.
- Bishop, C.-M., 2006. *Pattern Recognition and Machine Learning (Information Science and Statistics)*. Springer.
- Biswal, B.B., Mennes, M., Zuo, X.-N., Gohel, S., Kelly, C., Smith, S.M., Beckmann, C.F., Adelstein, J.S., Buckner, R.L., Colcombe, S., et al., 2010. Toward discovery science of human brain function. *Proc. Natl. Acad. Sci.* 107, 4734–4739.
- Bleich-Cohen, M., Jamshy, S., Sharon, H., Weizman, R., Intrator, N., Poyurovsky, M., Hendler, T., 2014. Machine learning fMRI classifier delineates subgroups of schizophrenia patients. *Schizophr. Res.* 160, 196–200. <http://dx.doi.org/10.1016/j.schres.2014.10.033>.
- Blum, A.L., Langley, P., 1997. Selection of relevant features and examples in machine learning. *Artif. Intell.* 97, 245–271.
- Bockholt, H.J., Scully, M., Courtney, W., Rachakonda, S., Scott, A., Caprihan, A., Fries, J., Kalyanam, R., Segall, J.M., de la Garza, R., et al., 2009. Mining the mind research network: a novel framework for exploring large scale, heterogeneous translational neuroscience research data sources. *Front. Neuroinform.* 3.
- Bohland, J.W., Saperstein, S., Pereira, F., Rapin, J., Grady, L., 2012. Network, anatomical, and non-imaging measures for the prediction of ADHD diagnosis in individual subjects. *Front. Syst. Neurosci.* 6, 78. <http://dx.doi.org/10.3389/fnsys.2012.00078>.
- Bottino, C.M.C., Castro, C.C., Gomes, R.L.E., Buchpiguel, A.C., Marchetti, R.L., Neto, M.R.L., 2002. Volumetric MRI measurements can differentiate Alzheimer's disease, mild cognitive impairment, and normal aging. *Int. Psychogeriatr.* 14, 59–72.
- Boubela, R.N., Kalcher, K., Huf, W., Seidel, E.-M., Derntl, B., Pezawas, L., Našelj, C., Moser, E., 2015. fMRI measurements of amygdala activation are confounded by stimulus correlated signal fluctuation in nearby veins draining distant brain regions. *Sci. Rep.* 5.

- Brookmeyer, R., Johnson, E., Ziegler-Graham, K., Arrighi, H.M., 2007. Forecasting the global burden of Alzheimer's disease. *Alzheimers Dement.* 3, 186–191.
- Brown, G., Pocock, A., Zhao, M.-J., Lujan, M., 2012a. Conditional likelihood maximisation: a unifying framework for mutual information feature selection. *J. Mach. Learn. Res.* 13, 27–66.
- Brown, M.R.G., Sidhu, G.S., Greiner, R., Asgarian, N., Bastani, M., Silverstone, P.H., Greenshaw, A.J., Dursun, S.M., 2012b. ADHD-200 global competition: diagnosing ADHD using personal characteristic data can outperform resting state fMRI measurements. *Front. Syst. Neurosci.* 6, 1–22. <http://dx.doi.org/10.3389/fnsys.2012.00069>.
- Buccigrossi, R., Ellisman, M., Grethe, J., Haselgrove, C., Kennedy, D.N., Martone, M., Preuss, N., Reynolds, K., Sullivan, M., Turner, J., et al., 2007. The neuroimaging informatics tools and resources clearinghouse (NITRC). AMIA Annual Symposium Proceedings/AMIA Symposium. AMIA Symposium, p. 1000.
- Caan, M.W. a, Vermeer, K.a., van Vliet, L.J., Majoie, C.B.L.M., Peters, B.D., den Heeten, G.J., Vos, F.M., 2006. Shaving diffusion tensor images in discriminant analysis: a study into schizophrenia. *Med. Image Anal.* 10, 841–849. <http://dx.doi.org/10.1016/j.media.2006.07.006>.
- Calderoni, S., Retico, A., Biagi, L., Tancredi, R., Muratori, F., Tosetti, M., 2012. Female children with autism spectrum disorder: an insight from mass-univariate and pattern classification analyses. *NeuroImage* 59, 1013–1022. <http://dx.doi.org/10.1016/j.neuroimage.2011.08.070>.
- Calhoun, V.D., Adali, T., 2009. Feature-based fusion of medical imaging data. *IEEE Trans. Inf. Technol. Biomed.* 13, 711–720. <http://dx.doi.org/10.1109/TITB.2008.923773>.
- Calhoun, V., Arbabshirani, M.R., 2012. Neuroimaging-based automatic classification of schizophrenia. In: Singh, I., Sinnott-Armstrong, W.P., Savulescu, J. (Eds.), *Bioprediction, Biomarkers and Bad Behavior*. Oxford Univ Press, pp. 206–230.
- Calhoun, V.D., Sui, J., 2016. Multimodal fusion of brain imaging data: a key to finding the missing link (s) in complex mental illness. *Biol. Psychiatry Cogn. Neurosci. Neuroimaging* (in press).
- Calhoun, V.D., Adali, T., Giuliani, N.R., Pekar, J.J., Kiehl, K.A., Pearlson, G.D., 2006b. Method for multimodal analysis of independent source differences in schizophrenia: combining gray matter structural and auditory oddball functional data. *Hum. Brain Mapp.* 27, 47–62. <http://dx.doi.org/10.1002/hbm.20166>.
- Calhoun, V.D., Adali, T., Kiehl, K.A., Astur, R., Pekar, J.J., Pearlson, G.D., 2006a. A method for multitask fMRI data fusion applied to schizophrenia. *Hum. Brain Mapp.* 27, 598–610.
- Calhoun, V.D., Maciejewski, P.K., Pearlson, G.D., Kiehl, K.A., 2008. Temporal lobe and "default" hemodynamic brain modes discriminate between schizophrenia and bipolar disorder. *Hum. Brain Mapp.* 29, 1265–1275. <http://dx.doi.org/10.1002/hbm.20463>.
- Cao, H., Duan, J., Lin, D., Calhoun, V., Wang, Y.-P., 2013. Integrating fMRI and SNP data for biomarker identification for schizophrenia with a sparse representation based variable selection method. *BMC Med. Genet.* 6 (Suppl. 3), S2. <http://dx.doi.org/10.1186/1755-8794-6-S3-S2>.
- Cao, L., Guo, S., Xue, Z., Hu, Y., Liu, H., Mwansinya, T.E., Pu, W., Yang, B., Liu, C., Feng, J., Chen, E.Y.H., Liu, Z., 2014. Aberrant functional connectivity for diagnosis of major depressive disorder: a discriminant analysis. *Psychiatry Clin. Neurosci.* 68, 110–119. <http://dx.doi.org/10.1111/pcn.12106>.
- Caprihan, a., Pearlson, G.D., Calhoun, V.D., 2008. Application of principal component analysis to distinguish patients with schizophrenia from healthy controls based on fractional anisotropy measurements. *NeuroImage* 42, 675–682. <http://dx.doi.org/10.1016/j.neuroimage.2008.04.255>.
- Casanova, R., Hsu, F.-C., Espeland, M.A., 2012. Classification of structural MRI images in Alzheimer's disease from the perspective of ill-posed problems. *PLoS One* 7, e44877. <http://dx.doi.org/10.1371/journal.pone.0044877>.
- Castellani, U., Rossato, E., Murino, V., Bellani, M., Rambaldelli, G., Perlini, C., Tomelleri, L., Tansella, M., Brambilla, P., 2012. Classification of schizophrenia using feature-based morphometry. *J. Neural Transm.* 119, 395–404. <http://dx.doi.org/10.1007/s00702-011-0693-7>.
- Castro, E., Gómez-Verdejo, V., Martínez-Ramón, M., Kiehl, K.A., Calhoun, V.D., 2014. A multiple kernel learning approach to perform classification of groups from complex-valued fMRI data analysis: application to schizophrenia. *NeuroImage* 87, 1–17. <http://dx.doi.org/10.1016/j.neuroimage.2013.10.065>.
- Castro, E., Martínez-Ramón, M., Pearlson, G., Sui, J., Calhoun, V.D., 2011. Characterization of groups using composite kernels and multi-source fMRI analysis data: application to schizophrenia. *NeuroImage* 58, 526–536. <http://dx.doi.org/10.1016/j.neuroimage.2011.06.044>.
- Castro, E., Ulloa, A., Plis, S.M., Turner, J.A., Calhoun, V.D., 2015. Simulation of structural magnetic resonance images for deep learning pre-training. *IEEE International Symposium on Biomedical Imaging*. New York, NY, USA.
- Cetin, M.S., Christensen, F., Abbott, C.C., Staphen, J.M., Mayer, A.R., Cañive, J.M., Bustillo, J.R., Pearlson, G.D., Calhoun, V.D., 2014. Thalamus and posterior temporal lobe show greater inter-network connectivity at rest and across sensory paradigms in schizophrenia. *NeuroImage* 97, 117–126.
- Çetin, M.S., Khullar, S., Damaraju, E., Michael, A.M., Baum, S.a., Calhoun, V.D., 2015. Enhanced disease characterization through multi network functional normalization in fMRI. *Front. Neurosci.* 9, 1–15. <http://dx.doi.org/10.3389/fnins.2015.00095>.
- Challis, E., Hurlley, P., Serra, L., Bozzali, M., Oliver, S., Cercignani, M., 2015. Gaussian process classification of Alzheimer's disease and mild cognitive impairment from resting-state fMRI. *NeuroImage* 112, 232–243. <http://dx.doi.org/10.1016/j.neuroimage.2015.02.037>.
- Chang, C.-W., Ho, C.-C., Chen, J.-H., 2012. ADHD classification by a texture analysis of anatomical brain MRI data. *Front. Syst. Neurosci.* 6, 66. <http://dx.doi.org/10.3389/fnsys.2012.00066>.
- Chaudhuri, K., Monteleoni, C., Sarwate, A.D., 2011. Differentially private empirical risk minimization. *J. Mach. Learn. Res.* 12, 1069–1109.
- Chen, C.P., Keown, C.L., Jahedi, A., Nair, A., Pflieger, M.E., Bailey, B.a., Müller, R.-A., 2015. Diagnostic classification of intrinsic functional connectivity highlights somatosensory, default mode, and visual regions in autism. *Neuroimage Clin.* 8, 238–245. <http://dx.doi.org/10.1016/j.nicl.2015.04.002>.
- Chen, Y., Storr, J., Tan, L., Mazlack, L.J., Lee, J.-H., Lu, L.J., 2014. Detecting brain structural changes as biomarker from magnetic resonance images using a local feature based SVM approach. *J. Neurosci. Methods* 221, 22–31. <http://dx.doi.org/10.1016/j.jneumeth.2013.09.001>.
- Cheng, B., Liu, M., Zhang, D., Munsell, B.C., Shen, D., 2015a. Domain transfer learning for MCI conversion prediction. *IEEE Trans. Biomed. Eng.* 62, 1805–1817. <http://dx.doi.org/10.1109/TBME.2015.2404809>.
- Cheng, H., Newman, S., Goñi, J., Kent, J.S., Howell, J., Bolbecker, A., Puce, A., O'Donnell, B.F., Hetrick, W.P., 2015b. Nodal centrality of functional network in the differentiation of schizophrenia. *Schizophr. Res.* 168, 345–352. <http://dx.doi.org/10.1016/j.schres.2015.08.011>.
- Chincarini, A., Bosco, P., Calvini, P., Gemme, G., Esposito, M., Olivieri, C., Rei, L., Squarcia, S., Rodriguez, G., Bellotti, R., Cerello, P., De Mitri, I., Retico, A., Nobili, F., 2011. Local MRI analysis approach in the diagnosis of early and prodromal Alzheimer's disease. *NeuroImage* 58, 469–480. <http://dx.doi.org/10.1016/j.neuroimage.2011.05.083>.
- Chu, C., Hsu, A.-L., Chou, K.-H., Bandettini, P., Lin, C., 2012. Does feature selection improve classification accuracy? impact of sample size and feature selection on classification using anatomical magnetic resonance images. *NeuroImage* 60, 59–70. <http://dx.doi.org/10.1016/j.neuroimage.2011.11.066>.
- Chyzyk, D., Savio, A., Graña, M., 2015. Computer aided diagnosis of schizophrenia on resting state fMRI data by ensembles of ELM. *Neural Netw.* 68, 23–33. <http://dx.doi.org/10.1016/j.neunet.2015.04.002>.
- Colby, J.B., Rudie, J.D., Brown, J.A., Douglas, P.K., Cohen, M.S., Shehzad, Z., 2012. Insights into multimodal imaging classification of ADHD. *Front. Syst. Neurosci.* 6, 59. <http://dx.doi.org/10.3389/fnsys.2012.00059>.
- Collingridge, D.S., 2013. A primer on quantized data analysis and permutation testing. *J. Mix. Methods Res.* 7, 81–97.
- Consortium, A.-200, et al., 2012. The ADHD-200 consortium: a model to advance the translational potential of neuroimaging in clinical neuroscience. *Front. Syst. Neurosci.* 6.
- Costafreda, S.G., Dinov, I.D., Tu, Z., Shi, Y., Liu, C.-Y., Kloszewska, L., Mecocci, P., Soininen, H., Tsolaki, M., Vellas, B., Wahlund, L.-O., Spenger, C., Toga, A.W., Lovestone, S., Simmons, A., 2011a. Automated hippocampal shape analysis predicts the onset of dementia in mild cognitive impairment. *NeuroImage* 56, 212–219. <http://dx.doi.org/10.1016/j.neuroimage.2011.01.050>.
- Costafreda, S.G., Fu, C.H.Y., Picchioni, M., Touloupoulou, T., McDonald, C., Kravariti, E., Walsh, M., Prata, D., Murray, R.M., McGuire, P.K., 2011b. Pattern of neural responses to verbal fluency shows diagnostic specificity for schizophrenia and bipolar disorder. *BMC Psychiatry* 11, 18. <http://dx.doi.org/10.1186/1471-244X-11-18>.
- Coupé, P., Eskildsen, S.F., Manjón, J.V., Fonov, V.S., Collins, D.L., 2012. Simultaneous segmentation and grading of anatomical structures for patient's classification: application to Alzheimer's disease. *NeuroImage* 59, 3736–3747. <http://dx.doi.org/10.1016/j.neuroimage.2011.10.080>.
- Csernansky, J.G., Schindler, M.K., Splinter, N.R., Wang, L., Gado, M., Selemon, L.D., Rastogi-Cruz, D., Posener, J.a., Thompson, P.a., Miller, M.I., 2004. Abnormalities of thalamic volume and shape in schizophrenia. *Am. J. Psychiatry* 161, 896–902. <http://dx.doi.org/10.1176/appi.ajp.161.5.896>.
- Cui, Y., Liu, B., Luo, S., Zhen, X., Fan, M., Liu, T., Zhu, W., Park, M., Jiang, T., Jin, J.S., 2011. Identification of conversion from mild cognitive impairment to Alzheimer's disease using multivariate predictors. *PLoS One* 6, e21896. <http://dx.doi.org/10.1371/journal.pone.0021896>.
- Cui, Y., Wen, W., Lipnicki, D.M., Beg, M.F., Jin, J.S., Luo, S., Zhu, W., Kochan, N.A., Reppermund, S., Zhuang, L., Raamana, P.R., Liu, T., Trollor, J.N., Wang, L., Brodaty, H., Sachdev, P.S., 2012. Automated detection of amnesic mild cognitive impairment in community-dwelling elderly adults: a combined spatial atrophy and white matter alteration approach. *NeuroImage* 59, 1209–1217. <http://dx.doi.org/10.1016/j.neuroimage.2011.08.013>.
- Cuingnet, R., Gerardin, E., Tessieras, J., Auzias, G., Lehericy, S., Habert, M.-O., Chupin, M., Benali, H., Colliot, O., 2011. Automatic classification of patients with Alzheimer's disease from structural MRI: a comparison of ten methods using the ADNI database. *NeuroImage* 56, 766–781. <http://dx.doi.org/10.1016/j.neuroimage.2010.06.013>.
- Cuingnet, R., Glaunès, J.A., Chupin, M., Benali, H., Colliot, O., 2013. Spatial and anatomical regularization of SVM: a general framework for neuroimaging data. *IEEE Trans. Pattern Anal. Mach. Intell.* 35, 682–696. <http://dx.doi.org/10.1109/TPAMI.2012.142>.
- Dai, D., Wang, J., Hua, J., He, H., 2012a. Classification of ADHD children through multimodal magnetic resonance imaging. *Front. Syst. Neurosci.* 6, 63. <http://dx.doi.org/10.3389/fnsys.2012.00063>.
- Dai, Z., Yan, C., Wang, Z., Wang, J., Xia, M., Li, K., He, Y., 2012b. Discriminative analysis of early Alzheimer's disease using multi-modal imaging and multi-level characterization with multi-classifier (M3). *NeuroImage* 59, 2187–2195. <http://dx.doi.org/10.1016/j.neuroimage.2011.10.003>.
- Davatzikos, C., Shen, D., Gur, R.C., Wu, X., Liu, D., Fan, Y., Huggert, P., Turetsky, B.I., Gur, R.E., 2005. Whole-brain morphometric study of schizophrenia revealing a spatially complex set of focal abnormalities. *Arch. Gen. Psychiatry* 62, 1218–1227. <http://dx.doi.org/10.1001/archpsyc.62.11.1218>.
- Dazzan, P., 2014. Neuroimaging biomarkers to predict treatment response in schizophrenia: the end of 30 years of solitude? *Dialogues Clin. Neurosci.* 16, 491–503.
- DeCarli, C., Murphy, D.G., McIntosh, A.R., Teichberg, D., Schapiro, M.B., Horwitz, B., 1995. Discriminant analysis of MRI measures as a method to determine the presence of dementia of the Alzheimer type. *Psychiatry Res.* 57, 119–130.
- Demirci, O., Clark, V.P., Calhoun, V.D., 2008a. A projection pursuit algorithm to classify individuals using fMRI data: application to schizophrenia. *NeuroImage* 39, 1774–1782. <http://dx.doi.org/10.1016/j.neuroimage.2007.10.012>.
- Demirci, O., Clark, V.P., Magnotta, V.a., Andreasen, N.C., Lauriello, J., Kiehl, K.a., Pearlson, G.D., Calhoun, V.D., 2008b. A review of challenges in the use of fMRI for disease

- classification/characterization and a projection pursuit application from a multi-site fMRI schizophrenia study. *Brain Imaging Behav.* 2, 207–226. <http://dx.doi.org/10.1007/s11682-008-9028-1>.
- Deshpande, G., Liberio, L.E., Sreenivasan, K.R., Deshpande, H.D., Kana, R.K., 2013. Identification of neural connectivity signatures of autism using machine learning. *Front. Hum. Neurosci.* 7, 670. <http://dx.doi.org/10.3389/fnhum.2013.00670>.
- Deshpande, G., Wang, P., Rangaprakash, D., Wilamowski, B., 2015. Fully connected Cascade Artificial neural network architecture for attention deficit hyperactivity disorder classification from functional magnetic resonance imaging data. *IEEE Trans Cybern* 45, 2668–2679. <http://dx.doi.org/10.1109/TCYB.2014.2379621>.
- Dey, S., Rao, A.R., Shah, M., 2012. Exploiting the brain's network structure in identifying ADHD subjects. *Front. Syst. Neurosci.* 6, 75. <http://dx.doi.org/10.3389/fnsys.2012.00075>.
- Dey, S., Rao, A.R., Shah, M., 2014. Attributed graph distance measure for automatic detection of attention deficit hyperactive disordered subjects. *Front. Neural. Circuits* 8, 64. <http://dx.doi.org/10.3389/fncir.2014.00064>.
- DeYoe, E.A., Bandettini, P., Neitz, J., Miller, D., Winans, P., 1994. Functional magnetic resonance imaging (fMRI) of the human brain. *J. Neurosci. Methods* 54, 171–187.
- Di Martino, A., Yan, C.-G., Li, Q., Denio, E., Castellanos, F.X., Alaerts, K., Anderson, J.S., Assaf, M., Bookheimer, S.Y., Dapretto, M., et al., 2014. The autism brain imaging data exchange: towards a large-scale evaluation of the intrinsic brain architecture in autism. *Mol. Psychiatry* 19, 659–667.
- DiLuca, M., Olesen, J., 2014. The cost of brain diseases: a burden or a challenge? *Neuron* 82, 1205–1208. <http://dx.doi.org/10.1016/j.neuron.2014.05.044>.
- Du, W., Calhoun, V.D., Li, H., Ma, S., Eichele, T., Kiehl, K.A., Pearlson, G.D., Adali, T., 2012. High classification accuracy for schizophrenia with rest and task fMRI data. *Front. Hum. Neurosci.* 6, 1–12. <http://dx.doi.org/10.3389/fnhum.2012.00145>.
- Dukart, J., Mueller, K., Barthel, H., Villringer, A., Sabri, O., Schroeter, M.L., 2013. Meta-analysis based SVM classification enables accurate detection of Alzheimer's disease across different clinical centers using FDG-PET and MRI. *Psychiatry Res.* 212, 230–236. <http://dx.doi.org/10.1016/j.pscychres.2012.04.007>.
- Dwork, C., 2006. Differential privacy. *Autom. Lang. Program.* 1–12.
- Dyrba, M., Ewers, M., Wegrzyn, M., Kilimann, I., Plant, C., Oswald, A., Meindl, T., Pievani, M., Bokke, A.L.W., Fellgiebel, A., Filippi, M., Hampel, H., Klöppel, S., Hauenstein, K., Kirste, T., Teipel, S.J., 2013. Robust automated detection of microstructural white matter degeneration in Alzheimer's disease using machine learning classification of multicenter DTI data. *PLoS One* 8, e64925. <http://dx.doi.org/10.1371/journal.pone.0064925>.
- Dyrba, M., Grothe, M., Kirste, T., Teipel, S.J., 2015. Multimodal analysis of functional and structural disconnection in Alzheimer's disease using multiple kernel SVM. *Hum. Brain Mapp.* 36, 2118–2131. <http://dx.doi.org/10.1002/hbm.22759>.
- Ecker, C., Marquand, A., Mourão-Miranda, J., Johnston, P., Daly, E.M., Brammer, M.J., Maltezos, S., Murphy, C.M., Robertson, D., Williams, S.C., Murphy, D.G.M., 2010a. Describing the brain in autism in five dimensions—magnetic resonance imaging-assisted diagnosis of autism spectrum disorder using a multiparameter classification approach. *J. Neurosci.* 30, 10612–10623. <http://dx.doi.org/10.1523/JNEUROSCI.5413-09.2010>.
- Ecker, C., Rocha-Rego, V., Johnston, P., Mourão-Miranda, J., Marquand, A., Daly, E.M., Brammer, M.J., Murphy, C., Murphy, D.G., 2010b. Investigating the predictive value of whole-brain structural MR scans in autism: a pattern classification approach. *NeuroImage* 49, 44–56. <http://dx.doi.org/10.1016/j.neuroimage.2009.08.024>.
- Eickhoff, S., Turner, J.A., Nichols, T.E., Van Horn, J.D., 2016. Sharing the wealth: neuroimaging data repositories. *NeuroImage* 124, 1065–1068.
- Epstein, J., Stern, E., Silbersweig, D., 2001. Neuropsychiatry at the millennium: the potential for mind/brain integration through emerging interdisciplinary research strategies. *Clin. Neurosci. Res.* 1, 10–18.
- Ernst, R.L., Hay, J.W., 1994. The US economic and social costs of Alzheimer's disease revisited. *Am. J. Public Health* 84, 1261–1264.
- Esikildsen, S.F., Coupé, P., García-Lorenzo, D., Fonov, V., Pruessner, J.C., Collins, D.L., Initiative, A.D.N., et al., 2013. Prediction of Alzheimer's disease in subjects with mild cognitive impairment from the ADNI cohort using patterns of cortical thinning. *NeuroImage* 65, 511–521.
- Fair, D.A., Nigg, J.T., Iyer, S., Bathula, D., Mills, K.L., Dosenbach, N.U.F., Schlaggar, B.L., Meneses, M., Gutman, D., Bangaru, D., Buitelaar, J.K., Dickstein, D.P., Di Martino, A., Kennedy, D.N., Kelly, C., Luna, B., Schweitzer, J.B., Velanova, K., Wang, Y.-F., Mostofsky, S., Castellanos, F.X., Millham, M.P., 2012. Distinct neural signatures detected for ADHD subtypes after controlling for micro-movements in resting state functional connectivity MRI data. *Front. Syst. Neurosci.* 6, 80. <http://dx.doi.org/10.3389/fnsys.2012.00080>.
- Falahati, F., Westman, E., Simmons, A., 2014. Multivariate data analysis and machine learning in Alzheimer's disease with a focus on structural magnetic resonance imaging. *J. Alzheimers Dis.* 41, 685–708. <http://dx.doi.org/10.3233/JAD-131928>.
- Fan, Y., Gur, R.E., Gur, R.C., Wu, X., Shen, D., Calkins, M.E., Davatzikos, C., 2008a. Unaffected family members and schizophrenia patients share brain structure patterns: a high-dimensional pattern classification study. *Biol. Psychiatry* 63, 118–124.
- Fan, Y., Liu, Y., Wu, H., Hao, Y., Liu, H., Liu, Z., Jiang, T., 2011. Discriminant analysis of functional connectivity patterns on Grassmann manifold. *NeuroImage* 56, 2058–2067. <http://dx.doi.org/10.1016/j.neuroimage.2011.03.051>.
- Fan, Y., Resnick, S.M., Wu, X., Davatzikos, C., 2008b. Structural and functional biomarkers of prodromal Alzheimer's disease: a high-dimensional pattern classification study. *NeuroImage* 41, 277–285.
- Fan, Y., Shen, D., Davatzikos, C., 2005. Classification of structural images via high-dimensional image warping, robust feature extraction, and SVM. *Med. Image Comput. Assist. Interv.* 8, 1–8. http://dx.doi.org/10.1007/11566465_1.
- Fan, Y., Shen, D., Gur, R.C., Gur, R.E., Davatzikos, C., 2007. COMPARE: classification of morphological patterns using adaptive regional elements. *Comp. A J. Comp. Educ.* 26, 93–105.
- Fang, P., Zeng, L.-L., Shen, H., Wang, L., Li, B., Liu, L., Hu, D., 2012. Increased cortical-limbic anatomical network connectivity in major depression revealed by diffusion tensor imaging. *PLoS One* 7, e45972. <http://dx.doi.org/10.1371/journal.pone.0045972>.
- Farhan, S., Fahiem, M.A., Tauseef, H., 2014. An ensemble-of-classifiers based approach for early diagnosis of Alzheimer's disease: classification using structural features of brain images. *Comput. Math. Methods Med.* 2014, 862307. <http://dx.doi.org/10.1155/2014/862307>.
- Farzan, A., Mashohor, S., Ramli, A.R., Mahmud, R., 2015. Boosting diagnosis accuracy of Alzheimer's disease using high dimensional recognition of longitudinal brain atrophy patterns. *Behav. Brain Res.* 290, 124–130. <http://dx.doi.org/10.1016/j.bbr.2015.04.010>.
- Fekete, T., Wilf, M., Rubin, D., Edelman, S., Malach, R., Mujica-Parodi, L.R., 2013. Combining classification with fMRI-Derived complex network measures for potential neurodiagnostics. *PLoS One* 8. <http://dx.doi.org/10.1371/journal.pone.0062867>.
- Filipovich, R., Davatzikos, C., Initiative, A.D.N., et al., 2011. Semi-supervised pattern classification of medical images: application to mild cognitive impairment (MCI). *NeuroImage* 55, 1109–1119.
- Fisher, S.R.A., Genetiker, S., Fisher, R.A., Genetician, S., Fisher, R.A., Généticien, S., 1960. *The Design of Experiments. Oliver and Boyd Edinburgh*.
- Foland-Ross, L.C., Sacchet, M.D., Prasad, G., Gilbert, B., Thompson, P.M., Gotlib, I.H., 2015. Cortical thickness predicts the first onset of major depression in adolescence. *Int. J. Dev. Neurosci.* 46, 125–131. <http://dx.doi.org/10.1016/j.ijdevneu.2015.07.007>.
- Ford, J.M., Roach, B.J., Jorgensen, K.W., Turner, J.A., Brown, G.G., Notestine, R., Bischoff-Grethe, A., Greve, D., Wible, C., Lauriello, J., et al., 2009. Tuning in to the voices: a multisite fMRI study of auditory hallucinations. *Schizophr. Bull.* 35, 58–66.
- Franke, K., Ziegler, G., Klöppel, S., Gaser, C., Initiative, A.D.N., et al., 2010. Estimating the age of healthy subjects from T1-weighted MRI scans using kernel methods: exploring the influence of various parameters. *NeuroImage* 50, 883–892.
- Freeborough, P.A., Fox, N.C., 1998. MR image texture analysis applied to the diagnosis and tracking of Alzheimer's disease. *IEEE Trans. Med. Imaging* 17, 475–479. <http://dx.doi.org/10.1109/42.712137>.
- Frisoni, G.B., Beltramello, A., Weiss, C., Geroldi, C., Bianchetti, A., Trabucchi, M., 1996. Linear measures of atrophy in mild Alzheimer disease. *AJNR Am. J. Neuroradiol.* 17, 913–923.
- Fung, G., Deng, Y., Zhao, Q., Li, Z., Qu, M., Li, K., Zeng, Y.-W., Jin, Z., Ma, Y.-T., Yu, X., Wang, Z.-R., Shum, D.H.K., Chan, R.C.K., 2015. Distinguishing bipolar and major depressive disorders by brain structural morphometry: a pilot study. *BMC Psychiatry* 15, 298. <http://dx.doi.org/10.1186/s12888-015-0685-5>.
- Gaonkar, B., Davatzikos, C., 2013. Analytic estimation of statistical significance maps for support vector machine based multi-variate image analysis and classification. *NeuroImage* 78, 270–283.
- Gauthier, S., Reisberg, B., Zaudig, M., Petersen, R.C., Ritchie, K., Broich, K., Belleville, S., Brodaty, H., Bennett, D., Chertkow, H., et al., 2006. Mild cognitive impairment. *Lancet* 367, 1262–1270.
- Gerardin, E., Chételat, G., Chupin, M., Cuingnet, R., Desgranges, B., Kim, H.-S., Niethammer, M., Dubois, B., Lehéricy, S., Garnero, L., Eustache, F., Colliot, O., 2009. Multidimensional classification of hippocampal shape features discriminates Alzheimer's disease and mild cognitive impairment from normal aging. *NeuroImage* 47, 1476–1486. <http://dx.doi.org/10.1016/j.neuroimage.2009.05.036>.
- Gill, P.M.W., 2007. Efficient calculation of p-values in linear-statistic permutation significance tests. *J. Stat. Comput. Simul.* 77, 55–61.
- Gollub, R.L., Shoemaker, J.M., King, M.D., White, T., Ehrlich, S., Sponheim, S.R., Clark, V.P., Turner, J.A., Mueller, B.A., Magnotta, V., et al., 2013. The MCIC collection: a shared repository of multi-modal, multi-site brain image data from a clinical investigation of schizophrenia. *Neuroinformatics* 11, 367–388.
- Gong, Q., Wu, Q., Scarpazza, C., Lui, S., Jia, Z., Marquand, A., Huang, X., McGuire, P., Mechelli, A., 2011. Prognostic prediction of therapeutic response in depression using high-field MR imaging. *NeuroImage* 55, 1497–1503. <http://dx.doi.org/10.1016/j.neuroimage.2010.11.079>.
- Good, P.I., 2006. *Permutation, Parametric, and Bootstrap Tests of Hypotheses*. Springer Science & Business Media.
- Gori, I., Giuliano, A., Muratori, F., Saviozzi, I., Oliva, P., Tancredi, R., Cosenza, A., Tosetti, M., Calderoni, S., Retico, A., 2015. Gray matter alterations in young children with autism spectrum disorders: comparing morphometry at the voxel and regional level. *J. Neuroimaging* 25, 866–874. <http://dx.doi.org/10.1111/jon.12280>.
- Goryawala, M., Zhou, Q., Barker, W., Loewenstein, D.A., Duara, R., Adjouadi, M., 2015. Inclusion of neuropsychological scores in atrophy models improves diagnostic classification of Alzheimer's disease and mild cognitive impairment. *Comput. Intell. Neurosci.* 2015, 865265. <http://dx.doi.org/10.1155/2015/865265>.
- Gould, I.C., Shepherd, A.M., Laurens, K.R., Cairns, M.J., Carr, V.J., Green, M.J., 2014. Multivariate neuroanatomical classification of cognitive subtypes in schizophrenia: a support vector machine learning approach. *NeuroImage Clin.* 6, 229–236. <http://dx.doi.org/10.1016/j.nicl.2014.09.009>.
- Graña, M., Termenon, M., Savio, A., Gonzalez-Pinto, A., Echeveste, J., Pérez, J.M.M., Besga, A., 2011. Computer aided diagnosis system for Alzheimer disease using brain diffusion tensor imaging features selected by Pearson's correlation. *Neurosci. Lett.* 502, 225–229. <http://dx.doi.org/10.1016/j.neulet.2011.07.049>.
- Granziera, C., Daducci, A., Donati, a., Bonnier, G., Romascano, D., Roche, a., Bach Cuadra, M., Schmitter, D., Klöppel, S., Meuli, R., von Gunten, a., Krueger, G., 2015. A multi-contrast MRI study of microstructural brain damage in patients with mild cognitive impairment. *NeuroImage Clin.* 8, 631–639. <http://dx.doi.org/10.1016/j.nicl.2015.06.003>.
- Gray, K.R., Aljabar, P., Heckemann, R.A., Hammers, A., Rueckert, D., Initiative, A.D.N., et al., 2013. Random forest-based similarity measures for multi-modal classification of Alzheimer's disease. *NeuroImage* 65, 167–175.
- Green, M.J., Cairns, M.J., Wu, J., Dragovic, M., Jablensky, A., Tooney, P.A., Scott, R.J., Carr, V.J., 2013. Genome-wide supported variant MIR137 and severe negative symptoms predict membership of an impaired cognitive subtype of schizophrenia. *Mol. Psychiatry* 18, 774–780.
- Greenstein, D., Malley, J.D., Weisinger, B., Clasen, L., Gogtay, N., 2012. Using multivariate machine learning methods and structural MRI to classify childhood onset

- schizophrenia and healthy controls. *Front. Psychiatry* 3, 53. <http://dx.doi.org/10.3389/fpsy.2012.00053>.
- Guo, H., Cheng, C., Cao, X., Xiang, J., Chen, J., Zhang, K., 2014a. Resting-state functional connectivity abnormalities in first-onset unmedicated depression. *Neural. Regen. Res.* 9, 153–163. <http://dx.doi.org/10.4103/1673-5374.125344>.
- Guo, W., Su, Q., Yao, D., Jiang, J., Zhang, J., Zhang, Z., Yu, L., Zhai, J., Xiao, C., 2014b. Decreased regional activity of default-mode network in unaffected siblings of schizophrenia patients at rest. *Eur. Neuropsychopharmacol.* 24, 545–552. <http://dx.doi.org/10.1016/j.euroneuro.2014.01.004>.
- Guyon, I., Elisseeff, A., 2003. An introduction to variable and feature selection. *J. Mach. Learn. Res.* 3, 1157–1182.
- Guyon, I., Weston, J., Barnhill, S., Vapnik, V., 2002. Gene selection for cancer classification using support vector machines. *Mach. Learn.* 46, 389–422.
- H2O [WWW Document], 2015. (URL <http://h2o.ai/>)
- Hall, M.A., Smith, L.A., 1998. Practical Feature Subset Selection for Machine Learning.
- Haller, S., Missonnier, P., Herrmann, F.R., Rodriguez, C., Deiber, M.-P.P., Nguyen, D., Gold, G., Lovblad, K.-O.O., Giannakopoulos, P., 2013. Individual classification of mild cognitive impairment subtypes by support vector machine analysis of white matter DTI. *AJNR Am. J. Neuroradiol.* 34, 283–291. <http://dx.doi.org/10.3174/ajnr.A3223>.
- Haller, S., Nguyen, D., Rodriguez, C., Emch, J., Gold, G., Bartsch, A., Lovblad, K.O., Giannakopoulos, P., 2010. Individual prediction of cognitive decline in mild cognitive impairment using support vector machine-based analysis of diffusion tensor imaging data. *J. Alzheimers Dis.* 22, 315–327. <http://dx.doi.org/10.3233/JAD-2010-100840>.
- Hampel, H., Teipel, S.J., Bayer, W., Alexander, G.E., Schwarz, R., Schapiro, M.B., Rapoport, S.I., Möller, H.-J., 2002. Age transformation of combined hippocampus and amygdala volume improves diagnostic accuracy in Alzheimer's disease. *J. Neurol. Sci.* 194, 15–19.
- Hart, H., Chantiluke, K., Cubillo, A.I., Smith, A.B., Simmons, A., Brammer, M.J., Marquand, A.F., Rubia, K., 2014a. Pattern classification of response inhibition in ADHD: toward the development of neurobiological markers for ADHD. *Hum. Brain Mapp.* 35, 3083–3094. <http://dx.doi.org/10.1002/hbm.22386>.
- Hart, H., Marquand, A.F., Smith, A., Cubillo, A., Simmons, A., Brammer, M., Rubia, K., 2014b. Predictive neurofunctional markers of attention-deficit/hyperactivity disorder based on pattern classification of temporal processing. *J. Am. Acad. Child Adolesc. Psychiatry* 53, 569–578.
- Hastie, T., Rosset, S., Tibshirani, R., Zhu, J., 2004. The entire regularization path for the support vector machine. *J. Mach. Learn. Res.* 5, 1391–1415.
- Hebert, L.E., Beckett, L.A., Scherr, P.A., Evans, D.A., 2001. Annual incidence of Alzheimer disease in the United States projected to the years 2000 through 2050. *Alzheimer Dis. Assoc. Disord.* 15, 169–173.
- Heinrichs, R.W., Zakzanis, K.K., 1998. Neurocognitive deficit in schizophrenia: a quantitative review of the evidence. *Neuropsychology* 12, 426.
- Hidalgo-Muñoz, A.R., Ramírez, J., Górriz, J.M., Padilla, P., 2014. Regions of interest computed by SVM wrapped method for Alzheimer's disease examination from segmented MRI. *Front. Aging Neurosci.* 6, 20. <http://dx.doi.org/10.3389/fnagi.2014.00020>.
- Hinrichs, C., Singh, V., Mukherjee, L., Xu, G., Chung, M.K., Johnson, S.C., 2009. Spatially augmented LPboosting for AD classification with evaluations on the ADNI dataset. *NeuroImage* 48, 138–149. <http://dx.doi.org/10.1016/j.neuroimage.2009.05.056>.
- Hinrichs, C., Singh, V., Xu, G., Johnson, S.C., 2011. Predictive markers for AD in a multi-modality framework: an analysis of MCI progression in the ADNI population. *NeuroImage* 55, 574–589. <http://dx.doi.org/10.1016/j.neuroimage.2010.10.081>.
- Hjelm, R.D., Calhoun, V.D., Salakhutdinov, R., Allen, E.A., Adali, T., Plis, S.M., 2014. Restricted Boltzmann machines for neuroimaging: an application in identifying intrinsic networks. *NeuroImage* 96, 245–260.
- Honorio, J., Tomasi, D., Goldstein, R.Z., Leung, H.C., Samaras, D., 2012. Can a single brain region predict a disorder? *IEEE Trans. Med. Imaging* 31, 2062–2072. <http://dx.doi.org/10.1109/TMI.2012.2206047>.
- Iannaccone, R., Hauser, T.U., Ball, J., Brandeis, D., Walitza, S., Brem, S., 2015. Classifying adolescent attention-deficit/hyperactivity disorder (ADHD) based on functional and structural imaging. *Eur. Child Adolesc. Psychiatry* 24, 1279–1289. <http://dx.doi.org/10.1007/s00787-015-0678-4>.
- Igual, L., Soliva, J.C., Escalera, S., Gimeno, R., Vilarroya, O., Radeva, P., 2012. Automatic brain caudate nuclei segmentation and classification in diagnostic of attention-deficit/hyperactivity disorder. *Comput. Med. Imaging Graphs.* 36, 591–600. <http://dx.doi.org/10.1016/j.compmedimag.2012.08.002>.
- Iidaka, T., 2015. Resting state functional magnetic resonance imaging and neural network classified autism and control. *Cortex* 63, 55–67. <http://dx.doi.org/10.1016/j.cortex.2014.08.011>.
- Ingalhalikar, M., Parker, D., Bloy, L., Roberts, T.P.L., Verma, R., 2011. Diffusion based abnormality markers of pathology: toward learned diagnostic prediction of ASD. *NeuroImage* 57, 918–927. <http://dx.doi.org/10.1016/j.neuroimage.2011.05.023>.
- Ingalhalikar, M., Smith, A.R., Bloy, L., Gur, R., Roberts, T.P.L., Verma, R., 2012. Identifying sub-populations via unsupervised cluster analysis on multi-edge similarity graphs. *Med. Image Comput. Assist. Interv.* 15, 254–261.
- Iwabuchi, S.J., Liddle, P.F., Palaniyappan, L., 2013. Clinical utility of machine-learning approaches in schizophrenia: improving diagnostic confidence for translational neuroimaging. *Front. Psychiatry* 4, 95. <http://dx.doi.org/10.3389/fpsy.2013.00095>.
- Jablensky, A., 2006. Subtyping schizophrenia: implications for genetic research. *Mol. Psychiatry* 11, 815–836.
- Jack, C.R., Bernstein, M.A., Fox, N.C., Thompson, P., Alexander, G., Harvey, D., Borowski, B., Britson, P.J., L. Whitwell, J., Ward, C., et al., 2008. The Alzheimer's disease neuroimaging initiative (ADNI): MRI methods. *J. Magn. Reson. Imaging* 27, 685–691.
- Jack, C.R., Petersen, R.C., Xu, Y.C., Waring, S.C., O'Brien, P.C., Tangalos, E.G., Smith, G.E., Ivnik, R.J., Kokmen, E., 1997. Medial temporal atrophy on MRI in normal aging and very mild Alzheimer's disease. *Neurology* 49, 786–794.
- Jafri, M.J., Pearlson, G.D., Stevens, M., Calhoun, V.D., 2008. A method for functional network connectivity among spatially independent resting-state components in schizophrenia. *NeuroImage* 39, 1666–1681.
- Janousova, E., Schwarz, D., Kasperek, T., 2015. Combining various types of classifiers and features extracted from magnetic resonance imaging data in schizophrenia recognition. *Psychiatry Res. Neuroimaging* 232, 237–249. <http://dx.doi.org/10.1016/j.pscychres.2015.03.004>.
- Jiao, Y., Chen, R., Ke, X., Chu, K., Lu, Z., Herskovits, E.H., 2010. Predictive models of autism spectrum disorder based on brain regional cortical thickness. *NeuroImage* 50, 589–599. <http://dx.doi.org/10.1016/j.neuroimage.2009.12.047>.
- Jie, B., Zhang, D., Gao, W., Wang, Q., Wee, C.-Y., Shen, D., 2014. Integration of network topological and connectivity properties for neuroimaging classification. *IEEE Trans. Biomed. Eng.* 61, 576–589. <http://dx.doi.org/10.1109/TBME.2013.2284195>.
- Jie, N., Zhu, M., Xiaoying, M., Osuch, E.A., Wammes, M., Théberge, J., Li, H., Zhang, Y., Jiang, T., Sui, J., Calhoun, V.D., 2015. Discriminating bipolar disorder from major depression based on SVM-FoBa: efficient feature selection with multimodal brain imaging data. *IEEE Trans. Auton. Ment. Dev. (In Press)*.
- Johnston, B.A., Mwangi, B., Matthews, K., Coghill, D., Konrad, K., Steele, J.D., 2014. Brainstem abnormalities in attention deficit hyperactivity disorder support high accuracy individual diagnostic classification. *Hum. Brain Mapp.* 35, 5179–5189. <http://dx.doi.org/10.1002/hbm.22542>.
- Jung, W.B., Lee, Y.M., Kim, Y.H., Mun, C.-W., 2015. Automated classification to predict the progression of Alzheimer's disease using whole-brain volumetry and DTI. *Psychiatry Investig.* 12, 92–102. <http://dx.doi.org/10.4306/pi.2015.12.1.92>.
- Just, M.A., Cherkassky, V.L., Buchweitz, A., Keller, T.A., Mitchell, T.M., 2014. Identifying autism from neural representations of social interactions: neurocognitive markers of autism. *PLoS One* 9, e113879. <http://dx.doi.org/10.1371/journal.pone.0113879>.
- Kambeitz, J., Kambeitz-Ilankovic, L., Leucht, S., Wood, S., Davatzikos, C., Malchow, B., Falkai, P., Koutsouleris, N., 2015. Detecting neuroimaging biomarkers for schizophrenia: a meta-analysis of multivariate pattern recognition studies. *Neuropsychopharmacology* 40 (7), 1742–1751.
- Karageorgiou, E., Schulz, S.C., Gollub, R.L., Andreasen, N.C., Ho, B.-C.C., Lauriello, J., Calhoun, V.D., Bockholt, H.J., Sponheim, S.R., Georgopoulos, A.P., 2011. Neuropsychological testing and structural magnetic resonance imaging as diagnostic biomarkers early in the course of schizophrenia and related psychoses. *Neuroinformatics* 9, 321–333. <http://dx.doi.org/10.1007/s12021-010-9094-6>.
- Kasperek, T., Thomaz, C.E., Sato, J.R., Schwarz, D., Janousova, E., Marecek, R., Prikyr, R., Vanicek, J., Fujita, A., Ceskova, E., 2011. Maximum-uncertainty linear discrimination analysis of first-episode schizophrenia subjects. *Psychiatry Res. Neuroimaging* 191, 174–181. <http://dx.doi.org/10.1016/j.pscychres.2010.09.016>.
- Kaufer, D.I., Miller, B.L., Itti, L., Fairbanks, L.A., Li, J., Fishman, J., Kushi, J., Cummings, J.L., 1997. Midline cerebral morphology distinguishes frontotemporal dementia and Alzheimer's disease. *Neurology* 48, 978–985.
- Kaufmann, T., Skatun, K.C., Alnaes, D., Doan, N.T., Duff, E.P., Tonnesen, S., Rousso, E., Ueland, T., Aminoff, S.R., Lagerberg, T.V., Agartz, I., Melle, I.S., Smith, S.M., Andreassen, O.A., Westlye, L.T., 2015. Disintegration of sensorimotor brain networks in schizophrenia. *Schizophr. Bull.* 1–10. <http://dx.doi.org/10.1093/schbul/sbv060>.
- Kawasaki, Y., Suzuki, M., Kherif, F., Takahashi, T., Zhou, S.Y., Nakamura, K., Matsui, M., Sumiyoshi, T., Seto, H., Kurachi, M., 2007. Multivariate voxel-based morphology successfully differentiates schizophrenia patients from healthy controls. *NeuroImage* 34, 235–242. <http://dx.doi.org/10.1016/j.neuroimage.2006.08.018>.
- Keator, D.B., Grethe, J.S., Marcus, D., Ozyurt, B., Gadde, S., Murphy, S., Pieper, S., Greve, D., Notestine, R., Bockholt, H.J., et al., 2008. A national human neuroimaging collaborative enabled by the Biomedical Informatics Research Network (BIRN). *IEEE Trans. Inf. Technol. Biomed.* 12, 162–172.
- Kessler, R.C., Berglund, P., Demler, O., Jin, R., Koretz, D., Merikangas, K.R., Rush, A.J., Walters, E.E., Wang, P.S., 2003. The epidemiology of major depressive disorder: results from the National Comorbidity Survey Replication (NCS-R). *JAMA* 289, 3095–3105.
- Kessler, R.C., McGonagle, K.A., Zhao, S., Nelson, C.B., Hughes, M., Eshleman, S., Wittchen, H.-U., Kendler, K.S., 1994. Lifetime and 12-month prevalence of DSM-III-R psychiatric disorders in the United States: results from the National Comorbidity Survey. *Arch. Gen. Psychiatry* 51, 8–19.
- Khazaei, A., Ebrahimzadeh, A., Babajani-Feremi, A., 2015. Identifying patients with Alzheimer's disease using resting-state fMRI and graph theory. *Clin. Neurophysiol.* 126, 2132–2141. <http://dx.doi.org/10.1016/j.clinph.2015.02.060>.
- Kim, J., Calhoun, V.D., Shim, E., Lee, J.-H., 2015. Deep neural network with weight sparsity control and pre-training extracts hierarchical features and enhances classification performance: evidence from whole-brain resting-state functional connectivity patterns of schizophrenia. *NeuroImage* 124, 127–146. <http://dx.doi.org/10.1016/j.neuroimage.2015.05.018>.
- Kim, D.I., Sui, J., Rachakonda, S., White, T., Manoach, D.S., Clark, V.P., Ho, B.C., Schulz, S.C., Calhoun, V.D., 2010. Identification of imaging biomarkers in schizophrenia: a coefficient-constrained independent component analysis of the mind multi-site schizophrenia study. *Neuroinformatics* 1–17.
- Klöppel, S., Abdulkadir, A., Jack, C.R., Koutsouleris, N., Mourão-Miranda, J., Vemuri, P., 2012. Diagnostic neuroimaging across diseases. *NeuroImage* 61, 457–463. <http://dx.doi.org/10.1016/j.neuroimage.2011.11.002>.
- Klöppel, S., Chu, C., Tan, G.C., Draganski, B., Johnson, H., Paulsen, J.S., Kienzle, W., Tabrizi, S.J., Ashburner, J., Frackowiak, R.S.J., et al., 2009. Automatic detection of preclinical neurodegeneration presymptomatic Huntington disease. *Neurology* 72, 426–431.
- Klöppel, S., Peter, J., Ludl, A., Pilatus, A., Maier, S., Mader, I., Heimbach, B., Frings, L., Egger, K., Dukart, J., Schroeter, M.L., Perneckzy, R., Häussermann, P., Vach, W., Urbach, H., Teipel, S., Hüll, M., Abdulkadir, A., 2015. Applying automated MR-based diagnostic methods to the memory clinic: a prospective study. *J. Alzheimers Dis.* 47, 939–954. <http://dx.doi.org/10.3233/JAD-150334>.

- Klöppel, S., Stonnington, C.M., Chu, C., Draganski, B., Scahill, R.I., Rohrer, J.D., Fox, N.C., Jack, C.R., Ashburner, J., Frackowiak, R.S.J., 2008. Automatic classification of MR scans in Alzheimer's disease. *Brain* 131, 681–689. <http://dx.doi.org/10.1093/brain/awm319>.
- Koch, S.P., Hägele, C., Haynes, J.-D., Heinz, A., Schlagenhaut, F., Sterzer, P., 2015. Diagnostic classification of schizophrenia patients on the basis of regional reward-related fMRI signal patterns. *PLoS One* 10, e0119089. <http://dx.doi.org/10.1371/journal.pone.0119089>.
- Kohavi, R., John, G.H., 1997. Wrappers for feature subset selection. *Artif. Intell.* 97, 273–324.
- Koutsouleris, N., Meisenzahl, E.M., Borgwardt, S., Riecher-Rössler, a., Frodl, T., Kambitz, J., Kohler, Y., Falkai, P., Moller, H.-J., Reiser, M., Davatzikos, C., 2015. Individualized differential diagnosis of schizophrenia and mood disorders using neuroanatomical biomarkers. *Brain* <http://dx.doi.org/10.1093/brain/awv111>.
- Kriegeskorte, N., 2015. Deep neural networks: a new framework for modelling biological vision and brain information processing. *Bioresources* xiv, 29876.
- Lahmiri, S., Boukadoum, M., Lahmiri, S., 2014. New approach for automatic classification of Alzheimer's disease, mild cognitive impairment and healthy brain magnetic resonance images. *Heal. Technol. Lett.* 1, 32–36. <http://dx.doi.org/10.1049/htl.2013.0022>.
- Landis, D., Courtney, W., Dieringer, C., Kelly, R., King, M., Miller, B., Wang, R., Wood, D., Turner, J.A., Calhoun, V.D., 2016. An open platform for compiling, curating, and disseminating neuroimaging data. *NeuroImage* 124, 1084–1088.
- Le Bihan, D., Mangin, J.F., Poupon, C., Clark, C.A., Pappata, S., Molko, N., Chabriat, H., 2001. Diffusion tensor imaging: concepts and applications. *J. Magn. Reson. Imaging* 13, 534–546.
- Lee, G.-Y., Kim, J., Kim, J.H., Kim, K., Seong, J.-K., 2014. Online learning for classification of Alzheimer disease based on cortical thickness and hippocampal shape analysis. *Heal. Inf. Res* 20, 61–68. <http://dx.doi.org/10.4258/hir.2014.20.1.61>.
- Lee, W., Park, B., Han, K., 2013. Classification of diffusion tensor images for the early detection of Alzheimer's disease. *Comput. Biol. Med.* 43, 1313–1320. <http://dx.doi.org/10.1016/j.compbiomed.2013.07.004>.
- Lemm, S., Blankertz, B., Dickhaus, T., Müller, K.R., 2011. Introduction to machine learning for brain imaging. *NeuroImage* 56, 387–399. <http://dx.doi.org/10.1016/j.neuroimage.2010.11.004>.
- Lerch, J.P., Pruessner, J., Zijdenbos, A.P., Collins, D.L., Teipel, S.J., Hampel, H., Evans, A.C., 2008. Automated cortical thickness measurements from MRI can accurately separate Alzheimer's patients from normal elderly controls. *Neurobiol. Aging* 29, 23–30. <http://dx.doi.org/10.1016/j.neurobiolaging.2006.09.013>.
- Levman, J., Takahashi, E., 2015. Multivariate analyses applied to fetal, neonatal and pediatric MRI of neurodevelopmental disorders. *NeuroImage Clin.* 9, 532–544. <http://dx.doi.org/10.1016/j.nicl.2015.09.017>.
- Lewinsohn, P.M., Duncan, E.M., Stanton, A.K., Hautzinger, M., 1986. Age at first onset for nonbipolar depression. *J. Abnorm. Psychol.* 95, 378.
- Li, M., Oishi, K., He, X., Qin, Y., Gao, F., Mori, S., 2014a. An efficient approach for differentiating Alzheimer's disease from normal elderly based on multicenter MRI using gray-level invariant features. *PLoS One* 9, e105563. <http://dx.doi.org/10.1371/journal.pone.0105563>.
- Li, M., Qin, Y., Gao, F., Zhu, W., He, X., 2014b. Discriminative analysis of multivariate features from structural MRI and diffusion tensor images. *Magn. Reson. Imaging* 32, 1043–1051. <http://dx.doi.org/10.1016/j.mri.2014.05.008>.
- Li, S., Shi, F., Pu, F., Li, X., Jiang, T., Xie, S., Wang, Y., 2007. Hippocampal shape analysis of Alzheimer disease based on machine learning methods. *AJNR Am. J. Neuroradiol.* 28, 1339–1345. <http://dx.doi.org/10.3174/ajnr.A0620>.
- Li, Y., Wang, Y., Wu, G., Shi, F., Zhou, L., Lin, W., Shen, D., 2012. Discriminant analysis of longitudinal cortical thickness changes in Alzheimer's disease using dynamic and network features. *Neurobiol. Aging* 33 (427). <http://dx.doi.org/10.1016/j.neurobiolaging.2010.11.008> (e15–30).
- Liang, Z.-P., Lauterbur, P.C., 2000. Principles of Magnetic Resonance Imaging. SPIE Optical Engineering Press.
- Libero, L.E., Deramus, T.P., Lahti, A.C., Deshpande, G., Kana, R.K., 2015. Multimodal neuroimaging based classification of autism spectrum disorder using anatomical, neurochemical, and white matter correlates. *Cortex* 66, 46–59. <http://dx.doi.org/10.1016/j.cortex.2015.02.008>.
- Lillemark, L., Sorensen, L., Pai, A., Dam, E.B., Nielsen, M., 2014. Brain region's relative proximity as marker for Alzheimer's disease based on structural MRI. *BMC Med. Imaging* 14, 21. <http://dx.doi.org/10.1186/1471-2342-14-21>.
- Lim, L., Marquand, A., Cubillo, A.A., Smith, A.B., Chantiluke, K., Simmons, A., Mehta, M., Rubia, K., 2013. Disorder-Specific Predictive Classification of Adolescents with Attention Deficit Hyperactivity Disorder (ADHD) Relative to Autism Using Structural Magnetic Resonance Imaging.
- Liu, X., Tosun, D., Weiner, M.W., Schuff, N., 2013. Locally linear embedding (LLE) for MRI based Alzheimer's disease classification. *NeuroImage* 83, 148–157. <http://dx.doi.org/10.1016/j.neuroimage.2013.06.033>.
- Liu, F., Wee, C.-Y., Chen, H., Shen, D., 2014a. Inter-modality relationship constrained multi-modality multi-task feature selection for Alzheimer's disease and mild cognitive impairment identification. *NeuroImage* 84, 466–475. <http://dx.doi.org/10.1016/j.neuroimage.2013.09.015>.
- Liu, M., Zhang, D., Adeli-Mosabbeh, E., Shen, D., 2015. Inherent structure based multi-view learning with multi-template feature representation for Alzheimer's disease diagnosis. *IEEE Trans. Biomed. Eng.* <http://dx.doi.org/10.1109/TBME.2015.2496233>.
- Liu, M., Zhang, D., Shen, D., 2014b. Hierarchical fusion of features and classifier decisions for Alzheimer's disease diagnosis. *Hum. Brain Mapp.* 35, 1305–1319. <http://dx.doi.org/10.1002/hbm.22254>.
- Lord, A., Horn, D., Breakpear, M., Walter, M., 2012. Changes in community structure of resting state functional connectivity in unipolar depression. *PLoS One* 7, e41282. <http://dx.doi.org/10.1371/journal.pone.0041282>.
- Lorenzetti, V., Allen, N.B., Fornito, A., Yücel, M., 2009. Structural brain abnormalities in major depressive disorder: a selective review of recent MRI studies. *J. Affect. Disord.* 117, 1–17.
- Ludman, E.J., Fullerton, S.M., Spangler, L., Trinidad, S.B., Fujii, M.M., Jarvik, G.P., Larson, E.B., Burke, W., 2010. Glad you asked: participants' opinions of re-consent for dbGap data submission. *J. Empir. Res. Hum. Res. Ethics* 5, 9–16.
- Ma, Z., Li, R., Yu, J., He, Y., Li, J., 2013. Alterations in regional homogeneity of spontaneous brain activity in late-life subthreshold depression. *PLoS One* 8, e53148. <http://dx.doi.org/10.1371/journal.pone.0053148>.
- MacMaster, F.P., Carrey, N., Langevin, L.M., Jaworska, N., Crawford, S., 2014. Disorder-specific volumetric brain difference in adolescent major depressive disorder and bipolar depression. *Brain Imaging Behav.* 8, 119–127. <http://dx.doi.org/10.1007/s11682-013-9264-x>.
- Magnin, B., Mesrob, L., Kinkingnéhun, S., Pélégriani-Issac, M., Colliot, O., Sarazin, M., Dubois, B., Lehericy, S., Benali, H., 2009. Support vector machine-based classification of Alzheimer's disease from whole-brain anatomical MRI. *Neuroradiology* 51, 73–83. <http://dx.doi.org/10.1007/s00234-008-0463-x>.
- Mahanand, B.S., Suresh, S., Sundararajan, N., Aswatha Kumar, M., 2012. Identification of brain regions responsible for Alzheimer's disease using a Self-adaptive Resource Allocation Network. *Neural Netw.* 32, 313–322. <http://dx.doi.org/10.1016/j.neunet.2012.02.035>.
- Marcus, D.S., Olsen, T.R., Ramaratnam, M., Buckner, R.L., 2007. The extensible neuroimaging archive toolkit. *Neuroinformatics* 5, 11–33.
- McAlonan, G.M., Cheung, V., Cheung, C., Suckling, J., Lam, G.Y., Tai, K.S., Yip, L., Murphy, D.G.M., Chua, S.E., 2005. Mapping the brain in autism. A voxel-based MRI study of volumetric differences and intercorrelations in autism. *Brain* 128, 268–276.
- McCarley, R.W., Nakamura, M., Shenton, M.E., Salisbury, D.F., 2008. Combining ERP and structural MRI information in first episode schizophrenia and bipolar disorder. *Clin. EEG Neurosci.* 39, 57–60.
- McEvoy, L.K., Fennema-Notestine, C., Roddey, J.C., Hagler, D.J., Holland, D., Karow, D.S., Pung, C.J., Brewer, J.B., Dale, A.M., 2009. Alzheimer disease: quantitative structural neuroimaging for detection and prediction of clinical and structural changes in mild cognitive impairment. *Radiology* 251, 195–205. <http://dx.doi.org/10.1148/radiol.2511080924>.
- McEvoy, L.K., Holland, D., Hagler, D.J., Fennema-Notestine, C., Brewer, J.B., Dale, A.M., 2011. Mild cognitive impairment: baseline and longitudinal structural MR imaging measures improve predictive prognosis. *Radiology* 259, 834–843. <http://dx.doi.org/10.1148/radiol.11101975>.
- Mehta, C.R., Patel, N.R., Senchaudhuri, P., 1988. Importance sampling for estimating exact probabilities in permutational inference. *J. Am. Stat. Assoc.* 83, 999–1005.
- Merboldt, K.-D., Hancic, W., Frahm, J., 1985. Self-diffusion NMR imaging using stimulated echoes. *J. Magn. Reson.* 64, 479–486.
- Michael, A.M., Baum, S.A., Fries, J.F., Ho, B.C., Pierson, R.K., Andreasen, N.C., Calhoun, V.D., 2009. A method to fuse fMRI tasks through spatial correlations: applied to schizophrenia. *Hum. Brain Mapp.* 30, 2512–2529.
- Miller, M.L., Priebe, C.E., Qiu, A., Fischl, B., Kolasny, A., Brown, T., Park, Y., Ratnanather, J.T., Busa, E., Jovicich, J., Yu, P., Dickerson, B.C., Buckner, R.L., 2009. Collaborative computational anatomy: an MRI morphometry study of the human brain via diffeomorphic metric mapping. *Hum. Brain Mapp.* 30, 2132–2141. <http://dx.doi.org/10.1002/hbm.20655>.
- Min, R., Wu, G., Cheng, J., Wang, Q., Shen, D., 2014. Multi-atlas based representations for Alzheimer's disease diagnosis. *Hum. Brain Mapp.* 35, 5052–5070. <http://dx.doi.org/10.1002/hbm.22531>.
- Minshew, N.J., Payton, J.B., 1988. New perspectives in autism. Part 2: The differential diagnosis and neurobiology of autism. *Curr. Probl. Pediatr.* 18, 618–694.
- Moradi, E., Pepe, A., Gaser, C., Huttunen, H., Tohka, J., 2015. Machine learning framework for early MRI-based Alzheimer's conversion prediction in MCI subjects. *NeuroImage* 104, 398–412. <http://dx.doi.org/10.1016/j.neuroimage.2014.10.002>.
- Morar, B., Dragović, M., Waters, F.A.V., Chandler, D., Kalaydjieva, L., Jablensky, A., 2011. Neuregulin 3 (NRG3) as a susceptibility gene in a schizophrenia subtype with florid delusions and relatively spared cognition. *Mol. Psychiatry* 16, 860–866.
- Mourão-Miranda, J., Hardoon, D.R., Hahn, T., Marquand, A.F., Williams, S.C.R.R., Shawe-Taylor, J., Brammer, M., 2011. Patient classification as an outlier detection problem: an application of the One-Class Support Vector Machine. *NeuroImage* 58, 793–804. <http://dx.doi.org/10.1016/j.neuroimage.2011.06.042>.
- Mourão-Miranda, J., Oliveira, L., Ladouceur, C.D., Marquand, A., Brammer, M., Birmaher, B., Axelson, D., Phillips, M.L., 2012. Pattern recognition and functional neuroimaging help to discriminate healthy adolescents at risk for mood disorders from low risk adolescents. *PLoS One* 7, e29482. <http://dx.doi.org/10.1371/journal.pone.0029482>.
- Mueller, S.G., Schuff, N., Yaffe, K., Madison, C., Miller, B., Weiner, M.W., 2010. Hippocampal atrophy patterns in mild cognitive impairment and Alzheimer's disease. *Hum. Brain Mapp.* 31, 1339–1347. <http://dx.doi.org/10.1002/hbm.20934>.
- Murdaugh, D.L., Shinkareva, S.V., Deshpande, H.R., Wang, J., Pennick, M.R., Kana, R.K., 2012. Differential Deactivation during Mentalizing and Classification of Autism Based on Default Mode Network Connectivity.
- Mwangi, B., Ebmeier, K.P., Matthews, K., Steele, J.D., 2012. Multi-centre diagnostic classification of individual structural neuroimaging scans from patients with major depressive disorder. *Brain* 135, 1508–1521. <http://dx.doi.org/10.1093/brain/awj084>.
- Nakamura, K., Kawasaki, Y., Suzuki, M., Hagino, H., Kurokawa, K., Takahashi, T., Niu, L., Matsui, M., Seto, H., Kurachi, M., 2004. Multiple structural brain measures obtained by three-dimensional magnetic resonance imaging to distinguish between schizophrenia patients and normal subjects. *Schizophr. Bull.* 30, 393–404.
- Ng, A.Y., 2004. Feature selection, L1 vs. L2 regularization, and rotational invariance. *Proceedings of the Twenty-first International Conference on Machine Learning*, p. 78.
- Nieuwenhuis, M., van Haren, N.E.M., Hulshoff Pol, H.E., Cahn, W., Kahn, R.S., Schnack, H.G., 2012. Classification of schizophrenia patients and healthy controls from structural

- MRI scans in two large independent samples. *NeuroImage* 61, 606–612. <http://dx.doi.org/10.1016/j.neuroimage.2012.03.079>.
- Nir, T.M., Villalón-Reina, J.E., Prasad, G., Jahanshad, N., Joshi, S.H., Toga, A.W., Bernstein, M.A., Jack, C.R., Weiner, M.W., Thompson, P.M., 2015. Diffusion weighted imaging-based maximum density path analysis and classification of Alzheimer's disease. *Neurobiol. Aging* 36 (Suppl. 1), S132–S140. <http://dx.doi.org/10.1016/j.neurobiolaging.2014.05.037>.
- O'Dwyer, L., Lambertson, F., Bokde, A.L., Ewers, M., Faluyi, Y.O., Tanner, C., Mazoyer, B., O'Neill, D., Bartley, M., Collins, D.R., et al., 2012. Using support vector machines with multiple indices of diffusion for automated classification of mild cognitive impairment. *PLoS One* 7, e32441.
- Ogawa, S., Lee, T.-M., Kay, A.R., Tank, D.W., 1990. Brain magnetic resonance imaging with contrast dependent on blood oxygenation. *Proc. Natl. Acad. Sci.* 87, 9868–9872.
- Oishi, K., Akhter, K., Mielke, M., Ceritoglu, C., Zhang, J., Jiang, H., Li, X., Younes, L., Miller, M.I., van Zijl, P.C.M., Albert, M., Lyketos, C.G., Mori, S., 2011. Multi-modal MRI analysis with disease-specific spatial filtering: initial testing to predict mild cognitive impairment patients who convert to Alzheimer's disease. *Front. Neurol.* 2, 54. <http://dx.doi.org/10.3389/fneur.2011.00054>.
- Oliveira, P.P. de M., Nitrini, R., Busatto, G., Buchpiguel, C., Sato, J.R., Amaro, E., 2010. Use of SVM methods with surface-based cortical and volumetric subcortical measurements to detect Alzheimer's disease. *J. Alzheimers Dis.* 19, 1263–1272. <http://dx.doi.org/10.3233/JAD-2010-1322>.
- Orrù, G., Pettersson-Yeo, W., Marquand, A.F., Sartori, G., Mechelli, A., 2012. Using support vector machine to identify imaging biomarkers of neurological and psychiatric disease: a critical review. *Neurosci. Biobehav. Rev.* 36, 1140–1152. <http://dx.doi.org/10.1016/j.neubiorev.2012.01.004>.
- Ortiz, A., Munilla, J., Álvarez-Illán, I., Górriz, J.M., Ramírez, J., 2015. Exploratory graphical models of functional and structural connectivity patterns for Alzheimer's disease diagnosis. *Front. Comput. Neurosci.* 9, 132. <http://dx.doi.org/10.3389/fncom.2015.00132>.
- Ota, M., Ishikawa, M., Sato, N., Hori, H., Sasayama, D., Hattori, K., Teraishi, T., Noda, T., Obu, S., Nakata, Y., Higuchi, T., Kunugi, H., 2013. Discrimination between schizophrenia and major depressive disorder by magnetic resonance imaging of the female brain. *J. Psychiatr. Res.* 47, 1383–1388. <http://dx.doi.org/10.1016/j.jpsychires.2013.06.010>.
- Ota, K., Oishi, N., Ito, K., Fukuyama, H., 2014. A comparison of three brain atlases for MCI prediction. *J. Neurosci. Methods* 221, 139–150. <http://dx.doi.org/10.1016/j.jneumeth.2013.10.003>.
- Ota, K., Oishi, N., Ito, K., Fukuyama, H., 2015. Effects of imaging modalities, brain atlases and feature selection on prediction of Alzheimer's disease. *J. Neurosci. Methods* 256, 168–183. <http://dx.doi.org/10.1016/j.jneumeth.2015.08.020>.
- Ota, M., Sato, N., Ishikawa, M., Hori, H., Sasayama, D., Hattori, K., Teraishi, T., Obu, S., Nakata, Y., Nemoto, K., Moriguchi, Y., Hashimoto, R., Kunugi, H., 2012. Discrimination of female schizophrenia patients from healthy women using multiple structural brain measures obtained with voxel-based morphometry. *Psychiatry Clin. Neurosci.* 66, 611–617. <http://dx.doi.org/10.1111/j.1440-1819.2012.02397.x>.
- Pardo, P.J., Georgopoulos, A.P., Kenny, J.T., Stuve, T.A., Findling, R.L., Schulz, S.C., 2006. Classification of adolescent psychotic disorders using linear discriminant analysis. *Schizophr. Res.* 87, 297–306. <http://dx.doi.org/10.1016/j.schres.2006.05.007>.
- Park, M.Y., Hastie, T., 2007. L1-regularization path algorithm for generalized linear models. *J. R. Stat. Soc. Ser. B (Stat. Methodol.)* 69, 659–677.
- Park, B.-Y., Kim, M., Seo, J., Lee, J., Park, H., 2015. Connectivity analysis and feature classification in attention deficit hyperactivity disorder sub-types: a task functional magnetic resonance imaging study. *Brain Topogr.* <http://dx.doi.org/10.1007/s10548-015-0463-1>.
- Patel, M.J., Andreescu, C., Price, J.C., Edelman, K.L., Reynolds, C.F., Aizenstein, H.J., 2015. Machine learning approaches for integrating clinical and imaging features in late-life depression classification and response prediction. *Int. J. Geriatr. Psychiatry* 30, 1056–1067. <http://dx.doi.org/10.1002/gps.4262>.
- Peng, X., Lin, P., Zhang, T., Wang, J., 2013. Extreme learning machine-based classification of ADHD using brain structural MRI data. *PLoS One* 8, e79476. <http://dx.doi.org/10.1371/journal.pone.0079476>.
- Pennanen, C., Kivipelto, M., Tuomainen, S., Hartikainen, P., Hänninen, T., Laakso, M.P., Hallikainen, M., Vanhanen, M., Nissinen, A., Helkala, E.-L., Vainio, P., Vanninen, R., Partanen, K., Soininen, H., 2004. Hippocampus and entorhinal cortex in mild cognitive impairment and early AD. *Neurobiol. Aging* 25, 303–310. [http://dx.doi.org/10.1016/S0197-4580\(03\)00084-8](http://dx.doi.org/10.1016/S0197-4580(03)00084-8).
- Pereira, F., Mitchell, T., Botvinick, M., 2009. Machine learning classifiers and fMRI: a tutorial overview. *NeuroImage* 45, S199–S209.
- Petersen, R.C., Negash, S., 2008. Mild cognitive impairment: an overview. *CNS Spectr.* 13, 45–53.
- Pina-Camacho, L., Garcia-Prieto, J., Parellada, M., Castro-Fornieles, J., Gonzalez-Pinto, A.M., Bombin, I., Graell, M., Paya, B., Rapado-Castro, M., Janssen, J., Baeza, I., Del Pozo, F., Desco, M., Arango, C., Pozo, F., Del Desco, M., Arango, C., 2015. Predictors of schizophrenia spectrum disorders in early-onset first episodes of psychosis: a support vector machine model. *Eur. Child Adolesc. Psychiatry* 24, 427–440. <http://dx.doi.org/10.1007/s00787-014-0593-0>.
- Plant, C., Teipel, S.J., Oswald, A., Böhm, C., Meindl, T., Mourao-Miranda, J., Bokde, A.W., Hampel, H., Ewers, M., 2010. Automated detection of brain atrophy patterns based on MRI for the prediction of Alzheimer's disease. *NeuroImage* 50, 162–174. <http://dx.doi.org/10.1016/j.neuroimage.2009.11.046>.
- Plis, S.M., Hjelm, D., Salakhutdinov, R., Allen, E.A., Bockholt, H.J., Long, J.D., Johnson, H.J., Paulsen, J., Turner, J.A., Calhoun, V.D., 2014. Deep learning for neuroimaging: a validation study. *Front. Neurosci.* 8.
- Plitt, M., Barnes, K.A., Martin, A., 2015. Functional connectivity classification of autism identifies highly predictive brain features but falls short of biomarker standards. *NeuroImage Clin.* 7, 359–366. <http://dx.doi.org/10.1016/j.nicl.2014.12.013>.
- Polat, F., Demirel, S.O., Kitis, O., Simsek, F., Haznedaroglu, D.I., Coburn, K., Kumral, E., Gonul, A.S., 2012. Computer based classification of MR scans in first time applicant Alzheimer patients. *Curr. Alzheimer Res.* 9, 789–794.
- Poldrack, R.A., Barch, D.M., Mitchell, J.P., Wager, T.D., Wagner, A.D., Devlin, J.T., Cumba, C., Koyejo, O., Milham, M.P., 2013. Toward open sharing of task-based fMRI data: the OpenfMRI project. *Front. Neuroinform.* 7. <http://dx.doi.org/10.3389/fninf.2013.00012>.
- Power, J.D., Barnes, K.A., Snyder, A.Z., Schlaggar, B.L., Petersen, S.E., 2012. Spurious but systematic correlations in functional connectivity MRI networks arise from subject motion. *NeuroImage* 59, 2142–2154.
- Power, J.D., Mitra, A., Laumann, T.O., Snyder, A.Z., Schlaggar, B.L., Petersen, S.E., 2014. Methods to detect, characterize, and remove motion artifact in resting state fMRI. *NeuroImage* 84, 320–341.
- Power, J.D., Schlaggar, B.L., Petersen, S.E., 2015. Recent progress and outstanding issues in motion correction in resting state fMRI. *NeuroImage* 105, 536–551.
- Prasad, G., Joshi, S.H., Nir, T.M., Toga, A.W., Thompson, P.M., 2015. Brain connectivity and novel network measures for Alzheimer's disease classification. *Neurobiol. Aging* 36 (Suppl. 1), S121–S131. <http://dx.doi.org/10.1016/j.neurobiolaging.2014.04.037>.
- Qiu, A., Younes, L., Miller, M.I., Csernansky, J.G., 2008. Parallel transport in diffeomorphisms distinguishes the time-dependent pattern of hippocampal surface deformation due to healthy aging and the dementia of the Alzheimer's type. *NeuroImage* 40, 68–76. <http://dx.doi.org/10.1016/j.neuroimage.2007.11.041>.
- Raamana, P.R., Wen, W., Kochan, N.A., Brodaty, H., Sachdev, P.S., Wang, L., Beg, M.F., 2014. Novel ThickNet features for the discrimination of amnesic MCI subtypes. *NeuroImage Clin.* 6, 284–295. <http://dx.doi.org/10.1016/j.nicl.2014.09.005>.
- Radulescu, E., Ganesan, B., Shergill, S.S., Medford, N., Chatwin, C., Young, R.C.D., Critchley, H.D., 2014. Grey-matter texture abnormalities and reduced hippocampal volume are distinguishing features of schizophrenia. *Psychiatry Res.* 223, 179–186. <http://dx.doi.org/10.1016/j.psychres.2014.05.014>.
- Retico, A., Bosco, P., Cerello, P., Fiorina, E., Chincarini, A., Fantacci, M.E., 2015. Predictive models based on support vector machines: whole-brain versus regional analysis of structural MRI in the Alzheimer's disease. *J. Neuroimaging* 25, 552–563. <http://dx.doi.org/10.1111/jon.12163>.
- Retico, A., Tosetti, M., Muratori, F., Calderoni, S., 2013. Neuroimaging-based methods for autism identification: a possible translational application? *Funct. Neurol.* 29, 231–239.
- Retico, A., Tosetti, M., Muratori, F., Calderoni, S., 2014. Neuroimaging-based methods for autism identification: a possible translational application? *Funct. Neurol.* 29, 231–239.
- Rice, D.P., 1999. The economic impact of schizophrenia. *J. Clin. Psychiatry* 60 (suppl 1), 1–478.
- Rosa, M.J., Portugal, L., Hahn, T., Fallgatter, A.J., Garrido, M.I., Shawe-Taylor, J., Mourao-Miranda, J., 2015. Sparse network-based models for patient classification using fMRI. *NeuroImage* 105, 493–506. <http://dx.doi.org/10.1016/j.neuroimage.2014.11.021>.
- Sabuncu, M.R., Van Leemput, K., 2012. The relevance voxel machine (RVoxM): a self-tuning Bayesian model for informative image-based prediction. *IEEE Trans. Med. Imaging* 31, 2290–2306. <http://dx.doi.org/10.1109/TMI.2012.2216543>.
- Sacchet, M.D., Livermore, E.E., Iglesias, J.E., Glover, G.H., Gotlib, I.H., 2015. Subcortical volumes differentiate major depressive disorder, bipolar disorder, and remitted major depressive disorder. *J. Psychiatr. Res.* 68, 91–98. <http://dx.doi.org/10.1016/j.jpsychires.2015.06.002>.
- Salvatore, C., Cerasa, A., Battista, P., Gilardi, M.C., Quattrone, A., Castiglioni, I., 2015. Magnetic resonance imaging biomarkers for the early diagnosis of Alzheimer's disease: a machine learning approach. *Front. Neurosci.* 9, 307. <http://dx.doi.org/10.3389/fnins.2015.00307>.
- Sarwate, A.D., Plis, S.M., Turner, J.A., Arbabshirani, M.R., Calhoun, V.D., 2014. Sharing privacy-sensitive access to neuroimaging and genetics data: a review and preliminary validation. *Front. Neuroinform.* 8, 35. <http://dx.doi.org/10.3389/fninf.2014.00035>.
- Sato, J.R., Hoexter, M.Q., Fujita, A., Rohde, L.A., 2012. Evaluation of pattern recognition and feature extraction methods in ADHD prediction. *Front. Syst. Neurosci.* 6, 68. <http://dx.doi.org/10.3389/fnsys.2012.00068>.
- Sato, J.R., Hoexter, M.Q., Oliveira, P.P.D.M., Brammer, M.J., Murphy, D., Ecker, C., 2013. Inter-regional cortical thickness correlations are associated with autistic symptoms: a machine-learning approach. *J. Psychiatr. Res.* 47, 453–459. <http://dx.doi.org/10.1016/j.jpsychires.2012.11.017>.
- Sato, J.R., Moll, J., Green, S., Deakin, J.F.W., Thomaz, C.E., Zahn, R., 2015. Machine learning algorithm accurately detects fMRI signature of vulnerability to major depression. *Psychiatry Res.* 233, 289–291. <http://dx.doi.org/10.1016/j.psychres.2015.07.001>.
- Schnack, H.G., Nieuwenhuis, M., van Haren, N.E.M., Abramow, L., Scheewe, T.W., Brouwer, R.M., Hulshoff Pol, H.E., Kahn, R.S., 2014. Can structural MRI aid in clinical classification? A machine learning study in two independent samples of patients with schizophrenia, bipolar disorder and healthy subjects. *NeuroImage* 84, 299–306. <http://dx.doi.org/10.1016/j.neuroimage.2013.08.053>.
- Scott, A., Courtney, W., Wood, D., la Garza, R., Lane, S., King, M., Wang, R., Roberts, J., Turner, J.A., Calhoun, V.D., 2011. COINS: an innovative informatics and neuroimaging tool suite built for large heterogeneous datasets. *Front. Neuroinform.* 5.
- Segovia, F., Holt, R., Spencer, M., Górriz, J.M., Ramírez, J., Puntonet, C.G., Phillips, C., Chura, L., Baron-Cohen, S., Suckling, J., 2014. Identifying endophenotypes of autism: a multivariate approach. *Front. Comput. Neurosci.* 8.
- Semrud-Clikeman, M., Hooper, S.R., Hynd, G.W., Hern, K., Presley, R., Watson, T., 1996. Prediction of group membership in developmental dyslexia, attention deficit hyperactivity disorder, and normal controls using brain morphometric analysis of magnetic resonance imaging. *Arch. Clin. Neuropsychol.* 11, 521–528.
- Serpa, M.H., Ou, Y., Schaufelberger, M.S., Doshi, J., Ferreira, L.K., Machado-Vieira, R., Menezes, P.R., Sczufca, M., Davatzikos, C., Busatto, G.F., Zanetti, M.V., 2014. Neuroanatomical classification in a population-based sample of psychotic major depression

- and bipolar I disorder with 1 year of diagnostic stability. *Biomed. Res. Int.* 2014, 706157. <http://dx.doi.org/10.1155/2014/706157>.
- Shen, H., Wang, L., Liu, Y., Hu, D., 2010. Discriminative analysis of resting-state functional connectivity patterns of schizophrenia using low dimensional embedding of fMRI. *NeuroImage* 49, 3110–3121. <http://dx.doi.org/10.1016/j.neuroimage.2009.11.011>.
- Shimizu, Y., Yoshimoto, J., Toki, S., Takamura, M., Yoshimura, S., Okamoto, Y., Yamawaki, S., Doya, K., 2015. Toward probabilistic diagnosis and understanding of depression based on functional MRI data analysis with logistic group LASSO. *PLoS One* 10, e0123524. <http://dx.doi.org/10.1371/journal.pone.0123524>.
- Sidhu, G.S., Asgarian, N., Greiner, R., Brown, M.R.G., 2012. Kernel principal component analysis for dimensionality reduction in fMRI-based diagnosis of ADHD. *Front. Syst. Neurosci.* 6, 74. <http://dx.doi.org/10.3389/fnsys.2012.00074>.
- Silva, R.F., Castro, E., Gupta, C.N., Cetin, M., Arbabshirani, M., Potluru, V.K., Plis, S.M., Calhoun, V.D., 2014. The tenth annual MLSP competition: schizophrenia classification challenge the mind research network, 1101 Yale Blvd., Albuquerque, New Mexico 87106. IEEE International Workshop on Machine Learning for Signal Processing, Remis, France.
- Stonington, C.M., Chu, C., Klöppel, S., Jack, C.R., Ashburner, J., Frackowiak, R.S.J., 2010. Predicting clinical scores from magnetic resonance scans in Alzheimer's disease. *NeuroImage* 51, 1405–1413. <http://dx.doi.org/10.1016/j.neuroimage.2010.03.051>.
- Su, L., Wang, L., Shen, H., Feng, G., Hu, D., 2013. Discriminative analysis of non-linear brain connectivity in schizophrenia: an fMRI study. *Front. Hum. Neurosci.* 7, 702. <http://dx.doi.org/10.3389/fnhum.2013.00702>.
- Sui, J., He, H., Pearlson, G.D., Adali, T., Kiehl, K.A., Yu, Q., Clark, V.P., Castro, E., White, T., Mueller, B.A., et al., 2013a. Three-way (N-way) fusion of brain imaging data based on mCCA + jICA and its application to discriminating schizophrenia. *NeuroImage* 66, 119–132.
- Sui, J., He, H., Yu, Q., Chen, J., Rogers, J., Pearlson, G.D., Mayer, A.R., Bustillo, J.R., Canive, J., Calhoun, V.D., 2013b. Combination of resting state fMRI, DTI, and sMRI data to discriminate schizophrenia by N-way mCCA + jICA. *Front. Hum. Neurosci.* 7, 235. <http://dx.doi.org/10.3389/fnhum.2013.00235>.
- Sui, J., Adali, T., Pearlson, G.D., Calhoun, V.D., 2009. An ICA-based method for the identification of optimal fMRI features and components using combined group-discriminative techniques. *NeuroImage* 46, 73–86.
- Sui, J., He, H., Liu, J., Yu, Q., Adali, T., Pearlson, G., Calhoun, V., 2012. Three-way fMRI-DTI-Methylation data fusion based on mCCA + jICA and its application to schizophrenia. *Eng. Med. Biol. Soc.* 2012 (EMBS 2012. 34th Annu. Int. Conf. IEEE).
- Sui, J., Pearlson, G., Caprihan, A., Adali, T., Kiehl, K.A., Liu, J., Yamamoto, J., Calhoun, V.D., 2011. Discriminating schizophrenia and bipolar disorder by fusing fMRI and DTI in a multimodal CCA + joint ICA model. *NeuroImage* 57, 839–855.
- Sui, J., Pearlson, G.D., Du, Y., Yu, Q., Jones, T.R., Chen, J., Jiang, T., Bustillo, J., Calhoun, V.D., 2015. In search of multimodal neuroimaging biomarkers of cognitive deficits in schizophrenia. *Biol. Psychiatry* 78 (11), 794–804.
- Suk, H.-I., Lee, S.-W., Shen, D., Initiative, A.D.N., et al., 2013. Latent feature representation with stacked auto-encoder for AD/MCI diagnosis. *Brain Struct. Funct.* 220, 841–859.
- Sun, D., van Erp, T.G.M., Thompson, P.M., Bearden, C.E., Daley, M., Kushan, L., Hardt, M.E., Nuechterlein, K.H., Toga, A.W., Cannon, T.D., 2009. Elucidating a magnetic resonance imaging-based neuroanatomic biomarker for psychosis: classification analysis using probabilistic brain atlas and machine learning algorithms. *Biol. Psychiatry* 66, 1055–1060. <http://dx.doi.org/10.1016/j.biopsych.2009.07.019>.
- Sundermann, B., Herr, D., Schwindt, W., Pfeleiderer, B., 2014. Multivariate classification of blood oxygen level-dependent fMRI data with diagnostic intention: a clinical perspective. *Am. J. Neuroradiol.* 39, 848–855. <http://dx.doi.org/10.3174/ajnr.A3713>.
- Tagliazucchi, E., Laufs, H., 2014. Decoding wakefulness levels from typical fMRI resting-state data reveals reliable drifts between wakefulness and sleep. *Neuron* 82, 695–708.
- Takayanagi, Y., Takahashi, T., Orikabe, L., Mozue, Y., Kawasaki, Y., Nakamura, K., Sato, Y., Itokawa, M., Yamasue, H., Kasai, K., Kurachi, M., Okazaki, Y., Suzuki, M., 2011. Classification of first-episode schizophrenia patients and healthy subjects by automated MRI measures of regional brain volume and cortical thickness. *PLoS One* 6, 1–10. <http://dx.doi.org/10.1371/journal.pone.0021047>.
- Tang, X., Holland, D., Dale, A.M., Younes, L., Miller, M.I., 2014. Shape abnormalities of subcortical and ventricular structures in mild cognitive impairment and Alzheimer's disease: detecting, quantifying, and predicting. *Hum. Brain Mapp.* 35, 3701–3725. <http://dx.doi.org/10.1002/hbm.22431>.
- Tang, X., Holland, D., Dale, A.M., Younes, L., Miller, M.I., 2015. Baseline shape diffeomorphometry patterns of subcortical and ventricular structures in predicting conversion of mild cognitive impairment to Alzheimer's disease. *J. Alzheimers Dis.* 44, 599–611. <http://dx.doi.org/10.3233/JAD-141605>.
- Tang, Y., Wang, L., Cao, F., Tan, L., 2012. Identify schizophrenia using resting-state functional connectivity: an exploratory research and analysis. *Biomed. Eng. Online* 11, 50. <http://dx.doi.org/10.1186/1475-925X-11-50>.
- Tangaro, S., Amoroso, N., Brescia, M., Cavuoti, S., Chincarini, A., Errico, R., Inglese, P., Longo, G., Maglietta, R., Tateo, A., Riccio, G., Bellotti, R., 2015. Feature selection based on machine learning in MRIs for hippocampal segmentation. *Comput. Math. Methods Med.* 2015, 814104. <http://dx.doi.org/10.1155/2015/814104>.
- Tognin, S., Pettersson-Yeo, W., Valli, I., Hutton, C., Woolley, J., Allen, P., McGuire, P., Mechelli, A., 2013. Using structural neuroimaging to make quantitative predictions of symptom progression in individuals at ultra-high risk for psychosis. *Front. Psychiatry* 4, 187. <http://dx.doi.org/10.3389/fpsy.2013.00187>.
- Tong, T., Wolz, R., Gao, Q., Guerrero, R., Hajnal, J.V., Rueckert, D., 2014. Multiple instance learning for classification of dementia in brain MRI. *Med. Image Anal.* 18, 808–818. <http://dx.doi.org/10.1016/j.media.2014.04.006>.
- Turner, J.A., 2014. The rise of large-scale imaging studies in psychiatry. *Gigascience* 3, 29.
- Uddin, L.Q., Menon, V., Young, C.B., Ryali, S., Chen, T., Khouzam, A., Minshew, N.J., Hardan, A.Y., 2011. Multivariate searchlight classification of structural magnetic resonance imaging in children and adolescents with autism. *Biol. Psychiatry* 70, 833–841.
- Uddin, L.Q., Supekar, K., Lynch, C.J., Khouzam, A., Phillips, J., Feinstein, C., Ryali, S., Menon, V., 2013. Salience network-based classification and prediction of symptom severity in children with autism. *JAMA Psychiatry* 70, 869–879.
- Van Essen, D.C., Smith, S.M., Barch, D.M., Behrens, T.E.J., Yacoub, E., Uğurbil, K., Consortium, W.-M.H.C.P., et al., 2013. The WU-Minn human connectome project: an overview. *NeuroImage* 80, 62–79.
- Vemuri, P., Gunter, J.L., Senjem, M.L., Whitwell, J.L., Kantarci, K., Knopman, D.S., Boeve, B.F., Petersen, R.C., Jack, C.R., 2008. Alzheimer's disease diagnosis in individual subjects using structural MR images: validation studies. *NeuroImage* 39, 1186–1197. <http://dx.doi.org/10.1016/j.neuroimage.2007.09.073>.
- Venkataraman, A., Whitford, T.J., Westin, C.-F., Golland, P., Kubicki, M., 2012. Whole brain resting state functional connectivity abnormalities in schizophrenia. *Schizophr. Res.* 139, 7–12. <http://dx.doi.org/10.1016/j.schres.2012.04.021>.
- Vergara, V.M., Damaraju, E., Mayer, A.B., Miller, R., Cetin, M.S., Calhoun, V., 2015. The impact of data preprocessing in traumatic brain injury detection using functional magnetic resonance imaging. *Engineering in Medicine and Biology Society (EMBC), 2015 37th Annual International Conference of the IEEE*, pp. 5432–5435.
- Veronese, E., Castellani, U., Peruzzo, D., Bellani, M., Brambilla, P., 2013. Machine learning approaches: from theory to application in schizophrenia. *Comput. Math. Methods Med.* 2013, 867924. <http://dx.doi.org/10.1155/2013/867924>.
- Wang, L., Beg, F., Ratnanather, T., Ceritoglu, C., Younes, L., Morris, J.C., Csernansky, J.G., Miller, M.I., 2007. Large deformation diffeomorphism and momentum based hippocampal shape discrimination in dementia of the Alzheimer type. *IEEE Trans. Med. Imaging* 26, 462–470. <http://dx.doi.org/10.1109/TMI.2005.853923>.
- Wang, Y., Fan, Y., Bhatt, P., Davatzikos, C., 2010. High-dimensional pattern regression using machine learning: from medical images to continuous clinical variables. *NeuroImage* 50, 1519–1535. <http://dx.doi.org/10.1016/j.neuroimage.2009.12.092>.
- Wang, X., Jiao, Y., Tang, T., Wang, H., Lu, Z., 2013. Altered regional homogeneity patterns in adults with attention-deficit hyperactivity disorder. *Eur. J. Radiol.* 82, 1552–1557. <http://dx.doi.org/10.1016/j.ejrad.2013.04.009>.
- Watanabe, T., Kessler, D., Scott, C., Angstadt, M., Sripada, C., 2014. Disease prediction based on functional connectomes using a scalable and spatially-informed support vector machine. *NeuroImage* 96, 183–202. <http://dx.doi.org/10.1016/j.neuroimage.2014.03.067>.
- Wee, C.-Y., Wang, L., Shi, F., Yap, P.-T., Shen, D., 2014. Diagnosis of autism spectrum disorders using regional and interregional morphological features. *Hum. Brain Mapp.* 35, 3414–3430.
- Wee, C.-Y., Yap, P.-T., Li, W., Denny, K., Browndyke, J.N., Potter, G.G., Welsh-Bohmer, K.A., Wang, L., Shen, D., 2011. Enriched white matter connectivity networks for accurate identification of MCI patients. *NeuroImage* 54, 1812–1822. <http://dx.doi.org/10.1016/j.neuroimage.2010.10.026>.
- Wee, C.-Y., Yap, P.-T., Shen, D., 2013. Prediction of Alzheimer's disease and mild cognitive impairment using cortical morphological patterns. *Hum. Brain Mapp.* 34, 3411–3425. <http://dx.doi.org/10.1002/hbm.22156>.
- Wee, C.-Y., Yap, P.-T., Zhang, D., Denny, K., Browndyke, J.N., Potter, G.G., Welsh-Bohmer, K.A., Wang, L., Shen, D., 2012. Identification of MCI individuals using structural and functional connectivity networks. *NeuroImage* 59, 2045–2056.
- Wei, M., Qin, J., Yan, R., Li, H., Yao, Z., Lu, Q., 2013. Identifying major depressive disorder using Hurst exponent of resting-state brain networks. *Psychiatry Res.* 214, 306–312. <http://dx.doi.org/10.1016/j.psychres.2013.09.008>.
- Wing, L., 1997. *The autistic spectrum*. *Lancet* 350, 1761–1766.
- Wolf, H., Grunwald, M., Kruggel, F., Riedel-Heller, S.G., Angerhöfer, S., Hojatoleslami, A., Hensel, A., Arendt, T., Gertz, H., 2001. Hippocampal volume discriminates between normal cognition; questionable and mild dementia in the elderly. *Neurobiol. Aging* 22, 177–186.
- Wolters, T., Buitelaar, J.K., Beckmann, C.F., Franke, B., Marquand, A.F., 2015. From estimating activation locality to predicting disorder: a review of pattern recognition for neuroimaging-based psychiatric diagnostics. *Neurosci. Biobehav. Rev.* 57, 328–349.
- Wolz, R., Julkunen, V., Koikkalainen, J., Niskanen, E., Zhang, D.P., Rueckert, D., Soininen, H., Lötjönen, J., 2011. Multi-method analysis of MRI images in early diagnostics of Alzheimer's disease. *PLoS One* 6, e25446. <http://dx.doi.org/10.1371/journal.pone.0025446>.
- Wu, X., Li, J., Ayutyanont, N., Protas, H., Jagust, W., Fleisher, A., Reiman, E., Yao, L., Chen, K., 2013. The receiver operational characteristic for binary classification with multiple indices and its application to the neuroimaging study of Alzheimer's disease. *IEEE/ACM Trans. Comput. Biol. Bioinform.* 10, 173–180. <http://dx.doi.org/10.1109/TCBB.2012.141>.
- Xu, L., Wu, X., Chen, K., Yao, L., 2015. Multi-modality sparse representation-based classification for Alzheimer's disease and mild cognitive impairment. *Comput. Methods Prog. Biomed.* 122, 182–190. <http://dx.doi.org/10.1016/j.cmpb.2015.08.004>.
- Yang, S.-T., Lee, J.-D., Chang, T.-C., Huang, C.-H., Wang, J.-J., Hsu, W.-C., Chan, H.-L., Wai, Y.-Y., Li, K.-Y., 2013. Discrimination between Alzheimer's disease and mild cognitive impairment using SOM and PSO-SVM. *Comput. Math. Methods Med.* 2013, 253670. <http://dx.doi.org/10.1155/2013/253670>.
- Yang, H., Liu, J., Sui, J., Pearlson, G., Calhoun, V.D., 2010. A hybrid machine learning method for fusing fMRI and genetic data: combining both improves classification of schizophrenia. *Front. Hum. Neurosci.* 4, 192. <http://dx.doi.org/10.3389/fnhum.2010.00192>.
- Yang, W., Lui, R.L.M., Gao, J.-H.H., Chan, T.-F., Yau, S.-T.T., Sperling, R.A., Huang, X., 2011. Independent component analysis-based classification of Alzheimer's disease MRI data. *J. Alzheimers Dis.* 24, 775–783. <http://dx.doi.org/10.3233/JAD-2011-101371>.
- Yoon, J.H., Nguyen, D.V., McVay, L.M., Deramo, P., Minzenberg, M.J., Ragland, J.D., Niendam, T., Solomon, M., Carter, C.S., 2012. Automated classification of fMRI during cognitive control identifies more severely disorganized subjects with schizophrenia. *Schizophr. Res.* 135, 28–33. <http://dx.doi.org/10.1016/j.schres.2012.01.001>.

- Yoon, J.H., Tamir, D., Minzenberg, M.J., Ragland, J.D., Ursu, S., Carter, C.S., 2008. Multivariate pattern analysis of functional magnetic resonance imaging data reveals deficits in distributed representations in schizophrenia. *Biol. Psychiatry* 64, 1035–1041. <http://dx.doi.org/10.1016/j.biopsych.2008.07.025>.
- Young, K., Du, A.-T., Kramer, J., Rosen, H., Miller, B., Weiner, M., Schuff, N., 2009. Patterns of structural complexity in Alzheimer's disease and frontotemporal dementia. *Hum. Brain Mapp.* 30, 1667–1677. <http://dx.doi.org/10.1002/hbm.20632>.
- Young, J., Modat, M., Cardoso, M.J., Mendelson, A., Cash, D., Ourselin, S., 2013. Accurate multimodal probabilistic prediction of conversion to Alzheimer's disease in patients with mild cognitive impairment. *NeuroImage Clin.* 2, 735–745. <http://dx.doi.org/10.1016/j.nicl.2013.05.004>.
- Yu, Y., Shen, H., Zeng, L.-L., Ma, Q., Hu, D., 2013a. Convergent and divergent functional connectivity patterns in schizophrenia and depression. *PLoS One* 8, e68250. <http://dx.doi.org/10.1371/journal.pone.0068250>.
- Yu, Y., Shen, H., Zhang, H., Zeng, L.-L., Xue, Z., Hu, D., 2013b. Functional connectivity-based signatures of schizophrenia revealed by multiclass pattern analysis of resting-state fMRI from schizophrenic patients and their healthy siblings. *Biomed. Eng. Online* 12, 10. <http://dx.doi.org/10.1186/1475-925X-12-10>.
- Yu, G., Liu, Y., Shen, D., 2015. Graph-guided joint prediction of class label and clinical scores for the Alzheimer's disease. *Brain Struct. Funct.* <http://dx.doi.org/10.1007/s00429-015-1132-6>.
- Yu, G., Liu, Y., Thung, K.-H., Shen, D., 2014. Multi-task linear programming discriminant analysis for the identification of progressive MCI individuals. *PLoS One* 9, e96458. <http://dx.doi.org/10.1371/journal.pone.0096458>.
- Yue, C., Wu, D., Bai, F., Shi, Y., Yu, H., Xie, C., Zhang, Z., 2015. State-based functional connectivity changes associate with cognitive decline in amnesic mild cognitive impairment subjects. *Behav. Brain Res.* 288, 94–102. <http://dx.doi.org/10.1016/j.bbr.2015.04.013>.
- Yun, H.J., Kwak, K., Lee, J.-M., 2015. Multimodal discrimination of Alzheimer's disease based on regional cortical atrophy and hypometabolism. *PLoS One* 10, e0129250. <http://dx.doi.org/10.1371/journal.pone.0129250>.
- Zaharia, M., Chowdhury, M., Franklin, M.J., Shenker, S., Stoica, I., 2010. *Spark: cluster computing with working sets*. *Proceedings of the 2nd USENIX Conference on Hot Topics in Cloud Computing*, p. 10.
- Zanetti, M.V., Schaufelberger, M.S., Doshi, J., Ou, Y., Ferreira, L.K., Menezes, P.R., Sczufca, M., Davatzikos, C., Busatto, G.F., 2013. Neuroanatomical pattern classification in a population-based sample of first-episode schizophrenia. *Prog. Neuro-Psychopharmacol. Biol. Psychiatry* 43, 116–125. <http://dx.doi.org/10.1016/j.pnpbp.2012.12.005>.
- Zarei, M., Damoiseaux, J.S., Morgese, C., Beckmann, C.F., Smith, S.M., Matthews, P.M., Scheltens, P., Rombouts, S.A.R.B., Barkhof, F., 2009. Regional white matter integrity differentiates between vascular dementia and Alzheimer disease. *Stroke* 40, 773–779. <http://dx.doi.org/10.1161/STROKEAHA.108.530832>.
- Zarogianni, E., Moorhead, T.W.J., Lawrie, S.M., 2013. Towards the identification of imaging biomarkers in schizophrenia, using multivariate pattern classification at a single-subject level. *NeuroImage Clin.* 3, 279–289. <http://dx.doi.org/10.1016/j.nicl.2013.09.003>.
- Zeng, L.-L., Shen, H., Liu, L., Hu, D., 2014. Unsupervised classification of major depression using functional connectivity MRI. *Hum. Brain Mapp.* 35, 1630–1641. <http://dx.doi.org/10.1002/hbm.22278>.
- Zhang, T., Davatzikos, C., 2011. ODVBA: optimally-discriminative voxel-based analysis. *IEEE Trans. Med. Imaging* 30, 1441–1454. <http://dx.doi.org/10.1109/TMI.2011.2114362>.
- Zhang, T., Davatzikos, C., 2013. Optimally-discriminative voxel-based morphometry significantly increases the ability to detect group differences in schizophrenia, mild cognitive impairment, and Alzheimer's disease. *NeuroImage* 79, 94–110. <http://dx.doi.org/10.1016/j.neuroimage.2013.04.063>.
- Zhang, D., Shen, D., 2012a. Multi-modal multi-task learning for joint prediction of multiple regression and classification variables in Alzheimer's disease. *NeuroImage* 59, 895–907. <http://dx.doi.org/10.1016/j.neuroimage.2011.09.069>.
- Zhang, D., Shen, D., 2012b. Predicting future clinical changes of MCI patients using longitudinal and multimodal biomarkers. *PLoS One* 7, e33182. <http://dx.doi.org/10.1371/journal.pone.0033182>.
- Zhang, Y., Dong, Z., Phillips, P., Wang, S., Ji, G., Yang, J., Yuan, T.-F., 2015. Detection of subjects and brain regions related to Alzheimer's disease using 3D MRI scans based on eigenbrain and machine learning. *Front. Comput. Neurosci.* 9, 66. <http://dx.doi.org/10.3389/fncom.2015.00066>.
- Zhang, Z., Huang, H., Shen, D., 2014. Integrative analysis of multi-dimensional imaging genomics data for Alzheimer's disease prediction. *Front. Aging Neurosci.* 6, 260. <http://dx.doi.org/10.3389/fnagi.2014.00260>.
- Zhang, D., Wang, Y., Zhou, L., Yuan, H., Shen, D., Initiative, A.D.N., et al., 2011. Multimodal classification of Alzheimer's disease and mild cognitive impairment. *NeuroImage* 55, 856–867. <http://dx.doi.org/10.1016/j.neuroimage.2011.01.008>.
- Zhou, J., Greicius, M.D., Gennatas, E.D., Growdon, M.E., Jang, J.Y., Rabinovici, G.D., Kramer, J.H., Weiner, M., Miller, B.L., Seeley, W.W., 2010. Divergent network connectivity changes in behavioural variant frontotemporal dementia and Alzheimer's disease. *Brain* 133, 1352–1367. <http://dx.doi.org/10.1093/brain/awq075>.
- Zhou, Y., Yu, F., Duong, T., 2014. Multiparametric MRI characterization and prediction in autism spectrum disorder using graph theory and machine learning. *PLoS One* 9, e90405. <http://dx.doi.org/10.1371/journal.pone.0090405>.
- Zhu, C.-Z., Zang, Y.-F., Cao, Q.-J., Yan, C.-G., He, Y., Jiang, T.-Z., Sui, M.-Q., Wang, Y.-F., 2008. Fisher discriminative analysis of resting-state brain function for attention-deficit/hyperactivity disorder. *NeuroImage* 40, 110–120.
- Zou, H., Hastie, T., 2005. Regularization and variable selection via the elastic net. *J. R. Stat. Soc. Ser. B (Stat Methodol.)* 67, 301–320.
- Zu, C., Jie, B., Liu, M., Chen, S., Shen, D., Zhang, D., 2015. Label-aligned multi-task feature learning for multimodal classification of Alzheimer's disease and mild cognitive impairment. *Brain Imaging Behav.* <http://dx.doi.org/10.1007/s11682-015-9480-7>.